Diversification and Local Adaptation in Western Fence Lizards, *Sceloporus occidentalis*

Nassima Mahdjouba Bouzid

A dissertation
submitted in partial fulfillment of the
requirements for the degree of

Doctor of Philosophy

University of Washington
2019

Reading Committee:
Lauren B. Buckley, Chair
Adam D. Leaché
Raymond B. Huey

Program Authorized to Offer Degree:
Biology

University of Washington

Abstract

Diversification and Local Adaptation in
Western Fence Lizards, *Sceloporus occidentalis*

Nassima Mahdjouba Bouzid

Chair of the Supervisory Committee:
Dr. Lauren B. Buckley
Department of Biology

I am fascinated by intraspecific variation–by both its sources and its potential implications for how organisms interact with their environments. The importance of intraspecific variation for predicting species responses to climate change has recently become a research priority (Moran et al., 2016; Urban et al., 2016). Differences in the sources of intraspecific variation–genetic divergence, phenotypic plasticity, and drift–can have profoundly different outcomes for species responses. Variation in traits produced by heritable differences in genes will be sensitive to future selection, while variation produced by phenotypic plasticity may be buffered. Time and again, mechanistic studies of species responses have highlighted the importance of considering trait variation to predict idiosyncratic responses (Albert et al., 2010; Bolnick et al., 2011; Buckley, 2010), and the sources of trait variation must also be considered.

I studied intraspecific variation in Western Fence Lizards (*Sceloporus occidentalis*) at three spatial scales and three levels of organization. In Chapter 1 I investigated species-wide phylogeographic patterns and demographic scenarios throughout western North America. In Chapter 2 I characterized clinal variation in genotypes and phenotypes and gene flow along an elevation gradient in Yosemite National Park. In Chapter 3 I disentangled the genetic and plastic

constituents of divergent phenotypes in a lab rearing experiment. My dissertation research provides an integrative framework for studying local adaptation in a polymorphic and well-established vertebrate system.

Chapter 1 is the culmination of over two decades of research on phylogeographic structure within *S. occidentalis*. We sampled 108 individuals from 83 localities throughout the range in western North America. We used 4,555 SNPs from ddRADseq to characterize population structure and estimate demographic history. We found five genetically distinct populations including: one in the southwest, south of the Transverse Ranges; two west of the Sierra Nevada-Cascades cordillera, separated from north-to-south just north of San Francisco Bay; and two east of the Sierra Nevada-Cascades cordillera, separated from east-to-west in the Great Basin desert. The branching pattern of populations suggests that populations south of the Transverse Ranges and west of the Sierra Nevada-Cascades cordillera are divergent from populations east of the Sierra Nevada-Cascades cordillera. The predominant mechanism of population divergence is allopatric divergence and contemporary secondary contact, which supports Quaternary glacial cycles as drivers of intraspecific genetic divergence.

Chapter 2 builds on foundational work by Leaché et al. (2010) to characterize genetic and phenotypic clines along an elevation gradient in Yosemite National Park. At high elevations lizards are larger and more melanistic, while at low elevations lizards are smaller and lighter-colored. We sampled 78 individuals from a 21 km stretch of the Grand Canyon of the Tuolumne River in northern Yosemite. The elevation gradient spanned 1321 m from N Hetch Hetchy Reservoir (37.9168°N, 119.6595°W, 1167 m) in the west to E Glen Aulin (37.9076°N, 119.4196°W, 2488 m) in the east. We used 721 SNPs from ddRADseq to characterize genetic

clines and estimate demographic history of populations along the elevation gradient. We found evidence for additional population structure and genetic divergence between phenotypically divergent individuals; one genetically distinct population corresponds to low elevation individuals and another corresponds to high elevation individuals. Analyses of SNPs, maximum size (snout-vent length, SVL), and coloration (ventral patch area) confirm that genes and phenotypes vary clinally, and not discretely, along the elevation gradient. Genetically distinct populations diverged in allopatry, but contemporary gene flow between populations is asymmetric. Genes flow uphill, with five times as many migrants entering the high elevation population from low elevation than the converse.

Chapter 3 delves into the underlying sources of trait divergence between low and high elevation individuals from the Grand Canyon of the Tuolumne River elevation gradient. While low and high elevation lizards mature at the same age (ca. 20 months; Jameson & Allison, 1976), high elevation lizards are larger and more melanistic than low elevation lizards. We disentangled the genetic and environmental constituents of phenotypic variation by rearing hatchling lizards under controlled lab conditions. We collected five gravid females from low elevation (N Hetch Hetchy Reservoir [37.96°N, -119.78°W, ca. 1200 m]) and eight gravid females from high elevation (Glen Aulin [37.91°N, -119.42°W, ca. 2400 m]), who produced 36 and 51 hatchling lizards, respectively. We evenly distributed hatchlings from both populations among two treatments that varied in potential activity time: short activity period (6 hrs) and long activity period (12 hrs). We varied activity time by limiting access to heat-lamp-produced thermal gradients, which are necessary for thermoregulation. We found evidence that differences in size are genetically-based; high elevation hatchlings were larger than low elevation hatchlings,

regardless of treatment. We found evidence that differences in color are at least partially produced by phenotypic plasticity; high elevation hatchlings were capable of plastically lightening to a color that was lighter than low elevation hatchlings. We found evidence that differences in behavior are genetically-based; high elevation hatchlings spent more time engaged in active behaviors. Overall, our findings are suggestive of local adaptation of high elevation hatchlings to restricted activity periods at high elevation.

References

Albert, C. H., Thuiller, W., Yoccoz, N. G., Soudant, A., Boucher, F., Saccone, P., & Lavorel, S. (2010). Intraspecific functional variability: extent, structure and sources of variation. Journal of Ecology, 98, 604–613.

Bolnick, D. I., Amarasekare, P., Araújo, M. S., Bürger, R., Levine, J. M., Novak, M., Rudolf, V. H. W., Schreiber S. J., Urban, M. C., & Vasseur, D. A. (2011). Why intraspecific trait variation matters in community ecology. Trends in Ecology & Evolution, 26, 183–192.

Buckley, L. B. (2010). The range implications of lizard traits in changing environments. Global Ecology and Biogeography, 19, 452–464.

Jameson Jr, E. W., & Allison, A. (1976). Fat and breeding cycles in two montane populations of *Sceloporus occidentalis* (Reptilia, Lacertilia, Iguanidae). Journal of Herpetology, 211–220.

Leache, A. D., Helmer, D. S., & Moritz, C. (2010). Phenotypic evolution in high-elevation populations of western fence lizards (*Sceloporus occidentalis*) in the Sierra Nevada Mountains. Biological Journal of the Linnean Society, 100, 630–641.

Moran, E. V., Hartig, F., & Bell, D. M. (2016). Intraspecific trait variation across scales: implications for understanding global change responses. Global Change Biology, 22, 137–150.

Urban, M. C., Bocedi, G., Hendry, A. P., Mihoub, J. B., Pe'er, G., Singer, A., Bridle, J. R., Crozier, L. G., De Meester, L., Godsoe, W., Gonzalez, A., Hellman, J. J., Holt, R. D., Huth, A., Johst, K., Krug, C. B., Leadley, P. W., Palmer, S. C. F., Pantel, J. H., Schmitz, A., Zollner, P. A., & Travis, J. M. J. (2016). Improving the forecast for biodiversity under climate change. Science, 353, aad8466.

Contents

Acknowledgments……...…2
Chapter 1: Phylogeography and diversification in a geographically widespread lizard (*Sceloporus occidentalis*)…….……6
Introduction…….…….……7
Materials and methods…….……...13
Results…….……...22
Discussion……...30
Acknowledgments……..……45
References……...46
Figures…….……...55
Tables……...……...64
Chapter 2: Potential for local adaptation in Western Fence Lizards (*Sceloporus occidentalis*) along an elevation gradient in Yosemite National Park…….…68
Introduction…….……..69
Materials and methods…….…..74
Results…….……...85
Discussion……...90
Acknowledgments……..……94
References……...95
Figures…….…….100
Tables……...……105
Chapter 3: Genetic divergence and phenotypic plasticity underlie trait differentiation in Western Fence Lizards (*Sceloporus occidentalis*)……..116
Introduction…….……..…117
Materials and methods…….….121
Results…….….135
Discussion…….141
Acknowledgments……..……..146
References……147
Figures…….…….152
Tables……...…….162
Appendix A: Photos of enclosures and experimental set-up…..…….166

Acknowledgments

My PhD has given me opportunities for personal and professional growth, and I am grateful. Over my almost five years as a graduate student I explored many exciting and motivating avenues of research and others that I found less so. I put myself in challenging situations that enabled me to become a more resilient person, both in research and in life. Ultimately, I've found that one of the most valuable skills I've gained is the ability to be resolute in my decisions regarding what I like and what I dislike. One of the things I've liked most about my graduate career has been the community. I feel fortunate to have had the support and guidance of many along the way.

First and foremost, I sincerely thank Adam Leaché and Lauren Buckley. Adam was always available to discuss exciting new projects and research strategies and he helped me defuse a number of research crises. He provided me with the encouragement to keep going, even when it seemed like the deck was stacked against me. Lauren helped me develop concise and clear reasoning and communication, both very valuable skills, and ones that are difficult to master. She also helped me identify interesting research questions, and encouraged me to invest my time in research endeavors that were likely to push the field forward. Being co-advised by Adam and Lauren made it possible for me to do the integrative research that I sought to do during my PhD.

Thanks to my committee members, Joe Felsenstein and Ray Huey, for taking time to help me brainstorm and pointing me towards interesting research topics. I've enjoyed our many conversations about natural history, cow genetics, mountaineering, etc. Thanks especially to Ray for taking my cold call in April 2014 and helping me solidify my decision to join UW Biology.

Thanks to members of the Leaché and Buckley lab groups for providing guidance, training, support, and much-needed research breaks. Thanks to Leonard Jones, Matt McElroy,

and Charles Linkem for training me in the lab. Thanks to Jared Grummer, Rebecca Harris, Matt McElroy, Rory Telemeco, Leonard Jones, and Itzue Caviedes-Solis for helping me prepare for presentations and committee meetings and for providing feedback on grants and papers. Thanks to my lab siblings, Itzue and Leonard, for going on snack breaks with me and for conversations on virtually everything. Thanks to Tony and Aji for your interesting perspectives on quantitative approaches to studying biology.

My fieldwork was made more fun and fruitful by organization extraordinaire Ann Trápaga, and by many stellar lizard wranglers, including Natasha Stepanova, Ellen Murphy, Olivia MacDonald, Charlotte Jennings, Dana Lin, Sabrina Horrack, Rachel Gittelman, Piotr Nowodworski, Dan Portik, Alison Ke, Sean Parnell, Ben Pridonoff, Cade Niles. Thanks to Leonard Jones for accompanying me on my initial scouting trip and ensuring we wouldn't be eaten by bears. My fieldwork in Yosemite would not have been possible without the coordination and support of the UC Natural Reserve System, the California Department of Fish and Wildlife (CDFW), and the National Park Service (NPS). Thanks to Anne Kelly (UC Merced) for facilitating my research at the Sierra Nevada Research Station/Yosemite Field Station, helping to care for pregnant lizards, and providing access to the park. Thanks to Rob Grasso, Rachel Mazur, Mitzi Thornley, and Gary Bias of NPS for helping me develop a sustainable and substantiated research plan and for providing permits for collecting in Yosemite. Thanks to Laura Patterson and Gina De La Rosa of CDFW for providing scientific collecting permits for Tuolumne County, California.

For help with live lizard care and logistics I am indebted to Barry Sinervo and his lab at UC Santa Cruz. I thank Regina Spranger and Pauline Blaimont for training me in lizard husbandry and helping me troubleshoot and streamline my experiments. Thanks to undergraduate

lizard care assistants Aaron Gormley and Josh Beasley for going above and beyond to make sure my project was a success. Thanks to Mike Angilletta, Steve Adolph, Roger Anderson, and Matthew McTernan for providing additional consultations about proper lab rearing and experimentation protocols for lizards.

I spent over a year of my PhD living outside of Washington, mostly in California and Arizona. Thanks to Carol Spencer, Bill Kerr and Gemma for hosting me during my stays in Berkeley; I'm glad I could visit often. Thanks to Philip Skipwith for providing words of encouragement and disparagement, usually in the same breath. Thanks to my MVZ family--Carol, Lydia, Michelle, Monica, Ann, Dave, Ted, Dana, Leleña, Terri, Jim, Charlotte, Skip, Luke, Ammon, and anyone I may have missed--for making me feel welcome, and like I had never left. Thanks to Carol Spencer for mentoring me as an undergraduate and for continuing to provide support and encouragement throughout my PhD. Thanks to Sean Reilly, Michaela Chavez-Reilly, and Bria and to Simone Des Roches and Max Segnitz for hosting and feeding me in Santa Cruz. Thanks to John Weins for providing me with space and resources for my dissertation writing sabbatical in Tucson.

I relied heavily on the support of my friends in Seattle over the course of my PhD. I thank Rachel Gittelman, Daniel Olsen, Gideon Dunster, and Diana Gergel for allowing me to vent my frustrations and forcing me to get outside and do fun things so I wouldn't have as much to vent about. Thanks to Rachel for teaching me to drive stick so that I could do my field work, offering me a fancy place to stay in Seattle, and graciously providing last-minute editing without (much) judgement. Thanks to Daniel for administering many food-related clubs, providing sage wisdom and Bay Area nostalgia, and opting to play devil's advocate in many arguments. Thanks to

Gideon for initiating arguments for which Daniel would play devil's advocate. Thanks to Diana for facilitating outdoor adventures and dog park excursions, rain or shine, or snow.

A huge thanks to Josh Schraiber. Though you left Seattle after my second year, I'm very thankful for your continued guidance and sage advice. Thank you for believing in me and taking the time to help me recognize my strengths. You've transitioned from a Pop Gen hipster to one of my closest friends.

Thanks to my husband Dan Portik for his seemingly limitless patience and support. Thank you for being my sounding board and putting my academic catastrophes into perspective. Thank you for sacrificing months of your time to watch our cats and dogs while I chased after lizards. And thank you for encouraging me to pursue this dream, even if it meant we would be apart for a while.

Chapter 1: Phylogeography and diversification in a geographically widespread lizard (*Sceloporus occidentalis*)

NASSIMA M. BOUZID[1,*], JAMES W. ARCHIE[2], ROGER A. ANDERSON[3], JARED A. GRUMMER[4], ADAM D. LEACHÉ[1]

[1]*Department of Biology & Burke Museum of Natural History and Culture, University of Washington, Box 351800, Seattle WA 98195-1800, USA*

[2]*Biological Sciences, California State University, 1250 Bellflower Blvd, Long Beach, California, 90840 USA*

[3]*Biology Department, Western Washington University, 516 High Street, Bellingham, WA 98225-9160, USA*

[4]*Department of Zoology, University of British Columbia, and Beaty Biodiversity Museum, 6270 University Blvd., Vancouver, BC, V6T1Z4*

**E-mail: bouzidnm@uw.edu*

Introduction

The ecological and evolutionary processes that generate intraspecific diversity have long been of interest. Species traits mediate responses to environmental conditions and can diverge under a multitude of scenarios (Zamudio, Bell, & Mason, 2016). Geographic variation in traits that have an underlying genetic component can reflect differences in selective regimes across a species range (Endler, 1977). In a well-known example, coat color of rock pocket mice (*Chaetodipus intermedius*), which is controlled by the MC1r locus, is under strong selection to reduce conspicuousness to predators on high contrast substrates (Barrett et al., 2019; Hoekstra, Drumm, & Nachman, 2004). Alternatively, variation in traits can be produced by phenotypic plasticity in gene expression (DeWitt & Scheiner, 2004; Pigliucci, 2001). Selection might favor phenotypic plasticity in populations that are exposed to variable or unpredictable conditions if plasticity broadens the range of conditions a single genotype can tolerate (Ghalambor et al., 2007; Crispo, 2007). For example, plasticity in growth rates and age of maturity helps the montane vole (*Mictroctus montanus*) cope with unpredictable durations of winter and drought (Negus, Berger, & Pinter, 1992). Similarly, plasticity in behavior and physiology enable invasive cane toads (*Rhinella marina*) to reduce the costs of colonizing new environments and thrive in arid conditions (Brown et al., 2011).

Demographic history also contributes to intraspecific variation. Demographic events like population subdivision can limit gene flow and produce genetic divergence with or without a corresponding change in phenotype (Bickford et al., 2007). Populations separated by physical or environmental barriers accumulate genetic differences over time and may develop different traits if selective regimes differ between them (Zamudio, Bell, & Mason, 2016; Lande, 1980). In the classic example of ring species, the degree of genetic divergence within salamanders in the genus *Ensatina* is linked to the duration of geographic isolation, with populations in different environments exhibiting divergent phenotypes and populations in similar environments exhibiting conserved phenotypes (Pereira & Wake, 2009).

In addition to elucidating processes that produce genetic and phenotypic divergences between populations, studies of intraspecific variation can improve predictions of species responses to climate change (Moran et al., 2016). However, for most species we lack key data concerning mechanisms of phenotypic divergence, distribution of genetic diversity, and estimates of gene flow between populations (Urban et al., 2016). Divergent populations within a species may have different responses to changes in environmental conditions and predictions can thus be improved by linking intraspecific variation to the environmental and demographic processes that shape it (Urban et al., 2016; Moran et al., 2016).

The combined influences of trait variation, demographic history, and gene flow on patterns of intraspecific variation are expected to impact species differently. Within low mobility or specialist species that are reliant on specific habitat types, initial divergences are primarily due to restricted gene flow (Avise, 2000; Jansson & Dynesius, 2002). Processes that drive intraspecific divergence within dispersive and generalist taxa are more complex. Widespread taxa inhabiting differing environments are likely to contain locally adapted, genetically distinct populations (Kawecki & Ebert, 2004; Felsenstein, 1976), even though gene flow among populations acts to homogenize genetic variation and can swamp out alleles underlying locally adapted phenotypes if selection is not sufficiently strong (Lenormand, 2002). Species in the process of or having recently undergone expansions may contain highly phenotypically plastic populations that are capable of adopting traits that increase fitness in novel environments (Ghalambor et al., 2007; Shine, 2012). Vicariance due to historical climatic and geologic events can promote genetic differentiation via genetic drift by temporarily isolating populations, and signatures for these demographic events are recorded in patterns of population genetic diversity (Gottscho, 2016; Calsbeek et al., 2003; Gutenkunst et al., 2009). The relative contribution of each of these four processes—selection, phenotypic plasticity, gene flow, and vicariance—to intraspecific variation depends on both the extrinsic properties of the species' geographic range

(e.g., climate, topographic barriers) and the intrinsic properties of the species (e.g., dispersal ability).

We investigated processes driving intraspecific divergence of fence lizards in western North America, a region that encompasses the California Floristic Province, is a global biodiversity hotspot, and one that is expected to experience species and population declines as a result of anthropogenic climate change (Myers et al., 2000; Sheffield & Wood, 2008; Cook et al., 2015, Williams et al., 2015; Sinervo et al., 2010). Western North America's topographic complexity, including the Sierra Nevada-Cascade mountain chain and southern California's Transverse mountain ranges, has produced topographic barriers and sharp environmental gradients that have driven allopatric divergence within species of reptiles, amphibians, birds, mammals, and spiders (Calsbeek et al., 2003; Lapointe & Rissler, 2005; Satler et al., 2013). As recently as 14,000 years ago (14 ka), glaciation at high latitudes and altitudes limited dispersal and restricted species range expansions (Moore & Moring, 2013; Dubey & Shine, 2012; Rosenbaum & Reynolds, 2004; Hewitt, 2000). These glaciers reached their current, reduced extents approximately 10,000 years ago (10 ka) (Davis, 1988). Western North America's major mountain ranges, the Sierra Nevada and the Cascades, remain sharp temperature and precipitation gradients that likely impede gene flow (Ghalambor et al., 2006). Regions at temperate latitudes, including western North America, are expected to experience the greatest

magnitude of climate change, and increases in the frequency of extreme and unpredictable temperature events are likely to result in population declines (Buckley & Huey, 2016; IPCC, 2007; Williams et al., 2017). In addition to impacting temperatures, climate change has made drought a recurring feature of the climate of western North America that is driving aridification of the California Floristic Province (Sheffield & Wood, 2008; Cook et al., 2015, Williams et al., 2015). As a result, we expect the following phenomena to characterize species with large ranges in western North America:

1a. Intraspecific phenotypic variation will have resulted from spatially variable selection across heterogeneous environmental conditions.

1b. Phenotypic plasticity, manifested as multiple phenotypes within a single genotype with, has facilitated rapid colonization of recently glaciated mountain ranges and northern latitudes.

2. Intermittent isolation of populations by Quaternary glacial cycles drove divergence in allopatry, yet the magnitudes and directions of gene flow determined whether population boundaries are being maintained or eroded.

3. Gene flow across a continuous species range has been impeded by sharp environmental clines (e.g., of elevation and aridity).

Here, we test the above hypotheses within a widespread terrestrial ectotherm, the western fence lizard (*Sceloporus occidentalis*). Terrestrial ectotherms rely on environmental temperatures for basic biological functions and will be inordinately impacted by climate change (Deutsch et al., 2008; Adolph & Porter, 1993; Huey & Stevenson, 1979). In temperate regions, terrestrial ectotherms use broad physiological tolerances and behavioral plasticity to cope with seasonal and daily variation in temperature (Deutsch et al., 2008; Huey et al., 2012; Kearney et al., 2009). *Sceloporus occidentalis* occurs in every major ecoregion in California with few apparent barriers to gene flow, and has colonized high latitude and high elevation regions that were glaciated during the Quaternary within the last 10–15,000 years (Bell & Price, 1996; Leaché et al., 2010). Previous studies of *S. occidentalis* have reported phenotypic variation, plasticity in growth rates and morphology, thermal sensitivity of performance, and acclimatization of metabolic rates and energy stores, though the processes responsible for this intraspecific variation are unclear (Bell & Price, 1996; Buckley et al., 2009; Jameson & Allison, 1976; Leaché et al., 2010; Sinervo & Adolph, 1994; Tsuji, 1988; van Berkum, 1988; but see Sinervo & Huey, 1990). We test whether intraspecific phenotypic variation can be attributed to genetic variation or plasticity by comparing the distributions of morphologically distinct subspecies with phylogeographic structure inferred from genome-wide single nucleotide polymorphism (SNP) data. Using the genetically distinct populations inferred from SNPs as a guide, we evaluate simple two-

population demographic models to test if allopatric divergence is a key factor in population histories. We contrast the magnitudes and directions of gene flow across populations to determine whether genetic variation is expected to be swamped out with continued gene flow, or if population boundaries will be maintained. Finally, we identify barriers to gene flow, and potential environmental stressors, by reconstructing patterns of effective migration across the continuous range. We discuss our results in the context of phylogeographic and biogeographic patterns reported for other North American taxa and conclude by highlighting research directions that can further elucidate processes responsible for producing intraspecific variation.

Materials and methods

Morphological subspecies

Bell and Price (1996) describe six subspecies of *Sceloporus occidentalis* based on morphological characters and geographic range. Subspecies were grouped into two major "exerges": the *occidentalis* exerge has smaller body sizes, divided or absent gular patches, and white to cream venters; the *biseriatus* exerge has larger size, singular gular patches, and darker venters (Smith et al., 1992). The two subspecies within the *occidentalis* exerge [*S. o. bocourtii* (Coast Range Fence Lizard) and *S. o. occidentalis* (Northwestern Fence Lizard)] generally occur along the Pacific coast from Point Conception in southern California to the Pacific Northwest

(Fig. 1a). The four subspecies within the *biseriatus* exerge [*S. o. longipes* (Great Basin Fence Lizard), *S. o. biseriatus* (San Joaquin Fence Lizard), *S. o. taylori* (Sierra Fence Lizard), *S. o. becki* (Island Fence Lizard)] occupy a larger proportion of the range, and generally occur inland from the southeastern corner of Washington and eastern Oregon to southern California, the Channel Islands, and Baja California. The hypothesis that *S. occidentalis* subspecies represent unique lineages has been evaluated only using genetic data for the Sierra Fence Lizard (*S. o. taylori;* Leaché et al., 2010), which was found to be paraphyletic with respect to other, deeply divergent populations. In the context of describing intraspecific genetic variation, we briefly discuss the concordance of Bell and Price's (1996) subspecies diagnoses with the major genetic groups we infer using SNP data (see *Results*).

Genetic data

We sampled 108 *Sceloporus occidentalis* from throughout their range in western North America (Fig. S1; Table S1). We used NaCl extraction (MacManes, 2013) or a Qiagen DNeasy kit to extract whole genomic DNA from liver tissue. We collected ddRADseq data following Peterson et al., (2012). We double-digested 500 ng of genomic DNA for each sample with 20 units each of a rare cutter SbfI (restriction site 5'-CCTGCAGG-3') and a common cutter MspI (restriction site 5'-CCGG-3') in a single reaction with the manufacturer recommended buffer

(New England Biolabs) for 8 hr at 37°C. Fragments were purified with SeraPure SpeedBeads before ligation of barcoded Illumina adaptors onto the fragments. Eight individuals with unique barcodes were combined into each pool, and each pool was given its own Illumina adapter, giving each individual a unique barcode-adapter combination. Oligonucleotide sequences used for barcoding and adding Illumina indexes during library preparation are provided in Peterson et al., (2012). Libraries were size-selected (between 415 and 515 bp after accounting for adapter length) on a Blue Pippin Prep size fractionator (Sage Science). The final library amplification used proofreading *Taq* and Illumina's indexed primers. The fragment size distribution and concentration of each pool was determined on an Agilent 2200 TapeStation, and qPCR was performed to determine sequenceable library concentrations before multiplexing equimolar amounts of each pool for sequencing on a single Illumina HiSeq 2500 lane (50-bp, single-end reads) at the Vincent J. Coates Genomics Sequencing Laboratory at UC Berkeley.

Bioinformatics

We used PyRAD v.3.0.3 (Eaton, 2014) to de-multiplex Illumina sequence reads based on their unique barcode-adapter sequence combinations. Each read was reduced from 50 to 39 bp after the removal of the 5 bp barcode and the 6 bp restriction site overhang. To filter out low

quality reads, we changed sites with Phred quality scores under 99% (Phred score = 20) into "N" characters; and reads with ≥ 10% N's were discarded.

Trimmed reads from PyRAD were processed in the program Stacks (Catchen et al., 2011), interfaced through a custom Python pipeline (https://github.com/dportik/Stacks_pipeline). Reads were aligned into stacks, or sets of similar sequences, with a minimum depth of coverage of 5 sequences. A maximum of 2 nucleotide differences was allowed between stacks, meaning that only stacks with ≤ 2 differences could be combined and assembled into loci. As a result, loci can have more than 2 haplotypes. We dropped stacks with unusually high coverage prior to assembling loci to avoid retaining highly repetitive and/or non-orthologous regions in the final dataset. We removed loci that were invariant, non-biallelic, or that contained more than 2 haplotypes per individual. We assembled multiple datasets that varied in the percentage of individuals required to process a locus. Generally, the higher the proportion of individuals needed, the lower the number of loci that were retained in the final dataset (Table S2). To retain a higher number of loci, and have more power for demographic modeling, we required at least 25% of samples (27 of 108 total individuals) to have sequence data at a locus for the locus to be processed in downstream analyses. With this threshold, we compiled two datasets allowing a maximum of either 50% or 70% missing data per sample, respectively, which limited the number of samples retained in the final datasets. For example, in the case of 50% missing data per

sample, all samples with more than 50% of their loci missing would be discarded. To retain a larger proportion of the original 108 samples for phylogeographic analyses, we allowed for a higher percentage of missing data per sample. In the final two datasets, we sampled one random SNP per 39bp locus.

Population structure

Population structure provides a characterization of genetic variation, some of which could represent locally adapted populations (D'Amen et al., 2013; Serra-Varela et al., 2017). Here, we refer to 'populations' within *S. occidentalis* as major genetically-distinct groups of individuals; 'demes' as subsets of individuals within genetically-distinct groups; and 'localities' as the specific localities from which individuals were sampled. We used two methods to estimate population structure. The first is parametric: ADMIXTURE (Alexander et al., 2009), which relies on the model implemented in the program STRUCTURE (Falush et al., 2003; Pritchard et al., 2000), but uses a maximum likelihood framework and cross-validation error to choose the optimal value for the number of populations (K). We ran ADMIXTURE for K = 1–10 and compared the cross-validation error from each analysis to determine which K minimized group assignment error. However, parametric methods for estimating population structure are likely sensitive to the violations of model assumptions prevalent in natural populations, including

demographic processes like selection and/or migration that could result in allele frequencies that fall outside of Hardy Weinberg proportions and linkage disequilibrium (Waples, 2015). To evaluate the robustness of our population structure analysis, we also used a non-parametric method that should be less sensitive to these model assumptions: k-means clustering, followed by a discriminant analysis of principle components (DAPC), in the "find.clusters" and "dapc" commands, respectively, from the R package *adegenet* (Jombart, 2008). First, we transformed the data using PCA to reduce dimensionality using 20 dimensions, which explained 26.3% of the variation in the dataset and speed up the analysis. We ran k-means clustering on values of K = 1–10 and used the Bayesian Information Criterion (BIC) to select the K value that maximized the variation between groups. Finally, we performed DAPC using the original data to visualize genetic groups in ordination space and assign group membership probabilities.

Species tree estimation

We used a coalescent analysis of SNP data with SNAPP v1.3.0 (Bryant et al., 2012), implemented in BEAST v2.4 (Bouckaert et al., 2014), to estimate phylogenetic relationships among populations of *S. occidentalis*. To increase computation speed and reduce the analysis run time, we down-sampled to 4–5 evenly geographically spaced individuals from each genetically-distinct population, estimated under the K = 5 population model (see Results). We estimated

mutation rate priors (*u* and *v*) from the 70% missing dataset (1.066 and 0.942, respectively) and set the Yule birth rate prior (λ) to 10. We set a diffuse prior on the expected divergence between populations (θ) using a gamma distribution with alpha and beta shape parameters (1.0 and 250, respectively) corresponding to a mean of 0.004. We ran two independent analyses, each for 500,000 generations, sampling every 1,000 generations. We used DensiTree (implemented in BEAST) to visualize the posterior distribution of trees and the uncertainty in topology and branch length, then we used TreeAnnotator (BEAST) to calculate a maximum clade credibility (MCC), discarding the first 10% of trees as burn in. To provide a time frame for population divergence, we used a mutation rate of 1.0×10^{-8} substitutions per site per generation to time-calibrate the branch lengths of the MCC tree. This mutation rate is based on one estimated for humans (Lynch, 2010), but we converted the rate to substitutions per site per million years by adjusting for the shorter generation time of fence lizards (ca. 2 years; Tinkle & Ballinger, 1972).

Demographic models

The major features of demographic history that we modeled included the relative timing of gene flow and divergences between populations (e.g., continuous gene flow with divergence versus secondary contact post-divergence) and the relative magnitude and direction of gene flow (e.g. symmetric versus asymmetric gene flow). We only compared populations that are

geographically contiguous, meaning that their current geographic distributions are directly adjacent to one another, which could facilitate an exchange of migrants. We used the program *moments* (Jouganous et al., 2017) to evaluate competing models of population demographic history. Similar to the commonly used program δaδi (diffusion approximation for demographic inference; Gutenkunst et al., 2009), *moments* simulates the evolution of site frequency spectra (SFS) under user-specified demographic scenarios (Jouganous et al., 2017).

We optimized demographic parameters for 21 two-dimensional (2D) candidate models, originally described in Portik et al. (2017) and converted into a Python pipeline for *moments* (https://github.com/dportik). The 21 models are relevant for divergences in western North American taxa that are known to have been impacted by climatic instability and refugia (Waltari et al., 2007; Swenson & Howard, 2005). The optimized parameters include effective population size (*nu*), migration rates (*m*), and time since the major demographic event (e.g. population size change) (*T*). We conducted model fitting over three independent rounds of analysis, using 30, 50, and 100 replicates per round, respectively. At the end of the third and final round of optimizations, we ranked candidate demographic models for each pairwise comparison of populations according to the Akaike information criterion (AIC; Akaike, 1973). We selected the model with the lowest AIC value as the most well supported hypothesis to explain recent demographic history and further evaluated this choice using Akaike weights. Akaike weights

incorporate both the deltaAIC and the relative log likelihoods of candidate models to assign a measure of statistical confidence in the selected model relative to alternative models (Wagenmakers & Farrell, 2004). The most heavily weighted models carry the highest probability of being the correct model, given the dataset and candidate models.

Effective migration and landscape connectivity

We used the program EEMS (Estimating Effective Migration Surfaces; Petkova et al., 2016) to assess connectivity between individuals and identified barriers to gene flow. EEMS estimates effective migration, and not actual migration (i.e., the number of migrants per generation), by comparing empirical dissimilarities in genetic structure to those expected under an isolation-by-distance (IBD) model. Georeferenced samples are assigned to one of a specified number of demes, and dissimilarities are calculated between adjacent demes, with the assumption that an infinite number of demes would approach a continuous estimate of gene flow across the landscape. We used EEMS for our 70%-missing-individual-cutoff dataset with 500 demes, run for 10 million iterations, discarding the first 10% of samples as burnin. We sampled every 9,999 iterations and summarized results from three independent chains. To visualize geographic features corresponding with higher- and lower-than-expected rates of change of genetic dissimilarity, we overlaid the *m* rates raster with a 1 km-resolution digital elevation

model (DEM; Jarvis et al., 2008) in QGIS v2.18 (QGIS Geographic Information System). We extracted the *m* rates raster, which is the estimate of effective migration, from the EEMS companion R package rEEMSplots (https://github.com/dipetkov). The combination of the *m* rates and the DEM allowed us to identify geographic features, which we confirmed using Google Earth (https://earth.google.com). We defined features overlaid by lower than expected under IBD *m* rates as barriers and features overlaid by higher than expected under IBD as corridors.

Results

Genetic data

The prefiltered ddRADseq dataset contained 6,517 loci, of which 1,362 were invariant, 591 had more than 2 haplotypes per individual, and 17 were non-biallelic. After filtering, the final dataset contained 4,555 SNPs (one randomly sampled SNP for each locus) for 65 and 105 samples, while allowing for 50% and 70% missing data per sample, respectively. The characteristics of the ddRADseq data are provided in Table S2.

Population structure

Parametric and non-parametric population structure estimation did not unequivocally support the same value for *K*. For ADMIXTURE, the amount of missing data (or number of

SNPs) changed the optimal value for *K*. For example, the 50% and 70% missing datasets supported $K = 4$ and $K = 5$, respectively (Fig. S3). The differences between the cross-validation error scores from ADMIXTURE were only slightly different, which suggests that the optimal value of *K* is uncertain. The *adegenet* results were more stable and favored $K = 5$ based on BIC results (Fig. S3). Because the non-parametric population structure estimation method is insensitive to missing data and within the realm of reasonable choices for *K* according to the parametric method, we selected $K = 5$ for downstream analyses. The five populations are Southern California (S CA), West Sierra (W Sierra), West Great Basin (W GB), East Great Basin (E GB), and Pacific Northwest (PNW) (Fig. 1b). We visualized admixture between genetic populations by comparing barplots of individuals separated by mountain ranges that are known biogeographic barriers, the Transverse Ranges in southern California and the Sierra Nevada-Cascade mountain chain (Gottscho, 2016; Calsbeek et al., 2003) (Fig. 2b).

A principle components analysis of 4,555 SNPs without *a priori* population assignments revealed three major groupings in ordination space of genetically distinct populations (Fig. 2c). The first two principle components explained 26.3% of the variation in the dataset, and the third and fourth principle components explained an additional 5.1% and 4.7%, respectively. In general, geographically proximate genetic populations occupied adjacent ordination space (Fig. 2).

We detected individuals with >5% admixture in six different geographic areas (Fig. 1b). First, between the PNW and W GB populations in central Oregon. Second, between the PNW and W Sierra populations in the western portion of the range from the San Francisco Bay to northern California. Third between the PNW, W Sierra, and W GB populations in the central range in northeastern California. Fourth, between the W Sierra and W GB populations in the central range. Fifth, between W GB and E GB populations in the eastern portion of the range in Nevada. Sixth, between the S CA, W Sierra Nevada, and W GB populations in the south of the range near the Transverse mountain range.

Morphological subspecies

Morphologically divergent subspecies of Bell and Price (1996) share few concordant geographic boundaries with genetically distinct populations diagnosed here. The three subspecies *S. o. taylori*, *S. o. biseriatus*, and *S. o. bocourtii*, which are divergent from each other in both body size and coloration, all correspond to the W Sierra Nevada (genetic) population. The widespread and polymorphic *S. o. longipes* subspecies is composed of three genetically distinct populations: W GB, E GB, and S CA. The disjunct and sexually dimorphic portion of *S. o. longipes* that extends from southern California into Baja California corresponds to the S CA genetic population. The remaining portion of *S. o. longipes* in the Great Basin is sexually

monomorphic and corresponds to the W GB genetic population in the west and to the E GB genetic population in the east. The *S. o. occidentalis* subspecies roughly corresponds to the PNW population, although individuals in the northern Central Valley belong to the W Sierra Nevada population. We did not obtain samples from the Channel Islands, and can therefore not assign *S. o. becki* to a population or comment on its genetic distinctness.

Areas of intergradation between morphological subspecies did not necessarily correspond to genetic population boundaries. Within the W Sierra Nevada genetic population, *S. o. taylori* and *S. o. biseriatus* phenotypes intergrade on the western slopes of the Sierra Nevada near 2100 m elevation (Bell & Price, 1996; Leaché et al., 2010). Also, within the W Sierra Nevada genetic population, *S. o. occidentalis*, *S. o. biseriatus*, and *S. o. bocourtii* phenotypes intergrade in the Coast Ranges, west of the Central Valley. At the boundary between the W Sierra Nevada and S CA genetic populations near the Transverse mountain range, *S. o. biseriatus* and *S. o. bocourtii* phenotypes intergrade with the *S. o. longipes* phenotype. At the boundary between the PNW and W GB genetic populations in northeastern California and south-central Oregon, the *S. o. occidentalis* phenotype intergrades with the *S. o. longipes* phenotype.

Species tree estimation

The MCC species tree for *Sceloporus occidentalis* suggested an initial divergence ca. 200,000 years ago followed by three divergences within the last 23,000 years (Fig. 3). All divergences were well supported with posterior probabilities (PP) equal to 1.0 (Fig. 3b), though estimates for the age of the deep divergence (95% highest posterior density (HPD) 0.097–0.325 Mya). Fig. 3a) varied considerably. The deepest divergence split the five populations on either side of the Sierra Nevada Mountains: the western group included populations S CA, W Sierra Nevada, and PNW, and the eastern group included W GB and E GB. The three more recent divergences in order from oldest to youngest were between S CA and W Sierra Nevada-PNW, W Sierra Nevada and PNW, and W GB and E GB, respectively. Of the recent divergences, the estimate for the age of the split between S CA and W Sierra Nevada-PNW held the most uncertainty (95% HPD = 0.003–0.023 Mya).

Demographic modeling

We evaluated six pairwise comparisons of area of contiguous populations identified with *adegenet* and the PCA using JSFS. For each area grouping pair, we evaluated 21 demographic models and used AIC to select the optimal model to infer the likely mechanisms of population divergence (Table 1). Model parameters present across all models were effective population size

before (*nu1a*, *nu2a*) and after (*nu1b*, *nu2b*) the demographic event, migration rate (*m*), and the time interval of demographic change (*T*) (Fig. 4). We focused on the timing and direction of gene flow between areas and on the relative change in effective population size, which is analogous to genetic diversity (Nei & Takahata, 1993). The S CA and W Sierra comparison supports a secondary contact with symmetric gene flow model in which the effective size of W Sierra becomes larger than S CA (wAIC=0.9970). The S CA and W GB comparison supports a continuous contact model in which the direction of gene flow is asymmetric from S CA into W GB and the relative effective sizes of both populations remain constant (wAIC=0.9612). The W Sierra and W GB comparison supports a secondary contact model in which the direction of gene flow is asymmetric from W Sierra into W GB and the effective size of W Sierra is larger (wAIC=1.00). The W Sierra and PNW comparison supports a secondary contact and subsequent isolation model in which the direction of gene flow was asymmetric from W Sierra into PNW prior to current isolation, and the effective size of W Sierra is larger (wAIC=1.00). The W GB and PNW comparison supports a secondary contact model in which the direction of gene flow is asymmetric from W GB into PNW, and the effective size of W GB becomes larger than PNW (wAIC=0.9865). The W GB and E GB comparison supports a secondary contact model in which the direction of gene flow is asymmetric from W GB into E GB, and the effective size of W GB is larger (wAIC=0.5141).

Effective migration and landscape connectivity

To test whether sharp environmental clines (namely elevation and aridity gradients) impeded gene flow, we estimated effective migration surfaces and genetic diversity based on the 70% missing dataset containing 105 samples. The estimates for mean migration rates highlight that several barriers to gene flow for *S. occidentalis* are primarily in arid regions. We refer to relevant geographic features in Figure 5. The most prominent barrier corresponds to the southern Sierra Nevada and the eastern escarpment and rain shadow of the Sierra Nevada range, rather than the mountains themselves. (Fig. 5) Another barrier is located due north of the first, at the junction of California, Nevada, and Oregon. This region corresponds to the Black Rock Desert in Nevada and the rain shadow of the Warner Mountains in northeastern California. The Black Rock-Warner barrier extends northward into the high desert of the Harney Basin (Harney Co., OR) and curves in a U-shape southward through semi-arid steppe in southeastern Oregon and northern Nevada. In north and south central Nevada, two other barriers overlap with high elevation arid regions, including the Amargosa range on the California-Nevada border. The barrier roughly corresponds to the Mojave Desert in California and Nevada. Less prominent barriers overlap with other arid regions, for example the south Central Valley, the Colorado and Mojave Deserts in southern California, and the rain shadow of the Cascade Mountains in western

Washington. Only two moderately prominent barriers do not correspond with somewhat arid regions, Siskiyou National Forest in northwestern California and southwestern Oregon, and Lassen National Forest and Volcanic Park in northern California.

Corridors with higher gene flow than expected under an IBD model, the converse of barriers highlighted by mean effective migration rates, generally correspond to regions of Mediterranean climate that receive more rainfall, though there are exceptions. Some prominent corridors along the Pacific Coast are the Columbia River Valley and Coast Ranges in western Oregon and Washington; the Coast Range in northwestern California at the Mendocino Triple Junction (Gottscho, 2016); the region surrounding Monterrey Bay; the western Transverse Ranges in Santa Barbara County, southern California; and the eastern San Gabriel Mountains and Peninsular Ranges in Orange, Riverside, and San Bernardino Counties, also in southern California. Other, less prominent corridors occur on the western slopes and foothills of the Sierra Nevada, Plumas National Forest in northeastern California, and the Panamint Mountains in southern California. Corridors in eastern and western Nevada, southeastern Oregon, and southwestern Idaho occur in arid regions in the Great Basin, interspersed by small mountain ranges.

Genetic diversity is estimated relative to the expected dissimilarity between adjacent demes under an IBD model. Regions in which demes that are geographically proximate are more dissimilar than expected are considered regions of high diversity. Two major regions of high genetic diversity include: 1) the Peninsular Ranges of southern California and northeast through the Panamint Mountains to southwestern Nevada, and 2) southwestern and central Oregon, through to south-central Washington and south into northwestern Nevada. (Fig. S4b).

Discussion

Our study synthesizes distributions of phenotypic variation, SNP-based population demographic modeling, and estimates of gene flow to understand the processes that have shaped intraspecific variation in *Sceloporus occidentalis*. We find evidence for five genetically distinct populations phenotypic variation within genetically distinct populations, and correspondence between phylogeographic and phenotypic breaks. Allopatric divergence with secondary contact appears to be the primary mode of population divergence: this is consistent with isolation during Quaternary glacial cycles, which might have facilitated phenotypic divergence. The relative timing of genetic divergences suggests that Quaternary glaciation of the Sierra Nevada temporarily isolated populations to the west and east of the mountain range. The general trend in

the magnitude and direction of gene flow between populations is northward and eastward, with the most recently diverged populations occupying the northern and eastern range edges (Fig. 3b).

Arid geographic features, most notably the eastern escarpment of the Sierra Nevada, impede gene flow. Genetic diversity in the northern extreme of the range is low, though secondary contact between genetically distinct populations in the north has created a region of unexpectedly high genetic diversity (Fig. S4b). The pattern of low genetic diversity is the northern extreme of the range is consistent with expectations of expanding populations. Here, we discuss intraspecific patterns of phenotypic and genetic variation, mechanisms of divergence, and gene flow in the context of other North American taxa. We conclude by highlighting promising avenues of research that, using *S. occidentalis* as a model, would shed light on the process of adaptation to past and future environmental conditions.

Phenotypic variation both within and between genetically distinct populations

Intraspecific variation in phenotypes can be due to either differences in the alleles underlying traits or due to plasticity (Pigliucci, 2001; Endler, 1977). To determine which mechanism is more likely to be responsible for the variation within *S. occidentalis*, we quantified phylogeographic structure across the species range and compared patterns from SNPs with observed phenotypic variation. We identified five genetically distinct populations that span large

geographic regions (Fig. 1b), which may be partially linked to the species's high dispersal ability (Massot et al., 2003).

Another highly dispersive reptile, the common garter snake (*Thamnophis sirtalis*), contains genetically distinct groups that occupy large geographic regions but have little population substructure (Janzen et al., 2002). Taxa with more limited dispersal, like California slender salamanders, northern alligator lizards, and trapdoor spiders exhibit considerably more phylogeographic structure (Lavin et al., 2018; Highton, 2014; Satler et al., 2013). We identified cases of both phenotypic variation within a genetically distinct population and phenotypic uniformity among multiple genetically distinct populations, a pattern similar to that found in the closely related eastern fence lizards (*Sceloporus "undulatus";* Leaché and Reeder 2002). The considerable phenotypic variation within the W Sierra genetic population may reflect either fine-scale, clinal variation in alleles that were not sampled in our dataset or phenotypic plasticity or both. Lizards in the W Sierra genetic population live in multiple habitat types: moist scrub and forests along the north and central California coast, arid woodlands in the Central Valley, and highly seasonal montane forests in the Sierra Nevada (Bell & Price, 1996). The distinctive phenotype of high elevation Sierra Nevada lizards has multiple independent origins and is associated with multiple mitochondrial haplotypes (Leaché et al., 2010). High elevations in the Sierra Nevada were fully glaciated until as recently as 14,000 years ago, shrinking to their

current extents 10,000 years ago, meaning that colonization and phenotypic divergence occurred relatively recently (Davis, 1988; Dubey & Shine, 2012; Moore & Moring, 2013). To cope with cooler temperatures and seasonal activity restrictions, colonizing *S. occidentalis* may have plastically developed adaptive phenotypes (Chevin & Lande, 2011; Ghalambor et al., 2007). Grasshoppers in the *Melanoplus sanguinipes/devastator* complex are distributed along the same elevation gradient from the Central Valley to the Sierra Nevada and exhibit developmental plasticity in behavior and physiology to cope with environmental challenges at high elevation (Samietz, Salser, & Dingle, 2005).

Phylogeographic structure in the absence of morphological divergence is common in North American taxa and may reflect genetic divergence across populations occupying similar environments (Zamudio, Bell, & Mason, 2016). Members of the W GB, E GB, and S CA *S. occidentalis* genetic populations are phenotypically similar and together occupy a large latitudinal range. Examples of North American taxa exhibiting genetic divergence without phenotypic divergence include black salamanders, brown creepers, trapdoor spiders, and southwestern springsnails, to name a few (Reilly & Wake, 2015; Manthey, Klicka, & Spellman, 2011; Liu, Hershler, & Clift, 2003, Satler et al., 2013). Despite phenotypic similarity, previous studies have demonstrated that *S. occidentalis* at the northern and southern ends of this latitudinal range are divergent in physiology and thermoregulatory behavior (McTernan, 2017;

Sinervo, 1990; Tsuji, 1988). The lack of corroboration between the morphological subspecies and genetic population boundaries, and from evidence of contemporary gene flow between populations, suggests that *S. occidentalis* is a single, polymorphic species, with a potentially large number of locally adapted demes.

Population demographic events and divergences reflect glacial history

Mountains were impassible to terrestrial taxa during Quaternary glaciation and remain formidable ecological barriers (Dubey & Shine, 2012; Ghalambor et al., 2006). Until 14,000 years ago, glaciers covered high elevations in California's Sierra Nevada and Trinity Alps and Washington and Oregon's Cascade and Klamath mountains, but shrank to their current extents 10,000 years ago (Sharp, 1960; Porter, 1976; Davis, 1988; Rosenbaum & Reynolds, 2004; Moore & Moring, 2013). During glacial periods, glaciers expanded to lower elevations and 'locked-up' terrestrial water sources, resulting in drier conditions (Hewitt, 2000; Guyton, 1998). Species persisted in glacial refugia in North American Mediterranean regions and warm and cold-deserts during glacial periods and came into secondary contact during warmer and wetter interglacial periods (Wilson & Pitts, 2012; Hewitt, 2011; Waltari et al., 2007; Swenson & Howard, 2005).

To test whether intermittent isolation-and-expansion events have driven genetic divergence, we compared two-population divergence scenarios for contiguous populations. We find support for allopatric divergence with secondary contact as the predominant mode of divergence in all pairwise population comparisons except for one. The only instance of parapatric divergence with continuous gene flow occurs between the S CA and W GB populations in the southern part of the range. Low elevation and low latitude regions were likely less impacted by glaciation, which may have facilitated divergence with gene flow between the S CA and W GB populations (Dubey & Shine, 2012). Phylogeographic studies of many North American taxa have revealed signatures of population isolation and secondary contact, suggesting this mode of divergence is common (Lavin et al., 2018; O'Connell et al., 2017; Pereira & Wake, 2009; Leaché, 2009; Swenson & Howard, 2005).

Glacial history is supported as a driver of intraspecific genetic variation based on 1) the locations of contact zones, 2) the phylogenetic relationships among populations, and 3) recent colonization of previously glaciated regions. Until recently (ca. 10 ka), glaciation precluded colonization of high elevation in the Sierra Nevada and the Puget Sound in western Washington (Hill, 2006; Porter, 1976). Glaciation also prevented east-west dispersal across the Sierra Nevada, potentially driving phylogeographic breaks within amphibians, reptiles, and mammals, in addition to the ancient (ca. 200,00 years; HPD = 97,000–325,000 years) divergence between

S. occidentalis populations to the east and west (Lavin et al., 2018; Calsbeek et al., 2003). The phenomenon of northward expansion following Quaternary glaciation is well documented and supported by relatively low levels of genetic diversity in recently established northern populations and by relatively high levels of genetic diversity in older southern populations (Lavin et al., 2018; Potter et al., 2015; Hewitt, 2004; Hewitt, 2000).

Considering that the order of divergences on the species trees (Fig. 3), and that the PNW population must have dispersed to Puget Sound no earlier than 10 ka, *S. occidentalis* probably colonized regions west of the Sierra Nevada from south (southern and Baja California) to north (California, Oregon, then Washington). East of the Sierra Nevada, the common ancestor of the W GB and E GB populations (W GB-E GB) diverged from S CA-W Sierra-PNW prior to the divergence between S CA and W Sierra-PNW. Considering that low latitude and low elevation regions were less impacted by glaciation, and that the S CA and W GB genetic populations diverged with continuous gene flow, we expect that *S. occidentalis* colonized regions east of the Sierra Nevada from south to north (eastern Washington) and east (E GB in western Utah). A center of high genetic variation in the southern extreme of the range, where *S. occidentalis* might have persisted throughout Quaternary glaciation, supports this expectation (Fig. S4b).

Higher than expected effective genetic diversity in central Oregon and southern Washington coincides with a contact zone between distantly divergent genetic populations, PNW

and W GB (Fig. 1b: 1). Near this contact zone, at the Oregon-Washington border, an east-west trending low elevation trough, formed during the orogeny of the Cascades, could have served as a conduit for bringing distantly divergent genetic populations into secondary contact (Newcomb, 1967).

The trajectories of expansion from south to north with allopatric divergence on either side of the glaciated and impassable Sierra Nevada and secondary contact between distantly diverged populations in the north is reminiscent of a ring species, with several key differences. Two ring species, *Ensatina* salamanders and dusky-footed woodrats *(Neotoma fuscipes*), colonized regions of suitable habitat, including the Coast ranges and Sierra Nevada, on either side of an impassable barrier, the Central Valley (Pereira & Wake, 2009; Matocq, 2002; Moritz et al., 1992). *Ensatina* colonized from north to south, while *Neotoma* colonized from south to north (like *S. occidentalis*) and both exhibit lower genetic diversity in more recently established populations (Kuchta et al., 2009; Matocq, 2002). Unlike *S. occidentalis*, *Ensatina* in the southern terminus of the ring are unable to interbreed (Pereira & Wake, 2009). This reproductive isolation may be related to the time needed to complete the ring; *Ensatina* have extremely limited dispersal abilities, while *S. occidentalis*, as evidenced by its colonization of recently glaciated regions, is capable of rapid dispersal (Leaché et al., 2010; Staub et al., 1995). *Sceloporus occidentalis* offers an interesting generalist contrast to known ring species in that it has colonized previously

impassable regions and populations diverged by 200,000 years (HPD = 97,000–325,000 years) remain capable of interbreeding. Contrary to expectations of lower genetic diversity at northern latitudes following post-Quaternary-glaciation expansion, *S. occidentalis*'s status as an ephemeral ring species has produced centers of high genetic diversity in both the north and south of the range.

Gene flow has potential to swamp out alleles and is impeded by arid regions

Gene flow between genetically distinct populations of *S. occidentalis* is mostly asymmetric and may homogenize divergences over time if not opposed by selection (Lenormand, 2002; Kirkpatrick & Barton, 1997). The boundary between the S CA, W Sierra, and W GB genetic populations coincides with the Transverse Ranges in southern California, a prominent biogeographic barrier in terrestrial taxa, and a junction of three *S. occidentalis* phenotypes (Fig. 1b: 6) (Gottscho, 2016). Although the Transverse Ranges were not were not fully glaciated during the Quaternary, glaciers were present on the easternmost and highest points in the Range as recently at 15-16 ka (Owen, Finkel, & Minnich, 2003). During periods of glacial advance, *S. occidentalis* might have persisted in low elevation regions like the southern Central Valley, Mojave Desert, and San Fernando Valley, accumulating genetic variation in allopatry before secondary contact across the Transverse Ranges. Contemporary gene flow is

symmetric between S CA and W Sierra and could be homogenizing these populations. Divergence between S CA and W GB occurred in the presence of continuous asymmetric gene flow trending northeast from S CA to W GB. The S CA and W GB genetic populations are phenotypically similar (both categorized as *S. o. longipes*), though S CA is sexually dimorphic, whereas W GB is sexually monomorphic (Bell & Price, 1996).

Two possible mechanisms could be driving genetic divergence between S CA and W GB: selection for different alleles in the Mediterranean climate of the Peninsular Ranges than in the arid climate of the Mojave Desert and Great Basin could maintain genetic divergence despite gene flow; or social interactions between sexually dimorphic and monomorphic individuals could be driving divergence (Cooper & Burns, 1987; Kirkpatrick & Barton, 1997). The Mojave Desert and Joshua Tree National Park are highlighted as barriers to gene flow, but deserts are expected to be replaced by herbaceous grasslands and woodlands as climate change increases precipitation, which may increase asymmetric gene flow from S CA into W GB (Bachelet et al., 2016). East-west divergences between W Sierra and W GB and between PNW and W GB also coincide with arid regions, the eastern escarpment and rain shadow of the Sierra Nevada and the eastern rain shadow of the Cascades range, respectively. The populations located west of Sierra Nevada experience a Mediterranean climate with hot summers and rainy winters (Myers et al., 2000), while their eastern counterparts experience a more arid climate. Gene flow is asymmetric

from W Sierra into W GB and likely began relatively recently, after Sierra Nevada glaciers receded.

We detect very few admixed individuals between W Sierra and W GB, which suggests that populations are either adapted to different environments (montane western and arid eastern conditions) and selection against hybrids is strong; or that the recent timeframe for this contact zone has not allowed enough time for gene flow between populations to form a contact zone. In the former case, if populations on either side of the Sierra Nevada are locally adapted, asymmetric gene flow could introduce maladapted W Sierra alleles into the W GB population (Lenormand, 2002). With the exception of gene flow from W GB into PNW, the net flow of migrants appears to be north- and eastward. We discuss a possible scenario explaining secondary contact between the distantly divergent PNW and W GB populations in central Oregon above. Contrary to patterns in the rest of the species range, asymmetric gene flow trends westward, from the W GB into the PNW population. W GB and E GB animals are substantially larger in body size than PNW animals, which may explain this gene flow trend if larger individuals are also more dispersive.

Contemporary gene flow between W Sierra and PNW genetic populations in northern California has ceased, and gene swamping from W GB could obliterate the PNW genetic population if selection does not maintain genetic divergence. Asymmetric gene flow from W

Sierra into PNW populations, which are now isolated, may represent northward range expansion. The contact zone between the PNW and W Sierra genetic populations occurs in northern California, beginning roughly at the San Francisco Bay and ending at the California-Oregon border (Fig. 1a: 2). The San Francisco Bay is the outlet for several major rivers that flow from the Sierra Nevada, and a prominent phylogeographic break in other reptiles and amphibians (Lavin et al., 2018; Reilly & Wake, 2015; Feldman & Spicer, 2006). The very recent (ca. 4,000 years; HPD = 1,000–9,000 years) divergence between the PNW and W Sierra genetic populations has occurred across the Trinity Alps and southern Cascade mountains, which were glaciated until recently ca. 14 ka (Rosenbaum & Reynolds, 2004; Sharp, 1960). During glacial periods that impeded dispersal across northern California mountains, *S. occidentalis* might have persisted in a proposed refugium in northwestern California, diverged in allopatry from W Sierra, and expanded northward following glacial receding (Swenson & Howard, 2005). Alternatively, *S. occidentalis* might have persisted in suitable habitat pockets within the Klamath Mountains, which have been proposed as a glacial refuge for flora (Potter et al., 2015; Sawyer, 2007).

Divergence between the W GB and E GB genetic populations also appears to be supported by allopatric divergence in glacial refugia and may represent eastward range expansion (Wilson & Pitts, 2012). Multiple species distributed across the Great Basin, including

the velvet ant (genus *Dilophotopsis*) and long-nose leopard lizard (*Gambelia wislizenii*), exhibit east-west divergences that are postulated to reflect isolation and allopatric divergence in cryptic refugia (Wilson & Pitts, 2012; Wilson & Pitts, 2010; Orange et al., 1999). A barrier to gene flow in central Nevada that is roughly parallel to the arid barrier in the rain shadow of the Sierra Nevada separates the W GB and E GB genetic populations (Fig. 5). This central Nevada barrier spans a series of small, north-to-south mountain ranges separated by arid lowlands which might have driven genetic divergence.

Generally, within-population barriers to gene flow in *S. occidentalis* are environmental gradients of temperature and aridity that might maintain intraspecific diversity despite ongoing gene flow. Low rates of effective migration indicate more between-deme genetic dissimilarity than expected, which could result from strong directional selection for alleles that give individuals living in arid environments an advantage. If arid-adapted alleles suffer a cost in non-arid environments, they could indicate local adaptation. Continued asymmetric gene flow has the potential to eventually homogenize populations and erode genetic variation, including variation in alleles responsible for adaptive phenotypes (Lenormand, 2002). Corridors are regions in which genetic dissimilarity between demes is lower than expected, which could be due to either high gene flow homogenizing adjacent populations or purifying selection in the region (Lenormand, 2002). Corridors of gene flow in *S. occidentalis* correspond to wetter, more mountainous regions.

These regions may facilitate dispersal by providing reliable and abundant food sources, as precipitation is correlated with higher insect abundances (Dunham, 1978).

Implications for future studies

Future work should capitalize on the extensive genetic, phenotypic and physiological variation within *Sceloporus occidentalis* to extrapolate population responses to future climate change. First, local variation in phenotypes and genotypes is not adequate support for local adaptation (Lenormand, 2002; Merïla & Hendry, 2014). To support the hypothesis of local adaptation, variable traits must confer a fitness advantage in the specific environment in which they evolved (Merïla & Hendry, 2014). The presence of intraspecific variation might be an indication of past capacities for adaptation, but additional information about how mechanistically traits confer advantages in certain environments is needed to predict the fate of trait differences between *S. occidentalis* populations. Lab and field-based experiments using *S. occidentalis* have the potential to determine whether trait differences are a product of local adaptation. Second, a targeted effort to understand the genetic architectures underlying intraspecific trait variation will improve predictions of the nature of trait responses to environmental change. If traits are primarily controlled by plasticity (e.g. gene regulation), populations will compensate rapidly, but may be buffered by behavior from evolving traits to keep up with the pace of climate change

(Huey, Hertz, & Sinervo, 2003; Huey et al., 2012). Third, the large and heterogeneous range of *S. occidentalis* provides ample replication for studying the process of adaptation *in situ*. Targeted population and landscape genetic studies with dense sampling across putative selective regimes (e.g. habitat ecotones, elevation gradients) have the potential to track the repeated evolution of alleles and traits that confer fitness advantages in different environments. Regardless of the past conditions under which intraspecific variation evolved in *S. occidentalis*, current and future conditions have the potential to put novel pressures on populations. We provide the phylogeographic, demographic, and biogeographic contexts necessary to realize *S. occidentalis* as an emerging model system to study the processes of adaptation in western North America.

Acknowledgments

Scientific specimens were collected with permission from the Oregon Department of Fish and Wildlife (067-13), the California Department of Fish and Wildlife (SC-0075 to J. Archie), and the Washington Department of Fish and Wildlife (Roger Anderson's permit) We thank D. M. Portik and D. Petkova for help with analyses, S. Des Roches for technical support, P. Zani and members of the Archie lab for assistance with field collections, and J. G. Schraiber and members of the Leaché and Buckley labs for useful comments and discussion. The manuscript benefitted greatly from comments by R. Huey and L. Buckley. This work was supported by grants from the National Science Foundation awarded to A.D.L. (DEB-1144630) and a Graduate Research Fellowship awarded to N.M.B.

References

Adolph, S. C., & Porter, W. P. (1993). Temperature, activity, and lizard life histories. The American Naturalist, 142, 273–295.

Akaike, H. (1973). Information theory and an extension of the maximum likelihood principle. In B. N. Petrov & F. Caski (Eds.), Proceedings of the Second International Symposium on Information Theory (pp. 267–281). Budapest: Akademiai Kiado.

Alexander, D. H., Novembre, J., & Lange, K. (2009). Fast model-based estimation of ancestry in unrelated individuals. Genome Research, 19, 1655–1664.

Avise, J. C. (2000). Phylogeography: the history and formation of species. Harvard University Press.

Bachelet, D., Ferschweiler, K., Sheehan, T., & Strittholt, J. (2016). Climate change effects on southern California deserts. Journal of Arid Environments, 127, 17–29.

Barrett, R. D., Laurent, S., Mallarino, R., Pfeifer, S. P., Xu, C. C. Y., Foll, M., Wakamatsu, K., Duke-Cohan, J. S., Jensen, J. D. & Hoekstra, H. E. (2019). Linking a mutation to survival in wild mice. Science, 363, 499–504.

Bell, E. L., & Price, A. H. (1996). *Sceloporus occidentalis*. Catalogue of American Amphibians and Reptiles (CAAR).

Bickford, D., Lohman, D. J., Sodhi, N. S., Ng, P. K., Meier, R., Winker, K., ... & Das, I. (2007). Cryptic species as a window on diversity and conservation. Trends in Ecology & Evolution, 22, 148–155.

Bouckaert, R., Heled, J., Kühnert, D., Vaughan, T., Wu, C. H., Xie, D., Suchard, M. A., Rambaut, A., & Drummond, A. J. (2014). BEAST 2: a software platform for Bayesian evolutionary analysis. PLoS Computational Biology, 10(4), e1003537.

Brown, G. P., Kelehear, C., & Shine, R. (2011). Effects of seasonal aridity on the ecology and behaviour of invasive cane toads in the Australian wet–dry tropics. Functional Ecology, 25, 1339–1347.

Bryant, D., Bouckaert, R., Felsenstein, J., Rosenberg, N. A., & Roy Choudhury, A. (2012). Inferring species trees directly from biallelic genetic markers: bypassing gene trees in a full coalescent analysis. Molecular Biology and Evolution, 29, 1917–1932.

Buckley, C. R., Irschick, D. J., & Adolph, S. C. (2009). The contributions of evolutionary divergence and phenotypic plasticity to geographic variation in the western fence lizard, *Sceloporus occidentalis*. Biological Journal of the Linnean Society, 99, 84–98.

Buckley, L. B., & Huey, R. B. (2016). How extreme temperatures impact organisms and the evolution of their thermal tolerance. Integrative and Comparative Biology, 56, 98–109.

Calsbeek, R., Thompson, J. N., & Richardson, J. E. (2003). Patterns of molecular evolution and diversification in a biodiversity hotspot: the California Floristic Province. Molecular Ecology, 12, 1021–1029.

Catchen, J. M., Amores, A., Hohenlohe, P., Cresko, W., & Postlethwait, J. H. (2011). Stacks: building and genotyping loci de novo from short-read sequences. G3: Genes, genomes, genetics, 1, 171–182.

Chevin, L. M., & Lande, R. (2011). Adaptation to marginal habitats by evolution of increased phenotypic plasticity. Journal of Evolutionary Biology, 24, 1462–1476.

Cook, B. I., Ault, T. R., & Smerdon, J. E. (2015). Unprecedented 21st century drought risk in the American Southwest and Central Plains. Science Advances, 1, e1400082.

Cooper Jr, W. E., & Burns, N. (1987). Social significance of ventrolateral coloration in the fence lizard, *Sceloporus undulatus*. Animal Behaviour, 35, 526–532.

Crispo, E. (2007). The Baldwin effect and genetic assimilation: revisiting two mechanisms of evolutionary change mediated by phenotypic plasticity. Evolution: International Journal of Organic Evolution, 61, 2469–2479.

D'Amen, M., Zimmermann, N. E., & Pearman, P. B. (2013). Conservation of phylogeographic lineages under climate change. Global Ecology and Biogeography, 22(1), 93-104.

Davis, P. T. (1988). Holocene glacier fluctuations in the American Cordillera. Quaternary Science Reviews, 7, 129–157.

Deutsch, C. A., Tewksbury, J. J., Huey, R. B., Sheldon, K. S., Ghalambor, C. K., Haak, D. C., & Martin, P. R. (2008). Impacts of climate warming on terrestrial ectotherms across latitude. Proceedings of the National Academy of Sciences, 105, 6668–6672.

DeWitt, T. J., & Scheiner, S. M. (Eds.). (2004). Phenotypic plasticity: functional and conceptual approaches. Oxford University Press.

Dubey, S., & Shine, R. (2012). Are reptile and amphibian species younger in the Northern Hemisphere than in the Southern Hemisphere? Journal of Evolutionary Biology, 25, 220–226.

Dunham, A. E. (1978). Food availability as a proximate factor influencing individual growth rates in the iguanid lizard *Sceloporus merriami*. Ecology, 59, 770–778.

Eaton, D. A. (2014). PyRAD: assembly of de novo RADseq loci for phylogenetic analyses. Bioinformatics, 30, 1844–1849.

Endler, J. A. (1977). Geographic variation, speciation, and clines (No. 10). Princeton University Press.

Falush, D., Stephens, M., & Pritchard, J. K. (2003). Inference of population structure using multilocus genotype data: linked loci and correlated allele frequencies. Genetics, 164, 1567–1587.

Feldman, C. R., & Spicer, G. S. (2006). Comparative phylogeography of woodland reptiles in California: repeated patterns of cladogenesis and population expansion. Molecular Ecology, 15, 2201–2222.

Felsenstein, J. (1976). The theoretical population genetics of variable selection and migration. Annual Review of Genetics, 10, 253–280.

Ghalambor, C. K., Huey, R. B., Martin, P. R., Tewksbury, J. J., & Wang, G. (2006). Are mountain passes higher in the tropics? Janzen's hypothesis revisited. Integrative and Comparative Biology, 46, 5–17.

Ghalambor, C. K., McKay, J. K., Carroll, S. P., & Reznick, D. N. (2007). Adaptive versus non-adaptive phenotypic plasticity and the potential for contemporary adaptation in new environments. Functional Ecology, 21, 394–407.

Gottscho, A. D. (2016). Zoogeography of the San Andreas Fault system: Great Pacific Fracture Zones correspond with spatially concordant phylogeographic boundaries in western North America. Biological Reviews, 91, 235–254.

Gutenkunst, R. N., Hernandez, R. D., Williamson, S. H., & Bustamante, C. D. (2009). Inferring the joint demographic history of multiple populations from multidimensional SNP frequency data. PLoS Genetics, 5, e1000695.

Guyton, B. (1998). Glaciers of California: Modern Glaciers, Ice Age Glaciers, the Origin of Yosemite Valley, and a Glacier Tour in the Sierra Nevada (Vol. 59). University of California Press.

Hewitt, G. (2000). The genetic legacy of the Quaternary ice ages. Nature, 405, 907–913.

Hewitt, G. M. (2004). Genetic consequences of climatic oscillations in the Quaternary. Philosophical Transactions of the Royal Society of London. Series B: Biological Sciences, 359, 183–195.

Hewitt, G. M. (2011). Quaternary phylogeography: the roots of hybrid zones. Genetica, 139, 617–638.

Hill, M. (2006). Geology of the Sierra Nevada: Revised Edition (Vol. 80). University of California Press.

Hoekstra, H. E., Drumm, K. E., & Nachman, M. W. (2004). Ecological genetics of adaptive color polymorphism in pocket mice: geographic variation in selected and neutral genes. Evolution, 58, 1329–1341.

Huey, R. B., & Stevenson, R. D. (1979). Integrating thermal physiology and ecology of ectotherms: a discussion of approaches. American Zoologist, 19, 357–366.

Huey, R. B., Hertz, P. E., & Sinervo, B. (2003). Behavioral drive versus behavioral inertia in evolution: a null model approach. The American Naturalist, 161, 357–366.

Huey, R. B., Kearney, M. R., Krockenberger, A., Holtum, J. A., Jess, M., & Williams, S. E. (2012). Predicting organismal vulnerability to climate warming: roles of behaviour, physiology and adaptation. Philosophical Transactions of the Royal Society B: Biological Sciences, 367, 1665–1679.

IPCC (2007). Climate Change 2007: Synthesis Report. Intergovernmental Panel on Climate Change, Geneva.

Jameson Jr, E. W., & Allison, A. (1976). Fat and breeding cycles in two montane populations of *Sceloporus occidentalis* (Reptilia, Lacertilia, Iguanidae). Journal of Herpetology, 10, 211-220.

Jansson, R., & Dynesius, M. (2002). The fate of clades in a world of recurrent climatic change: Milankovitch oscillations and evolution. Annual Review of Ecology and Systematics, 33, 741–777.

Janzen, F. J., Krenz, J. G., Haselkorn, T. S., Brodie Jr, E. D., & Brodie III, E. D. (2002). Molecular phylogeography of common garter snakes (*Thamnophis sirtalis*) in western North America: implications for regional historical forces. Molecular Ecology, 11, 1739–1751.

Jarvis, A., Reuter, H.I., Nelson, A., Guevara, E. (2008). Hole-filled seamless SRTM data V4, International Centre for Tropical Agriculture (CIAT), available from http://srtm.csi.cgiar.org.

Jombart T. (2008) adegenet: a R package for the multivariate analysis of genetic markers Bioinformatics 24: 1403-1405. doi: 10.1093/bioinformatics/btn129

Jouganous, J., Long, W., Ragsdale, A. P., & Gravel, S. (2017). Inferring the joint demographic history of multiple populations: beyond the diffusion approximation. Genetics, 206 1549–1567.

Kawecki, T. J., & Ebert, D. (2004). Conceptual issues in local adaptation. Ecology Letters, 7, 1225–1241.

Kearney, M., Shine, R., & Porter, W. P. (2009). The potential for behavioral thermoregulation to buffer “cold-blooded” animals against climate warming. Proceedings of the National Academy of Sciences, 106, 3835–3840.

Kirkpatrick, M., & Barton, N. H. (1997). Evolution of a species' range. The American Naturalist, 150, 1–23.

Kuchta, S. R., Parks, D. S., Mueller, R. L., & Wake, D. B. (2009). Closing the ring: historical biogeography of the salamander ring species Ensatina eschscholtzii. Journal of Biogeography, 36, 982–995.

Lande, R. (1980). Genetic variation and phenotypic evolution during allopatric speciation. The American Naturalist, 116(4), 463-479.

Lapointe, F. J., & Rissler, L. J. (2005). Congruence, consensus, and the comparative phylogeography of codistributed species in California. The American Naturalist, 166, 290–299.

Lavin, B. R., Wogan, G. O., McGuire, J. A., & Feldman, C. R. (2018). Phylogeography of the Northern Alligator Lizard (Squamata, Anguidae): Hidden diversity in a western endemic. Zoologica Scripta, 47, 462–476.

Leaché, A. D. (2009). Species tree discordance traces to phylogeographic clade boundaries in North American fence lizards (*Sceloporus*). Systematic Biology, 58, 547–559.

Leaché, A. D., & Reeder, T. W. (2002). Molecular systematics of the eastern fence lizard (*Sceloporus undulatus*): a comparison of parsimony, likelihood, and Bayesian approaches. Systematic Biology, 51, 44–68.

Leaché, A. D., Helmer, D. S., & Moritz, C. (2010). Phenotypic evolution in high-elevation populations of western fence lizards (*Sceloporus occidentalis*) in the Sierra Nevada Mountains. Biological Journal of the Linnean Society, 100, 630–641.

Lenormand, T. (2002). Gene flow and the limits to natural selection. Trends in Ecology & Evolution, 17(4), 183-189.

Liu, H. P., Hershler, R., & Clift, K. (2003). Mitochondrial DNA sequences reveal extensive cryptic diversity within a western American springsnail. Molecular Ecology, 12, 2771–2782.

Lynch, M. (2010). Rate, molecular spectrum, and consequences of human mutation. Proceedings of the National Academy of Sciences USA, 107, 961–968.

MacManes, M. MacManes salt extraction protocol, 2013 Figshare. Available from: https://doi.org/10.6084/m9.figshare.658946

Manthey, J. D., Klicka, J., & Spellman, G. M. (2011). Cryptic diversity in a widespread North American songbird: phylogeography of the Brown Creeper (*Certhia americana*). Molecular Phylogenetics and Evolution, 58, 502–512.

Massot, M., Huey, R. B., Tsuji, J., & van Berkum, F. H. (2003). Genetic, prenatal, and postnatal correlates of dispersal in hatchling fence lizards (*Sceloporus occidentalis*). Behavioral Ecology, 14, 650–655.

Matocq, M. D., Patton, J. L., & Da Silva, M. N. F. (2000). Population genetic structure of two ecologically distinct Amazonian spiny rats: separating history and current ecology. Evolution, 54, 1423–1432.

McTernan, Matthew R., "How do lizards use behavior and physiology to inhabit different climate zones?" (2017). WWU Graduate School Collection. 604. https://cedar.wwu.edu/wwuet/604

Merilä, J., & Hendry, A. P. (2014). Climate change, adaptation, and phenotypic plasticity: the problem and the evidence. Evolutionary Applications, 7, 1–14.

Moore, J. G., & Moring, B. C. (2013). Rangewide glaciation in the Sierra Nevada, California. Geosphere, 9, 1804–1818.

Moran, E. V., Hartig, F., & Bell, D. M. (2016). Intraspecific trait variation across scales: implications for understanding global change responses. Global Change Biology, 22, 137–150.

Moritz, C., Schneider, C. J., & Wake, D. B. (1992). Evolutionary relationships within the *Ensatina eschscholtzii* complex confirm the ring species interpretation. Systematic biology, 41, 273–291.

Myers, N., Mittermeier, R. A., Mittermeier, C. G., Da Fonseca, G. A., & Kent, J. (2000). Biodiversity hotspots for conservation priorities. Nature, 403, 853–858.

Negus, N. C., Berger, P. J., & Pinter, A. J. (1992). Phenotypic plasticity of the montane vole (*Microtus montanus*) in unpredictable environments. Canadian Journal of Zoology, 70, 2121–2124.

Nei, M., & Takahata, N. (1993). Effective population size, genetic diversity, and coalescence time in subdivided populations. Journal of Molecular Evolution, 37, 240–244.

Newcomb, R. C. (1967). The Dalles-Umatilla syncline, Oregon and Washington. US Geological Survey Professional Paper, B88-B93.

O'Connell, K. A., Streicher, J. W., Smith, E. N., & Fujita, M. K. (2017). Geographical features are the predominant driver of molecular diversification in widely distributed North American whipsnakes. Molecular ecology, 26, 5729–5751.

Orange, D. I., Riddle, B. R., & Nickle, D. C. (1999). Phylogeography of a wide-ranging desert lizard, *Gambelia wislizenii* (Crotaphytidae). Copeia, 1999, 267-273.

Owen, L. A., Finkel, R. C., Minnich, R. A., & Perez, A. E. (2003). Extreme southwestern margin of late Quaternary glaciation in North America: timing and controls. Geology, 31, 729–732.

Pereira, R. J., & Wake, D. B. (2009). Genetic leakage after adaptive and nonadaptive divergence in the *Ensatina eschscholtzii* ring species. Evolution: International Journal of Organic Evolution, 63, 2288–2301.

Peterson, B. K., Weber, J. N., Kay, E. H., Fisher, H. S., & Hoekstra, H. E. (2012). Double digest RADseq: an inexpensive method for de novo SNP discovery and genotyping in model and non-model species. PLoS One, 7, e37135.

Petkova, D., Novembre, J., & Stephens, M. (2016). Visualizing spatial population structure with estimated effective migration surfaces. Nature Genetics, 48, 94–100.

Pigliucci, M. (2001). Phenotypic plasticity: beyond nature and nurture. JHU Press.

Porter, S. C. (1976). Pleistocene glaciation in the southern part of the North Cascade Range, Washington. Geological Society of America Bulletin, 87, 61–75.

Portik, D. M., Leaché, A. D., Rivera, D., Barej, M. F., Burger, M., Hirschfeld, M., Rödel, M., Blackburn, D. C., & Fujita, M. K. (2017). Evaluating mechanisms of diversification in a Guineo-Congolian tropical forest frog using demographic model selection. Molecular Ecology, 26, 5245–5263.

Potter, K. M., Hipkins, V. D., Mahalovich, M. F., & Means, R. E. (2015). Nuclear genetic variation across the range of ponderosa pine (*Pinus ponderosa*): Phylogeographic, taxonomic and conservation implications. Tree Genetics & Genomes, 11:38.

Pritchard, J. K., Stephens, M., & Donnelly, P. (2000). Inference of population structure using multilocus genotype data. Genetics, 155, 945–959.

QGIS Development Team (2018). QGIS Geographic Information System. Open Source Geospatial Foundation Project. http://qgis.osgeo.org.

Reilly, S. B., & Wake, D. B. (2015). Cryptic diversity and biogeographical patterns within the black salamander (*Aneides flavipunctatus*) complex. Journal of Biogeography, 42, 280–291.

Rosenbaum, J. G., & Reynolds, R. L. (2004). Record of Late Pleistocene glaciation and deglaciation in the southern Cascade Range. II. Flux of glacial flour in a sediment core from Upper Klamath Lake, Oregon. Journal of Paleolimnology, 31, 235–252.

Samietz, J., Salser, M. A., & Dingle, H. (2005). Altitudinal variation in behavioural thermoregulation: local adaptation vs. plasticity in California grasshoppers. Journal of Evolutionary Biology, 18, 1087–1096.

Satler, J. D., Carstens, B. C., & Hedin, M. (2013). Multilocus species delimitation in a complex of morphologically conserved trapdoor spiders (Mygalomorphae, Antrodiaetidae, *Aliatypus*). Systematic Biology, 62, 805–823.

Sawyer, J. O. (2007). Why are the Klamath Mountains and adjacent North Coast floristically diverse. Fremontia, 35, 3–11.

Serra-Varela, M. J., Alía, R., Daniels, R. R., Zimmermann, N. E., Gonzalo-Jiménez, J., & Grivet, D. (2017). Assessing vulnerability of two Mediterranean conifers to support genetic conservation management in the face of climate change. Diversity and Distributions, 23, 507–516.

Sharp, R. P. (1960). Pleistocene glaciation in the Trinity Alps of northern California. American Journal of Science, 258, 305–340.

Sheffield, J., & Wood, E. F. (2008). Projected changes in drought occurrence under future global warming from multi-model, multi-scenario, IPCC AR4 simulations. Climate Dynamics, 31, 79–105.

Shine, R. (2012). Invasive species as drivers of evolutionary change: cane toads in tropical Australia. Evolutionary Applications, 5, 107–116.

Sinervo, B. (1990). Evolution of thermal physiology and growth rate between populations of the western fence lizard (*Sceloporus occidentalis*). Oecologia, 83, 228–237.

Sinervo, B., & Adolph, S. C. (1994). Growth plasticity and thermal opportunity in *Sceloporus* lizards. Ecology, 75, 776–790.

Sinervo, B., & Huey, R. B. (1990). Allometric engineering: an experimental test of the causes of interpopulational differences in performance. Science, 248, 1106–1109.

Sinervo, B., Mendez-De-La-Cruz, F., Miles, D. B., Heulin, B., Bastiaans, E., Villagrán-Santa Cruz, M., Lara-Resendiz, R., Martínez-Méndez, N., Calderón-Espinosa, M. L., Meza-Lázaro, R. N., Gadsden, H., Avila, L. J., Morando, M., De la Riva, I. J., Sepulveda, P. V., Duarte Rocha, C. F., Ibargüengoytía, N., Puntriano, C. A., Massot, M., Lepetz, V., Oksanen, T. A., Chapple, D. G., Bauer, A. M., Branch, W. R., Clobert, J., Sites, J. W. (2010). Erosion of lizard diversity by climate change and altered thermal niches. Science, 328, 894–899.

Smith, H. M., Bell, E. L., Applegarth, J. S., & Chiszar, D. (1992). Adaptive convergence in the lizard superspecies *Sceloporus undulatus*. Bulletin of the Maryland Herpetological Society, 28, 123-149.

Staub, N. L., Brown, C. W., & Wake, D. B. (1995). Patterns of growth and movements in a population of *Ensatina eschscholtzii platensis* (Caudata: Plethodontidae) in the Sierra Nevada, California. Journal of Herpetology, 1995, 593-599.

Swenson, N. G., & Howard, D. J. (2005). Clustering of contact zones, hybrid zones, and phylogeographic breaks in North America. The American Naturalist, 166, 581–591.

Tinkle, D. W., & Ballinger, R. E. (1972). *Sceloporus undulatus*: a study of the intraspecific comparative demography of a lizard. Ecology, 53, 570–584.

Tsuji, J. S. (1988). Seasonal profiles of standard metabolic rate of lizards (*Sceloporus occidentalis*) in relation to latitude. Physiological Zoology, 61, 230–240.

Urban, M. C., Bocedi, G., Hendry, A. P., Mihoub, J. B., Pe'er, G., Singer, A., ... & Gonzalez, A. (2016). Improving the forecast for biodiversity under climate change. Science, 353, aad8466.

Wagenmakers, E. J., & Farrell, S. (2004). AIC model selection using Akaike weights. Psychonomic Bulletin & Review, 11, 192–196.

van Berkum, F. H. (1988). Latitudinal patterns of the thermal sensitivity of sprint speed in lizards. The American Naturalist,132, 327–343.

Waltari, E., Hijmans, R. J., Peterson, A. T., Nyári, Á. S., Perkins, S. L., & Guralnick, R. P. (2007). Locating Pleistocene refugia: comparing phylogeographic and

ecological niche model predictions. PLoS One, 2(7), e563.
Waples, R. S. (2014). Testing for Hardy–Weinberg proportions: have we lost the plot? Journal of Heredity, 106, 1–19.
Williams, A. P., Seager, R., Abatzoglou, J. T., Cook, B. I., Smerdon, J. E., & Cook, E. R. (2015). Contribution of anthropogenic warming to California drought during 2012–2014. Geophysical Research Letters, 42, 6819–6828.
Williams, C. M., Ragland, G. J., Betini, G., Buckley, L. B., Cheviron, Z. A., Donohue, K., ... & Schmidt, P. S. (2017). Understanding evolutionary impacts of seasonality: an introduction to the symposium. Integrative and Comparative Biology, 57, 921–933.
Wilson, J. S., & Pitts, J. P. (2010). Phylogeographic analysis of the nocturnal velvet ant genus *Dilophotopsis* (Hymenoptera: Mutillidae) provides insights into diversification in the Nearctic deserts. Biological Journal of the Linnean Society, 101, 360–375.
Wilson, J. S., & Pitts, J. P. (2012). Identifying Pleistocene refugia in North American cold deserts using phylogeographic analyses and ecological niche modelling. Diversity and Distributions, 18, 1139–1152.
Zamudio, K. R., Bell, R. C., & Mason, N. A. (2016). Phenotypes in phylogeography: Species' traits, environmental variation, and vertebrate diversification. Proceedings of the National Academy of Sciences, 113, 8041–8048.

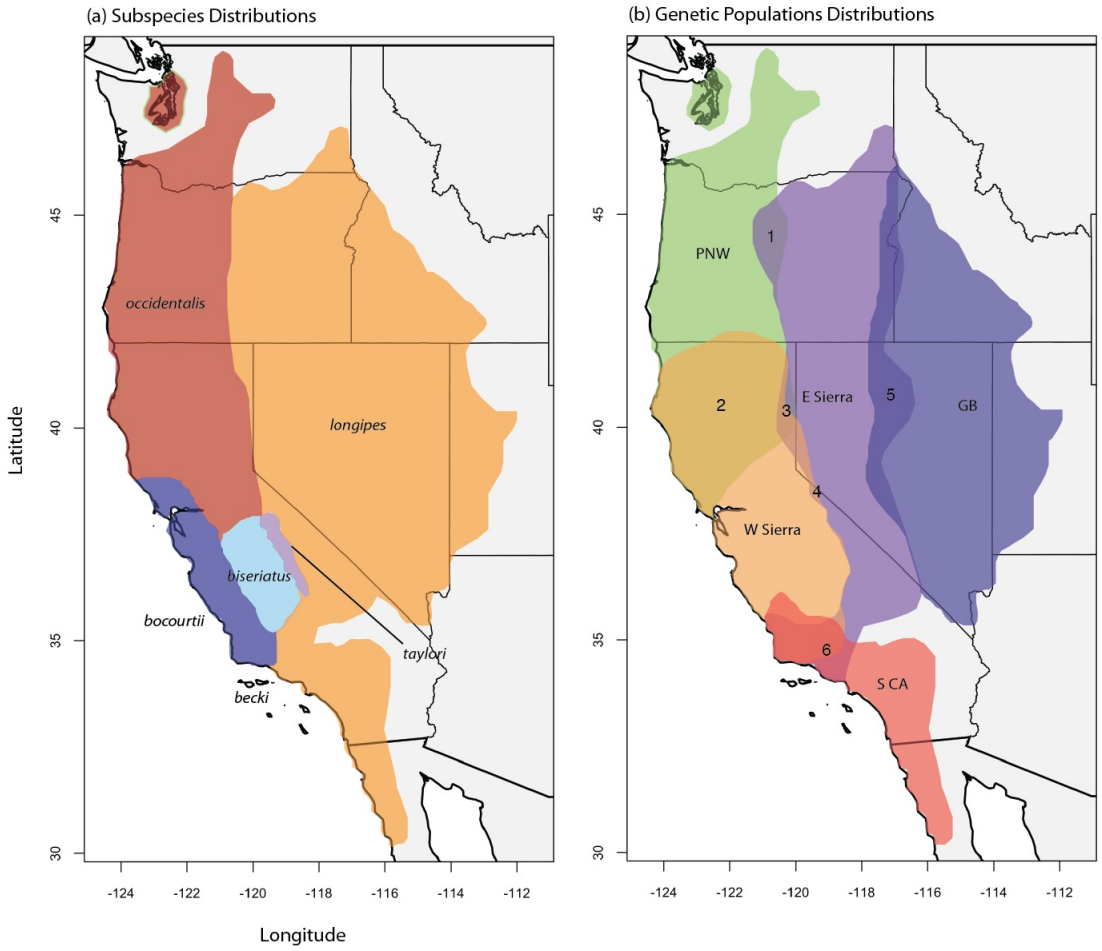

Figure 1. Comparison of phenotypic (subspecies) and genetic patterns of geographic variation within *Sceloporus occidentalis.* (a) Distribution of traditionally recognized subspecies diagnosed by morphology and geography, based on Bell & Price (1996). (b) Genetic-based population boundaries estimated using SNP data in ADMIXTURE, assuming a model with $K = 5$ populations. Six distinct areas of overlap in (b) represent zones of admixture between genetically distinct populations, inferred by the presence of admixed individuals

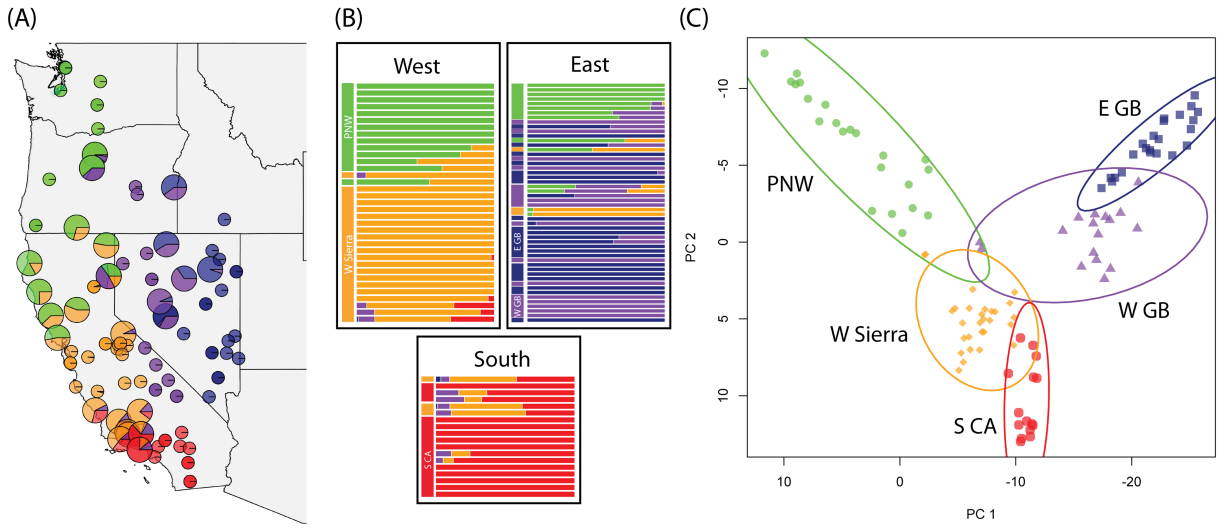

Figure 2. Population structure results for *S. occidentalis*. (a) Spatial distribution of ADMIXTURE results. Enlarged pies represent individuals with admixture >5%. (b) Barplots showing population membership results from ADMIXTURE, separated north-south by the Transverse Ranges (South) and east-west by the Sierra Nevada-Cascade mountain change (East and West). Individuals are ordered vertically by latitude, and population membership is color-coded and indicated with vertical bars. (c) PCA plot based on allele frequencies from 4,555 SNPs. Elliptical contours represent 95% confidence levels for genetically distinct groups. Individuals are colored by population membership. The five populations are Southern California (S CA, red); West Sierra (W Sierra, orange); West Great Basin (W GB, purple); East Great Basin (E GB, navy); Pacific Northwest (PNW, green).

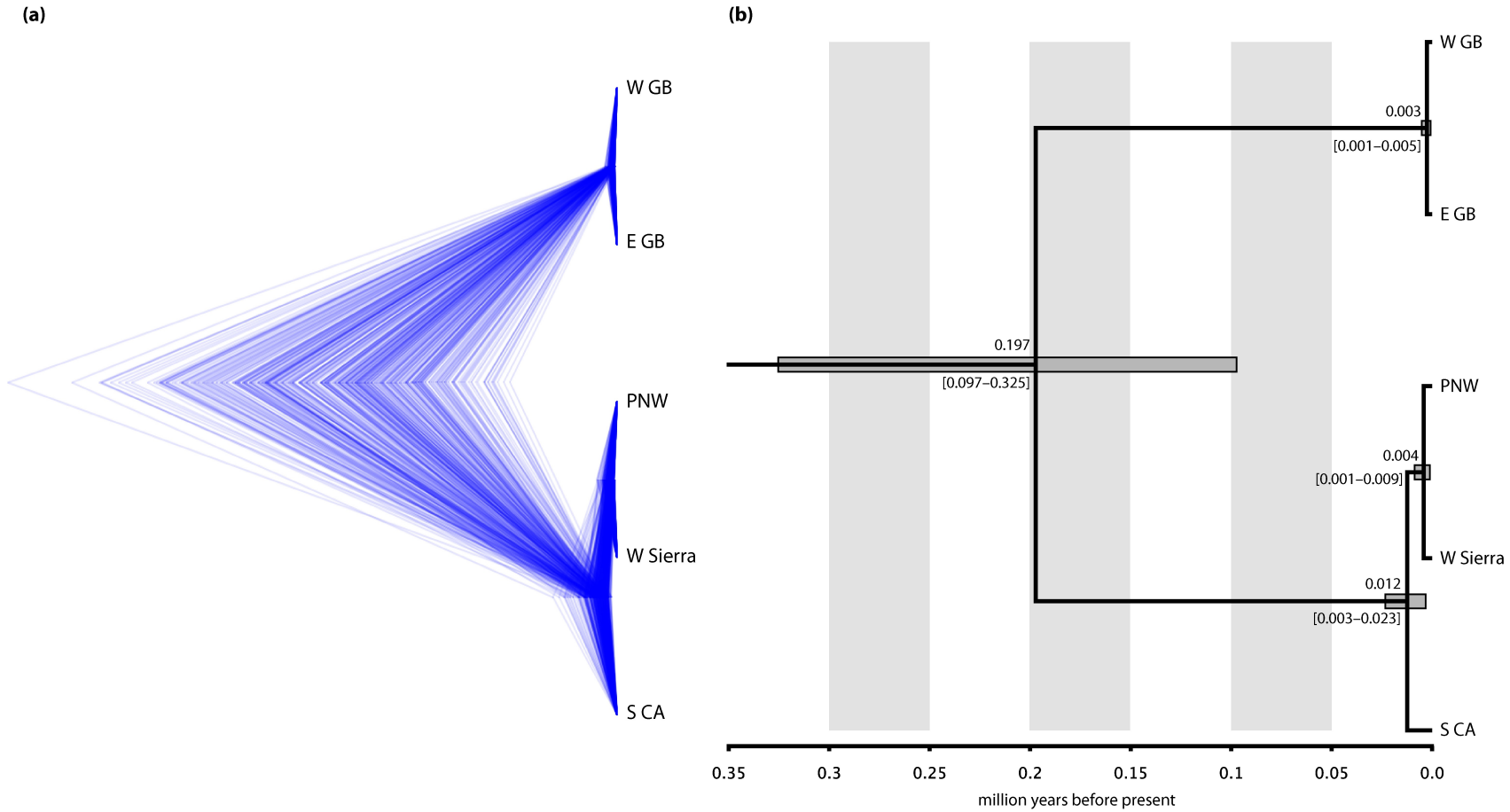

Figure 3. Species tree for *S. occidentalis* populations estimated using SNAPP. (a) Densitree plot illustrating uncertainty in the species tree topology and branch lengths. Densely colored regions near the tips of the tree show agreement in tree topologies and branch lengths, while the diffuse distribution near the root shows uncertainty in the divergence time estimate. (b) MCC tree calculated from the posterior distribution of topologies shown in (a). Numbers on branches are point estimates for divergence times (mean) and the HPD range (in brackets).

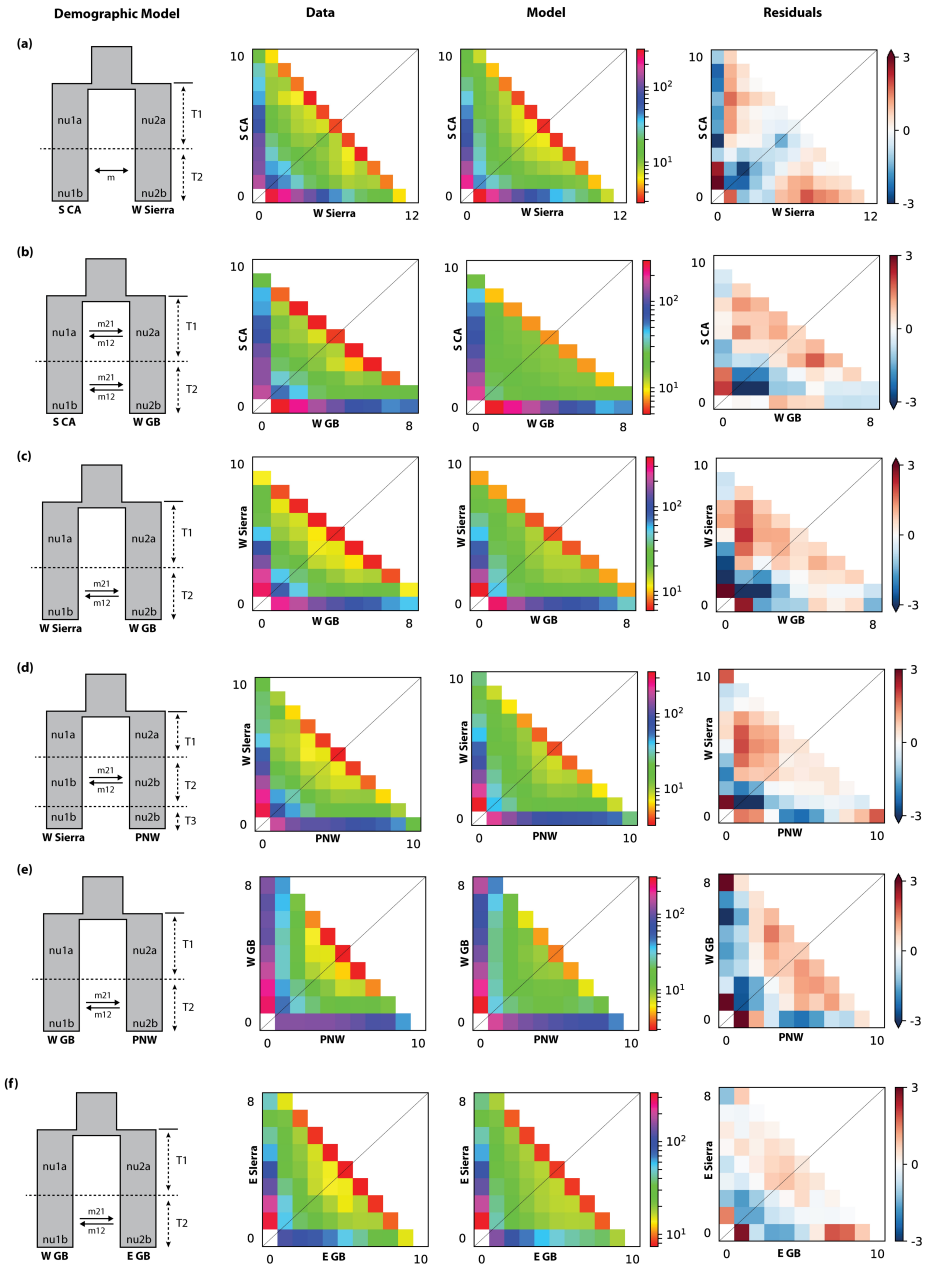

Figure 4. 2D demographic model results for six population pairs (a-f) in *S. occidentalis*. The best-fit demographic model for each population pair is represented with all relevant population parameters. The vertical axis is the frequency of the allele in the first population and the horizontal axis is the frequency of the allele in the second population. The color in each cell represents the counts of alleles at certain frequencies in the two populations. The residuals measure the differences in model fit, where lower residuals indicate better fit. The demographic model parameter estimates are provided in Table 1.

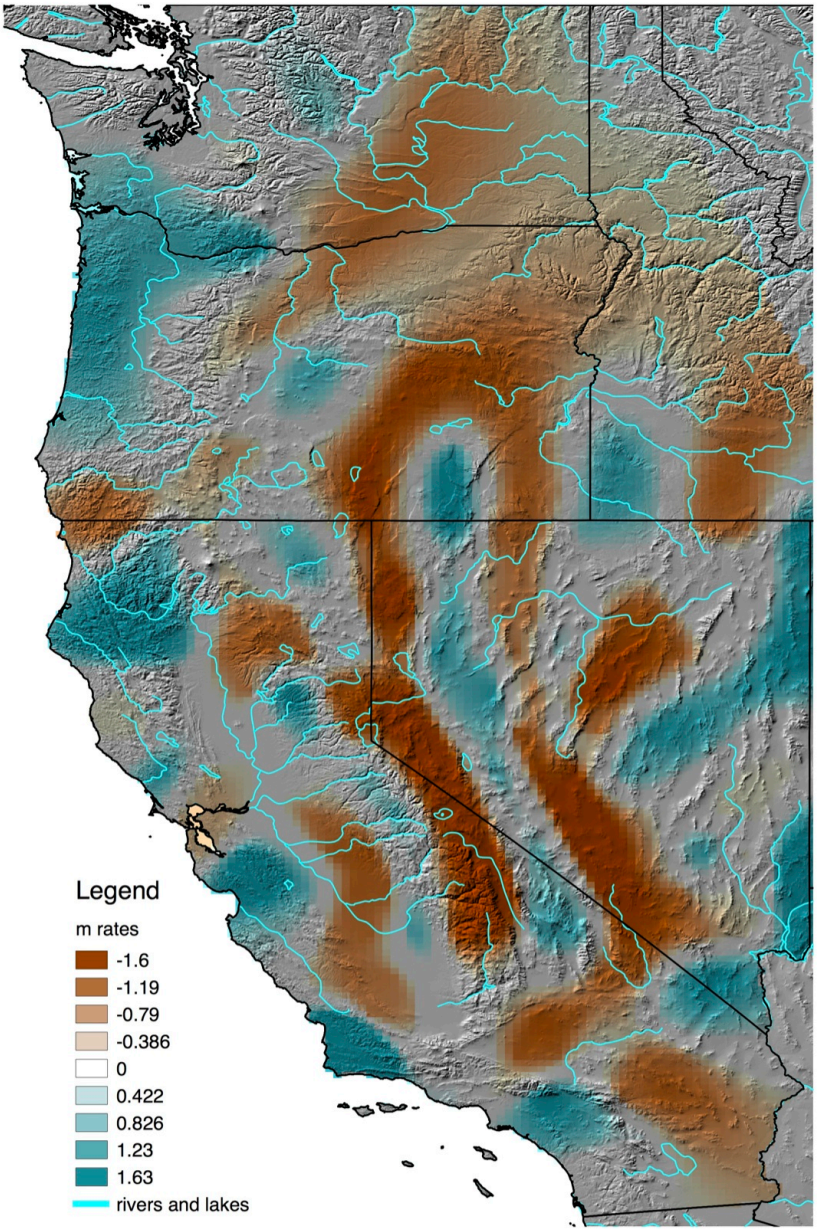

Figure 5. Effective migration surface from EEMS overlaid with a digital elevation model (DEM) at 1 km resolution. Barriers to migration with effective migration rates lower than expected under IBD are shown in rust. Corridors of migration with effective migration rates higher than expected under IBD are shown in turquoise. Major rivers and lakes are shown in light blue.

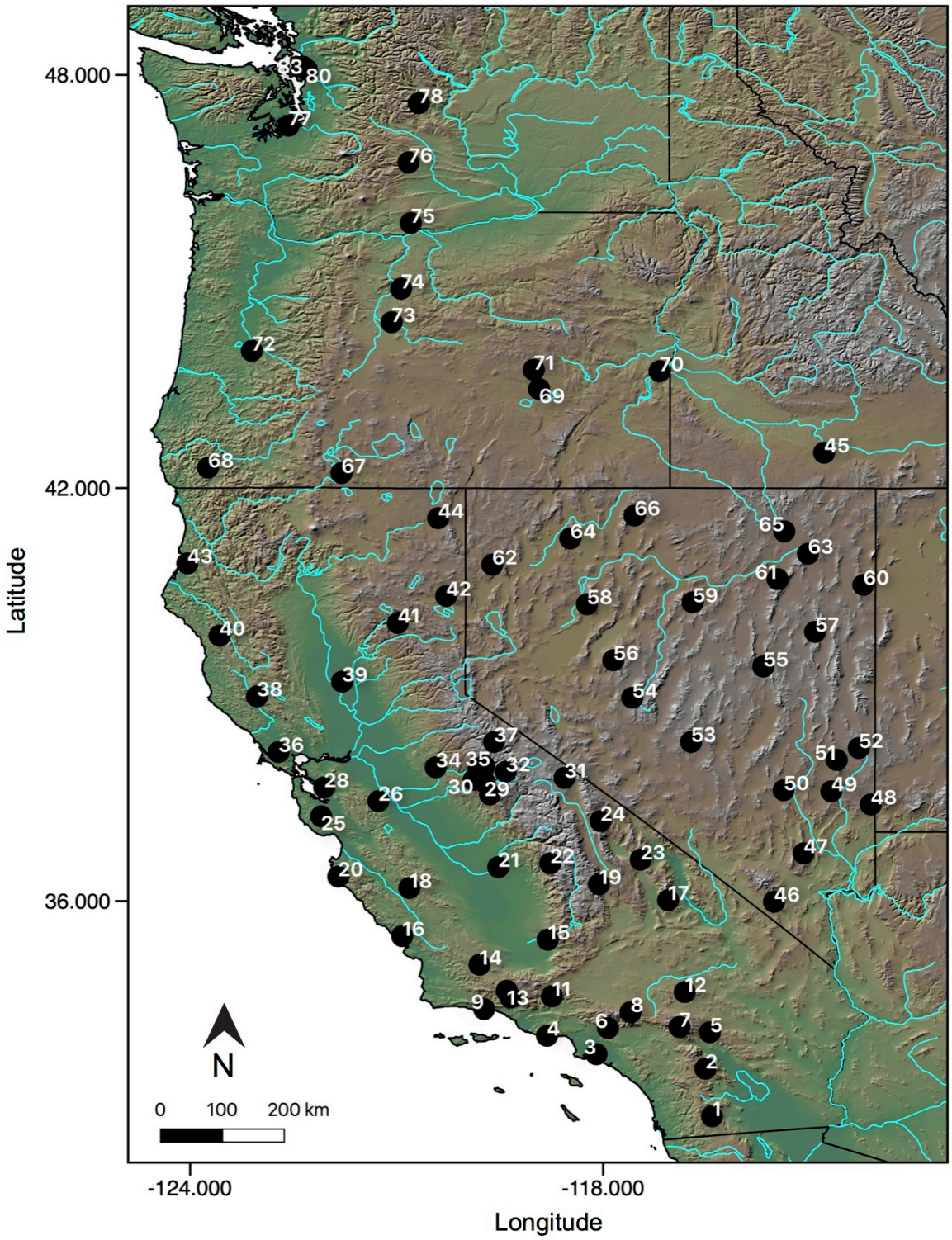

Figure S1. Sampling localities of *Sceloporus occidentalis*. Detailed locality data for numbered sampling localities are provided in **Table S1**.

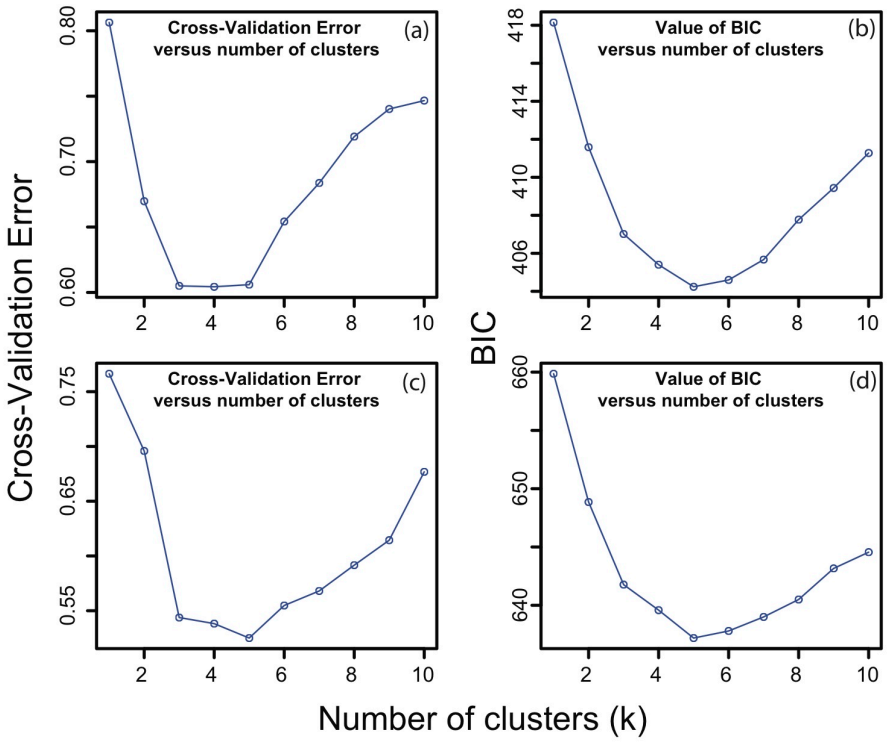

Figure S2. Cross-validation error from parametric (ADMIXTURE; a, c) and change in BIC from non-parametric (DAPC/k-means clustering; b, d) methods of population structure estimation. The top row (a, b) shows results from both methods for a dataset composed of 65 samples, allowing ≤50% missing data per sample. The bottom row (c, d) shows results from both methods for a dataset composed of 105 samples, allowing ≤70% missing data per sample.

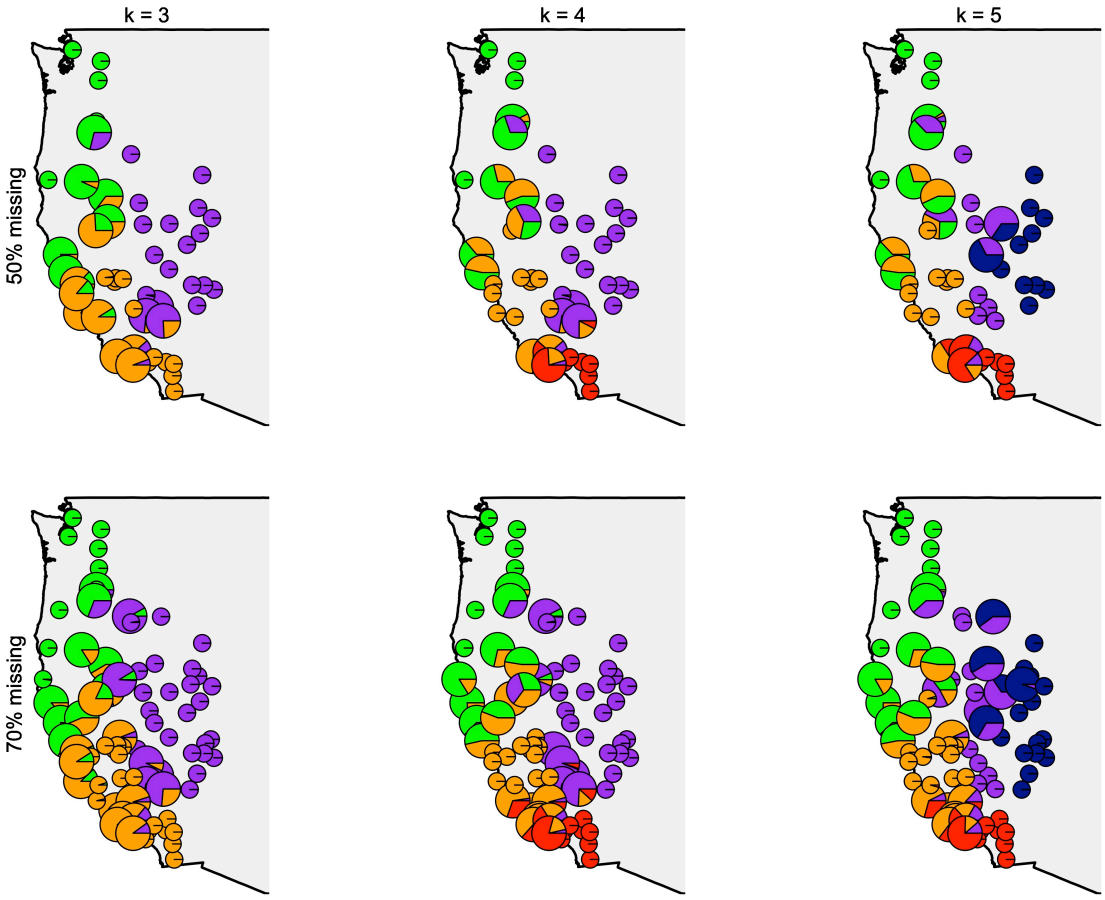

Figure S3. Estimates of population structure for k=3,4,5 for the 50% and 70% missing data per individual datasets using Admixture**.** Small pies are individuals with <5% admixed identity and larger pies are individuals with >5% admixed identity. Color corresponds to population identity as follows: S California (red); W Sierra Nevada (orange); W GB (purple); Great Basin (navy); Pacific Northwest (green).

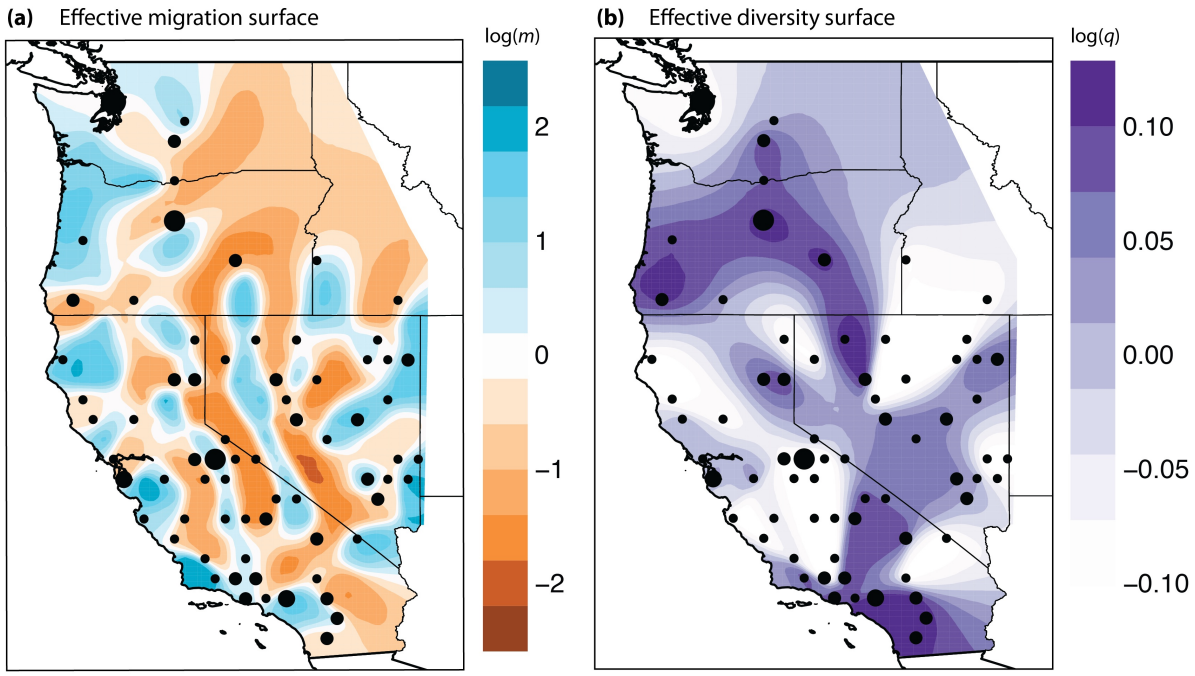

Figure S4. Effective migration and diversity estimates from EEMS. (a) Warmers colors represent effective migration rates lower than expected under isolation by distance, or "barriers" to migration. Cooler colors represent effective migration rates higher than expected under isolation by distance, or "corridors" of migration. (b) Effective diversity estimates calculated based on pairwise within and between deme dissimilarity. Regions with higher genetic diversity are darker in color.

Table 1. Pairwise comparisons of contiguous populations of *S. occidentalis*. Log-likelihoods (LL) and AIC weights (wAIC) used to evaluate best-fit models for each comparison. Theta is the estimated mutation rate, proportional to the effective ancestral population size N_e^{anc} ($\theta=4N_e^{anc}\mu$). nu1a, nu2a and nu1b, nu2b are effective population sizes of populations 1 and 2 before and after instantaneous size change. Populations 1 and 2 are the first and second populations listed in each comparison, respectively.

Comparison	Model	LL	wAIC	Theta	nu1a	nu2a	nu1b	nu2b	m12	m21	T1	T2	T3
S CA vs. W Sierra	Divergence in isolation, continuous symmetric secondary contact with size change	-232.3	1.00	324.9	7.332	2.945	0.235	0.411	1.553		1.631	0.274	
S CA vs. W GB	Divergence with continuous asymmetric migration, size change	-174.0	0.96	336.5	3.285	3.383	0.144	0.176	0.697	1.251	5.184	0.144	
W Sierra vs. W GB	Divergence in isolation, continuous asymmetric secondary contact with size change	-191.4	1.00	176.9	4.964	2.433	1.821	0.938	0.087	0.908	5.783	1.269	
W Sierra vs. PNW	Divergence in isolation, continuous asymmetric secondary contact with size change, isolation	-207.1	1.00	216.8	3.832	1.343	0.531	0.306	1.031	7.771	4.213	0.097	0.040
E Sierra vs. PNW	Divergence in isolation, continuous asymmetric secondary contact with size change	-198.2	0.99	444.1	1.919	2.327	0.288	0.137	0.885	1.963	2.088	0.233	
E Sierra vs. E GB	Divergence in isolation, continuous asymmetric secondary contact with size change	-157.1	0.51	812.1	0.657	0.193	0.207	0.083	0.794	5.662	0.121	0.095	

Table S1. Detailed locality data for samples used in this study.

Ref. #	Abbreviation	N	Locality	County	State	Latitude	Longitude	Elev. (m)
1	MLG	2	Mount Laguna	San Diego	CA	32.87200	-116.4182	5972
2	SRM	2	Santa Rosa Mountains	Riverside	CA	33.56240	-116.5143	4825
3	LBH	1	Long Beach	Los Angeles	CA	33.77350	-118.0962	20
4	ZUM	2	Zuma Canyon	Ventura	CA	34.04187	-118.8144	160
5	YUC	1	Yucca Valley	San Bernardino	CA	34.09290	-116.4493	3800
6	FCT	1	Fish Canyon Trail	Los Angeles	CA	34.15460	-117.9283	816
7	BAR	1	Barton Creek	San Bernardino	CA	34.16940	-116.8923	6336
8	WTW	2	Wrightwood	Los Angeles	CA	34.38460	-117.6020	3517
9	SBR	1	Santa Barbara	Santa Barbara	CA	34.42950	-119.7282	193
10	REY	1	Reyes Creek	Ventura	CA	34.59700	-119.3420	4093
11	PRU	2	Piru Creek, Pyramid Lake	Los Angeles	CA	34.61640	-118.7434	2246
12	ORD	1	Ord Mountain	San Bernardino	CA	34.67680	-116.8147	6214
13	NUV	1	Rancho Nuevo Campground	Ventura	CA	34.69500	-119.3985	3535
14	CAR	1	Caliente Ridge, Chimineas Rnch	San Luis Obispo	CA	35.07230	-119.7972	4062
15	KRV	1	Kern River Valley	Kern	CA	35.43700	-118.8040	721
16	CYR	1	Cayucos Creek Road	San Luis Obispo	CA	35.48940	-120.9191	187
17	RPS	2	Rogers Pass	Inyo	CA	36.01110	-117.0572	7368
18	PT	1	Peach Tree Lane	Monterrey	CA	36.18780	-120.8150	1853
19	OLA	2	Olancha	Inyo	CA	36.24290	-118.0596	5215
20	BOT	1	Bottcher Gap	Monterrey	CA	36.35440	-121.8467	2495
21	KBG	1	Kingsburg	Tulare	CA	36.49190	-119.5209	275
22	MRO	1	Moro Rock, Sequoia NF	Tulare	CA	36.54644	-118.7660	6404
23	HNT	1	Hunter Mountain	Inyo	CA	36.60010	-117.4551	5014
24	LCV	1	Little Cowhorn Valley	Inyo	CA	37.16090	-118.0390	7292
25	SKY	2	Skyline Drive	San Mateo	CA	37.23040	-122.0953	2993
26	MNR	1	Minnear Campground	Stanislaus	CA	37.45100	-121.2650	560
27	WAW	1	Wawona	Mariposa	CA	37.54785	-119.6416	4165
28	HAY	1	Hayward	Alameda	CA	37.64870	-122.0512	500
29	BOF	1	Big Oak Flat Road	Mariposa	CA	37.72386	-119.7194	4511
30	CTR	1	South Crocker Ridge	Tuolumne	CA	37.75870	-119.8810	5172
31	BNT	1	Benton Crossing Road	Mono	CA	37.78830	-118.5614	6609
32	POT	1	Pothole Dome	Tuolumne	CA	37.87863	-119.4123	8403
33	HHR	1	Hetch Hetchy Road	Tuolumne	CA	37.90945	-119.8097	4674
34	WDC	2	Woods Creek	Tuolumne	CA	37.94090	-120.4329	1367
35	TTC	2	TilTill Creek	Tuolumne	CA	37.95932	-119.7276	4139
36	WHR	1	Wilson Hill Road	Marin	CA	38.16290	-122.7133	488
37	LFV	1	Leavitt Falls Vista area	Mono	CA	38.30930	-119.5833	8165
38	HOP	1	Hopland	Lake	CA	38.97190	-123.0269	973
39	SUT	1	Sutter Buttes	Sutter	CA	39.18550	-121.7913	209
40	BEL	1	Bell Springs Road (Low)	Mendocino	CA	39.85430	-123.5730	2898
41	INK	2	Indian Creek	Plumas	CA	40.03800	-120.9830	2981
42	LTF	2	Litchfield (aka Honey Lake)	Lassen	CA	40.43010	-120.2805	4525
43	BLL	1	Blue Lake	Humboldt	CA	40.90450	-124.0408	152
44	ALT	1	East of Alturas	Modoc	CA	41.56120	-120.3972	4960

Continued on next page

Table S1 – continued from previous page

Ref. #	Abbreviation	N	Locality	County	State	Latitude	Longitude	Elev. (m)
45	SLF	1	Salmon Falls Road	Twin Falls	ID	42.51250	-114.7908	5183
46	MPS	1	Mountain Pass	Clark	NV	35.98700	-115.5170	5989
47	MWR	2	Mormon Well Road	Clark	NV	36.69140	-115.0881	5320
48	BNK	1	Bunker Pass Road	Lincoln	NV	37.40090	-114.1127	5634
49	DEL	1	Delamar Mountains	Lincoln	NV	37.59270	-114.6856	6248
50	MTI	2	Mount Irish	Lincoln	NV	37.60830	-115.3776	5727
51	CNP	1	Connors Pass	White Pine	NV	38.04850	-114.6068	7212
52	BHR	1	Buckhorn Range Road	Lincoln	NV	38.22190	-114.2881	7023
53	GEO	1	Georges Canyon	Nye	NV	38.31050	-116.7229	6662
54	ION	2	Ione	Nye	NV	38.95200	-117.5770	6258
55	PAN	2	Pancake Range	White Pine	NV	39.40500	-115.6730	6487
56	CAM	1	Clan Alpine Mountains	Churchill	NV	39.49680	-117.8515	6153
57	CCS	1	Cherry Creek Summit Road	White Pine	NV	39.90900	-114.9220	9707
58	ORA	2	East Oreana, Limerick Canyon	Pershing	NV	40.31000	-118.2342	4915
59	INC	1	Indian Creek Road	Lander	NV	40.33690	-116.6993	5316
60	TOA	2	Toano Range	Elko	NV	40.59100	-114.2213	5543
61	LML	1	Lamoille Canyon	Elko	NV	40.67470	-115.4655	6747
62	LJC	1	Lone Juniper Canyon	Washoe	NV	40.88620	-119.6094	5788
63	ANG	1	Angel Creek	Elko	NV	41.04440	-115.0246	6789
64	JKM	1	Jackson Mountain, Trout Creek	Humboldt	NV	41.26620	-118.4764	5730
65	HYR	1	Haystack Ranch Road	Elko	NV	41.36880	-115.3688	5929
66	IND	1	Indian Creek, Santa Rosas	Humboldt	NV	41.60010	-117.5440	5364
67	KLF	1	Klamath Falls	Klamath	OR	42.21550	-121.8005	4385
68	SLM	2	Selma	Josephine	OR	42.29530	-123.7410	1180
69	WRT	1	Wright Point	Harney	OR	43.43700	-118.9290	4103
70	SNV	1	Snively Gulch Road	Malheur	OR	43.69493	-117.1810	2631
71	DEV	1	Devine Canyon	Harney	OR	43.71610	-119.0071	4456
72	SPB	1	Spencer Butte, Eugene	Lane	OR	43.99090	-123.1022	1450
73	SKK	2	Skunk Hollow	Jefferson	OR	44.40750	-121.0729	3188
74	SHN	2	Shaniko Jct Rest Area	Wasco	OR	44.89480	-120.9357	3093
75	GDZ	1	Goldendale	Klickitat	WA	45.84790	-120.7937	1784
76	YAK	2	Oak Creek Road	Yakima	WA	46.72770	-120.8275	1892
77	PF	1	Point Fosdick	Pierce	WA	47.26274	-122.5687	20
78	LEV	1	Leavenworth	Chelan	WA	47.58880	-120.6775	1394
79	NTB	1	North Tulalip Bay	Snohomish	WA	48.07200	-122.3020	20
80	TS	1	Tulalip Shores	Snohomish	WA	48.08800	-122.3220	20
81	SBD	1	Spee Bi Dah	Snohomish	WA	48.09322	-122.3263	16
82	TB	1	Tulare Beach	Snohomish	WA	48.10532	-122.3449	16
83	MK	1	McKee's Beach	Snohomish	WA	48.11957	-122.3604	16

Table S2. Summary of single nucleotide polymorphism (SNP) datasets. One random SNP from each locus was sampled and two datasets were assembled, one containing individuals with less than 50% data missing and one containing individuals with less than 70% data missing. Datasets vary in loci recovered based on r, the percent of samples required to share a locus for the locus to be retained.

r (percent of samples sharing locus)	Raw # loci	Invariant	>2 Haplotypes	Non-biallelic	Ave. Perc. Missing	Max. Perc. Missing	Filtered # loci	# Samples Retained (limited to <50% missing per sample)	# Samples Retained (limited to <70% missing per sample)
5	27419	11270	1659	55	79.6	93.2	14465	2	19
10	15898	5198	1096	36	70.0	89.0	9584	18	49
15	10543	2780	816	27	61.1	84.3	6932	28	80
20	7946	1860	681	22	54.1	80.2	5394	49	94
25	6517	1362	591	17	48.9	76.8	4555	65	105
50	2971	413	281	7	29.4	60.2	2274	104	108
60	2166	275	201	4	23.6	52.0	1687	107	108
70	1428	183	131	3	17.9	41.9	1112	108	108
75	1083	149	100	2	14.9	39.2	833	108	108
80	781	102	76	1	12.0	38.4	603	108	108
90	219	33	22	0	5.8	28.8	164	108	108
100	4	2	0	0	0.0	0.0	2	108	108

Chapter 2: Potential for local adaptation in Western Fence Lizards (*Sceloporus occidentalis*) along an elevation gradient in Yosemite National Park

NASSIMA M. BOUZID[1,2,*], LAUREN B. BUCKLEY[1], & ADAM D. LEACHÉ[1,2]

[1]*Department of Biology, University of Washington, Box 351800, Seattle WA 98195–1800, USA*

[2] *Burke Museum of Natural History and Culture, University of Washington, Seattle, WA 98195, USA*

**E-mail: bouzidnm@uw.edu*

Introduction

Intraspecific variation in species traits provides a window to processes of incipient ecological divergence. Widespread species often contain populations that exhibit geographic clines in traits structured along environmental gradients (Aitken & Whitlock, 2013; Endler, 1977; Hereford, 2009; Huey, Gilchrist, et al., 2000; Kawecki & Ebert, 2004; Keller et al., 2013). Traits that contribute to increased fitness of genotypes native to specific environments are considered products of local adaptation, which refers to both the pattern and the process that produces a tradeoff between high fitness in native and low fitness in foreign environments (Kawecki & Ebert, 2004). Studies of local adaptation within species are an opportunity to identify traits that are under selection and to understand the mechanisms driving trait divergence.

Recent colonization of a new environment with accompanying clinal variation in traits offers an ideal scenario to study local adaptation. However, are differences in traits produced by rapid genetic adaptation, or by adaptive phenotypic plasticity? Furthermore, how have the relative strengths of migration and selection enabled the establishment of clines? Local adaptation occurs when variable environments exert differential selective pressure on populations (Kawecki & Ebert, 2004; Lenormand, 2002). Gene flow along the environmental gradient can produce maladapted genotypes and erode clinal variation if it is sufficiently strong (Aitken & Whitlock, 2013; Lenormand, 2002). Therefore, clines can be maintained if (1) traits are linked to genotypes and gene flow is limited along the gradient or (2) traits are adaptively plastic and can be maintained under strong gene flow (Crispo, 2008; Ghalambor et al., 2007; Kawecki & Ebert, 2004).

Lizards in the genus *Sceloporus* are a model system for studying life history evolution and thermal ecology, with demonstrated links between environmental temperatures and fitness (Adolph, 1990; Sears & Angilletta, 2004; Sinervo, 1990; Sinervo & Adolph, 1994; Sinervo et al.,

2010). By using behavior to regulate body temperatures, these ectotherms are able to thrive in diverse habitats, ranging from extreme desert with ambient temperatures exceeding 38°C to montane forests where temperatures drop below 0°C (Adolph, 1990; Sears & Angilletta, 2004). Despite considerable variation in environmental temperatures, lizards maintain narrow body temperature ranges via behavioral thermoregulation and opt to become inactive when environmental temperatures become either too hot or too cold (Adolph, 1990; Adolph & Porter, 1993; Andrews, 1998; Bogert, 1949). Consequently, cooler environments at high elevation and high latitudes limit activity duration, which also limits opportunities for feeding, digestion, growth, and reproduction (Adolph & Porter, 1993; Sears & Angilletta, 2004). Traits that enable extended activity or more efficient growth are thought to potentially increase fitness in temporally limited environments (Buckley, 2010; Clusella-Trullas et al., 2007; Levy et al., 2016).

High and low elevation populations of Western Fence Lizards (*Sceloporus occidentalis*) in the Sierra Nevada of California exhibit clinal variation in traits that may increase fitness in temporally limited environments. Cooler temperatures and seasonality at high elevation limit both daily and seasonal activity periods, meaning lizards may be inactive due to snow for up to 9 months (Jameson & Allison, 1976). Reduced activity periods constrain fitness by limiting opportunities for feeding, digestion, and assimilation, which in turn limit growth and reproduction (Adolph & Porter, 1993). Selection on traits that facilitate increased activity in environments that limit activity periods can increase fitness (Buckley, 2010; Levy et al., 2016). With increasing elevation, *S. occidentalis* achieve larger body sizes and darker, more melanistic coloration (Camp, 1916; Leaché et al., 2010). Larger body sizes have been linked to both the ability to produce larger clutches and to slower cooling rates in lizards, which would increase

reproductive output and heat retention, respectively (Du et al., 2005; McKenna & Packard, 1975; Moreno Azócar et al., 2016; Sears & Angilletta, 2004). Darker coloration has been linked to faster heating rates and may also block harmful solar radiation (more intense at high elevations), which would extend activity durations in colder environments and prevent skin damage during basking, respectively (Reguera et al., 2014; Clusella-Trullas et al., 2007; Cope et al., 2001). A study that compared high and low elevation *S. occidentalis* from the central Sierra Nevada confirmed that high elevation lizards experience shorter activity periods and accelerated reproductive timelines and found that low and high elevation lizards matured at approximately the same age (20 months), suggesting that growth rates may also differ (Jameson & Allison, 1976). Demonstrated shifts in life history at high elevations suggest that the environment exerts selective pressure on high elevation populations (Ruth, 1977). A study investigating the phenotypic evolution of high elevation populations in Yosemite National Park suggested that high and low elevation populations are genetically distinct in mitochondrial DNA and found evidence for multiple, independent origins along different river drainages (Leaché et al., 2010). Convergence in traits among divergent lineages that have recently colonized high elevation may be a product of either rapid genetic adaptation or adaptive phenotypic plasticity (Ghalambor et al., 2007; Hoffman & Sgrò, 2011).

Glaciation provided constraints on the timing and direction of colonization of high elevations in the Sierra Nevada by *S. occidentalis.* The Grand Canyon of the Tuolumne River (GCT) ascends gradually over ca. 40 km from Hetch Hetchy Valley in the west to Tuolumne Meadows in the east (Fig. 1). The geologic and glacial history of the GCT suggests that current residents colonized higher elevations from the west, rather than from the north or the south. Westward uplift of the Sierra Nevada mountain block, hinging at the eastern margin of the

Central Valley, created a steep eastern escarpment that likely impeded colonization of the Sierra Nevada from the east (Huber, 1990; Wakabayashi & Sawyer, 2001). The GCT is V-shaped, which is atypical of glacially carved valleys, with steep canyon walls carved by preglacial stream incision and subsequently modified by glaciers (Huber, 1990). In contrast to Yosemite Valley, a classic glacially-carved U-shaped valley that was last filled with ice ca. 750,000 years before the present (ybp), the GCT was filled with ice (ca. 1220 m from valley floor to rim) much more recently: 15,000–20,000 ybp (Tioga glaciation; Huber, 1990). Glaciers in the Sierra Nevada receded to post-glacial-maximum extents by approximately 10,000 ybp, suggesting colonization of high elevations via the GCT occurred recently (Chapter 1; Davis, 1988).

Recent colonization of high elevation (Chapter 1) and a clear morphological cline in *S. occidentalis* offers a promising opportunity to study local adaptation. Larger and darker phenotypes are exclusive to high elevations in the central Sierra Nevada, which were inaccessible to lizards until ca. 10,000-15,000 years before the present (ybp) (Huber, 1990). Development of a locally exclusive–and potentially locally adapted–phenotype might have facilitated rapid expansion to high elevation following glaciation. Considering this requirement, phenotypic clines produced by adaptive phenotypic plasticity cannot be considered local adaptation because a single genotype might have high fitness in both native and foreign environments (Ghalambor et al., 2007). Due to the logistic challenges of conducting common garden and reciprocal transplant experiments in non-model vertebrate systems, a preliminary assessment of local adaptation can include (1) comparisons of cline characteristics for multiple traits and (2) estimates of the magnitude and direction of gene flow along the environmental gradient. This preliminary assessment would confirm that traits vary clinally across transitions

between environments and inform predictions of whether phenotypic plasticity or genetic divergence underlies trait variation.

We investigate phenotypic clines and gene flow among populations of *S. occidentalis* along a sharp and recently colonized elevation gradient in the Sierra Nevada. The phenotypic clines encompass larger body size and darker skin color at high elevation (Leaché et al., 2010). Our study is focused on an approximately 21 km long stretch of the Grand Canyon of the Tuolumne River in northern Yosemite National Park spanning ca. 1300 m elevation (Fig. 1). We combine new single nucleotide polymorphism (SNP) data with previously published mitochondrial DNA (mtDNA) and morphological data (Leaché et al., 2010) to gain an integrative assessment of clinal variation along the elevation gradient. Properties of clines including cline width and slope at cline center provide estimates of both the strength of selection needed to maintain clines and the impact of environmental variation on trait variation (Slatkin, 1973). Broad clines can be produced by weak selection and/or fine-scale transitions between environments. Broad or absent clines can also result from strong gene flow and weak selection against foreign genotypes. In the special case of closely linked, neutral alleles, however, even strong gene flow can produce steep, "step-like" clines in allele frequencies, similar to those expected across a physical barrier (Barton, 1979). The magnitude and direction of gene flow along the gradient can also provide an estimate of whether trait divergence is produced by genetic adaptation or phenotypic plasticity (Hendry, 2015). Balanced symmetric or strong asymmetric gene flow, also called "gene swamping," tends to homogenize genetic variation (Lenormand, 2002). As a result, maintenance of a cline in the face of gene flow would suggest that divergence in traits is produced by phenotypic plasticity.

We test the specific hypothesis that weak gene flow or isolation following initial colonization of high elevation has facilitated local adaptation in Yosemite *S. occidentalis*. If our hypothesis is supported, we predict that low and high elevation lizards will be genetically divergent and that gene flow between them will be limited. If our hypothesis is supported we also predict that changes in traits will be abrupt, manifesting as steep clines. If our hypothesis is not supported, we predict that gene flow will be strong (either asymmetric or symmetric) and that trait clines will be broad. To extend our preliminary assessment of local adaptation in *S. occidentalis*, we also identify and determine the function of potential candidate loci that are significantly correlated with elevation.

Materials and methods

Study area and phenotypic cline

Our study is focused on populations of *S. occidentalis* distributed along an elevation gradient in Yosemite National Park, Tuolumne County, California. The Museum of Vertebrate Zoology (MVZ; UC Berkeley) conducted the Grinnell Resurvey Project (GRP) in Yosemite National Park from 2003–2006, a large-scale study aimed at quantifying changes in distribution and community composition of vertebrate taxa nearly 100 years following original surveys by MVZ Director Joseph Grinnell from 1911–1920 (Grinnell & Storer, 1924; Moritz et al., 2008). As part of the GRP, sampling of vertebrate animals was expanded into new regions, including the Grand Canyon of the Tuolumne River (GCT).

We used phenotypic data collected for *S. occidentalis* as part of the GRP to assess clinal variation in the GCT (Leaché et al., 2010). With increasing elevation, lizards achieve larger body sizes and darker coloration. While body size in *Sceloporus* is usually determined by age at

maturity (e.g., larger lizards mature later), lizards with different body sizes in the Sierra Nevada reach maturity at the same age (Jameson & Allison, 1976; Sears & Angilletta, 2004). This suggests that body sizes clines might be produced by variation in growth rates; to achieve larger body sizes in the same amount of time, high elevation lizards must grow faster than low elevation lizards. A trend of darker color in ectotherms living in cold environments (high latitudes and high elevations) has suggested that color may be relevant to thermoregulation (Clusella-Trullas et al., 2007).

Genetic sampling, DNA extraction, and sequencing

Lizards were collected opportunistically along the Grand Canyon of the Tuolumne River trail from E of Hetch Hetchy Reservoir (37.9168°N, 119.6595°W) to E of Glen Aulin (37.90764°N, 119.4196°W) from August 5–23, 2003. (Table S1). Lizards were collected along the trail from west to east in an approximately linear transect because the trail borders the Tuolumne River to the south and the steep wall of the GCT to the north. Our sampling of the elevation gradient along the GCT ranges from 1167–2488 m elevation over ca. 21 km. (Fig. 1).

We obtained 80 tissue samples for *Sceloporus occidentalis* from the GCT elevation gradient from the Museum of Vertebrate Zoology (University of California, Berkeley), and used a high-salt protocol to extract whole genomic DNA from liver tissue (MacManes, 2013). We collected double-digest restriction-site associated DNA sequencing (ddRADseq; Peterson et al., 2012). Briefly, the ddRADseq protocol involved using restriction enzymes to digest genomic DNA targeting rare (SbfI 5'-CCTGCAGG-3') and common (MspI 5'-CCGG-3') cut-sites (New England Biolabs); purification and ligation of barcoded Illumina adapters onto digested fragments; combining eight individuals with unique barcodes into pools and assigning each pool

a unique Illumina adapter; using a Blue Pippin Prep size fractionator (Sage Science) to select fragments between 415 and 515 base pairs (bp) in length; amplifying final libraries with proofreading *Taq* and Illumina's indexed primers; and using an Agilent 2200 TapeStation to determine the fragment size distribution and concentration of each pool. We sent final libraries to the Vincent J. Coates Genomics Sequencing Laboratory (UC Berkeley), where qPCR was used to determine sequenceable library concentrations before pools were combined in quantities that evenly distributed sequencing effort across individuals; libraries were sequences on a single Illumina HiSeq-4000 lane (51-bp, single-end reads).

Bioinformatics

We used STACKS version 1.37 (Catchen et al., 2013) to process raw sequencing reads and assemble SNP loci, interfaced through a custom Python pipeline (Portik et al., 2017; https://github.com/dportik/Stacks_pipeline). Briefly, we extracted individual sequences from raw Illumina reads using individual barcodes for each sequencing pool; we used FastQC (Babraham Bioinformatics, 2011) to assess read quality; and we used fastx_trimmer (Gordon & Hannon, 2012) to trim the 6-bp restriction-site overhang sequence. We reduced raw sequencing reads from 51 to 40 bp after removing the 5 bp barcode and 6 bp restriction site overhang. We assembled loci in STACKS by aligning reads into sets of similar sequences with a minimum depth of coverage of 5 sequences, allowing a maximum of 2 nucleotide differences between sets and a minimum minor allele frequency of 0.05. We discarded sets with unusually high coverage to avoid retaining highly repetitive and/or non-orthologous loci in the final dataset.

Some loci may contain multiple SNPs in linkage disequilibrium, meaning that they are non-randomly associated, or linked (Slatkin, 2008). Quantifying linkage disequilibrium across

the genome can elucidate patterns of selection and demographic processes in model systems (Slatkin, 2008). However, in systems for which we are only beginning to explore genomic architecture, it may be difficult to distinguish between sequencing biases and true linkage disequilibrium. Furthermore, many methods make simplifying assumptions that each site is unlinked (Chifman & Kubatko, 2014; Gutenkunst et al., 2009). By digesting whole genomic DNA at rare and common cut-sites, we can assume that ddRAD loci are randomly distributed throughout the genome (Peterson et al., 2012). To ensure that unlinked SNPs are retained, one can either calculate a linkage disequilibrium statistic to determine which sites to prune (Slatkin, 2008), or sample a single SNP per locus. In our final dataset, we sampled one random SNP per 40 bp locus, meaning that the number of loci recovered by STACKS and the number of SNPs in our final dataset were the same.

Population structure

We used ADMIXTURE version 1.3.0 (Alexander et al., 2009) to characterize genetic variation among individuals from the elevation gradient. ADMIXTURE implements a maximum likelihood (ML) framework and cross-validation error to choose the number of genetic clusters (*K*) that best describes the variation between individuals. Here, we refer to genetic clusters as 'populations.' We used PLINK version 1.07 (Purcell et al., 2007) to convert output files from the STACKS pipeline to the binary PLINK format required by ADMIXTURE. We ran ADMIXTURE with cross-validation enabled for values of *K* from 1 to 10 and selected the value of *K* that minimized cross-validation error.

Cline analysis

Characteristics of trait clines can elucidate the strength of selection across environmental gradients (Brown & Pavlovic, 1992; Endler, 1977; Slatkin, 1973). Cline widths are determined by both dispersal (i.e., gene flow) and selection across environmental gradients (Slatkin, 1973). If environmental variables that are relevant to fitness change on a scale that is larger than average dispersal distance (e.g., "coarse-grained environment"; Levins, 1968), a cline will be established. Alternatively, if environmental variables change on a scale that is smaller than average dispersal distance (e.g., "fine-grained environment"), organisms will be unable to respond to environmental variation and no cline will be established (Slatkin, 1973). Slatkin (1973) coined "characteristic length" as a term to describe the minimum distance over which selection could produce a trait cline. Over distances less than the characteristic length even strong selection will not produce a cline (Slatkin, 1973). The characteristic length (l_c) is proportional to the average dispersal distance traveled at the dispersal stage (l) and inversely proportional to the strength of selection (s):

$$l_c = \frac{l}{\sqrt{s}} \qquad (1).$$

Therefore, strong gene flow and weak selection would produce trait variation over a large distance, or a broad cline. Weak gene flow and strong selection would produce trait variation over a small distance, or a narrow cline.

Here, we used the term 'trait' to refer to any variable character, which included allele frequencies for SNPs, mitochondrial haplotype frequencies, and morphological traits including body size (snout-vent length; SVL) and color (ventral color patches). We interpreted the characteristic length to be roughly equivalent to cline width (w), and rewrote equation (1) to estimate the strength of selection (s) with known w and l:

$$s = \left(\frac{l}{l_{50}}\right)^{2} \qquad (2)$$

or

$$s = \left(\frac{l}{l_{500}}\right)^{2}. \qquad (3)$$

Sceloporus occidentalis is a territorial species in which adults defend and occupy territories in the same area year after year (Davis & Ford, 1983; Sheldahl & Martins, 2000). In one mark and recapture study, however, an adult *S. occidentalis* traveled 1 km within 24 hr (Bromwich & Schall, 1986). Dispersal generally occurs at the juvenile stage; individuals can disperse at least 420 m, although there is considerable variation even between individuals from the same clutch (Massot et al., 2003). For example, in another mark and recapture study, siblings dispersed between 4 and 420 m, and across families the average dispersal distance 38.86 m for females and 51.33 m for males (Massot et al., 2003). We compared the strength of selection for two possible dispersal distances (l): 50 m and 500 m.

We used the R (R Core Team, 2017) package HZAR (Derryberry et al., 2014) to fit ML clines to multiple traits along the GCT elevation gradient: (1) SNP data; (2) mitochondrial sequence (mtDNA) data; and (3) morphological data (color and SVL). Analysis of genetic variation within continuously distributed populations usually requires grouping individuals into discrete bins (Petkova et al., 2016). We grouped individuals into 11 bins along the elevation gradient first by geographic proximity and second by ensuring that each bin contained at least two individuals (Table S1; Fig. S1). If possible, we grouped individuals from geographically proximate localities into separate bins to capture fine scale variation related to changes in elevation. Cline-fitting methods require that sampling localities vary geographically in only one dimension. We converted two-dimensional variation in latitudes and longitudes of sampling localities into one dimension by calculating a pairwise Great Circle dissimilarity matrix and

performing classical multidimensional scaling to ordinate localities into one dimension, while also preserving the variation in the dissimilarity matrix. We equated the ordinated dimension with geographic localities along the elevation gradient, which started at 0 km at the western extent of the elevation gradient at low elevation and extended east for approximately 21 km to the eastern extent of the elevation gradient to high elevation.

We fit ML clines for each trait by comparing 4 cline models and a null model: Model 1 assumed trait intervals fixed between 0 and 1 with no exponential tails; Model 2 assumed trait intervals fit to the observed minimum and maximum trait values with no exponential tails; Model 3 assumed trait intervals fit to the observed minimum and maximum trait values with exponential tails; Model 4 assumed trait intervals varied freely with exponential tails; and the Null Model assumed that traits did not vary with distance. We used the following parameters for the ML search for different models and traits: chain length of 100,000 steps, burnin of 10,000 steps, and random starting seed.

SNP clines. We compared the centers and widths of clines fit to (1) a composite estimate of SNP variation, the proportion of membership to one of two populations in each bin, and (2) individual SNPs. We used STRUCTURE version 2.3.4 (Falush et al., 2007; Pritchard et al., 2000) to calculate the average admixture proportion (Q) within elevation bins based on the complete SNP dataset, which can be considered a composite estimate of genetic variation because it combines patterns from individual SNPs. We prepared the STRUCTURE analysis with StrAuto version 1.0 (Chhatre & Emerson, 2017), predefined two populations ($K = 2$) for calculations of Q, ran the analysis for 10,000 replicates, and discarded the first 1,000 replicates as burnin.

In addition to fitting a cline to the population membership proportions, we fit clines to individual SNPs. We identified "cline-like" SNPs by comparing allele frequencies (p) among

low-, mid-, and high elevation bins. We combined three elevation bins at low-, mid-, and high elevations, respectively, and calculated averages of allele frequencies within the combined three elevation bins. We retained SNPs for which the allele frequencies of the mid-elevation combined bin were intermediate to allele frequencies of the low- and high elevation combined bins, or for which:

$$p_{Low} < p_{Mid} < p_{High}$$

or

$$p_{Low} > p_{Mid} > p_{High}.$$

We discarded SNPs that exhibited a "bowl-like" pattern in allele frequencies, or for which allele frequencies of the mid-elevation bins were lower than allele frequencies in both the low- and high elevation bins. After isolating "cline-like" SNPs, we calculated allele frequencies within each elevation bin.

mtDNA cline. We fit a cline to the frequency of mtDNA haplotypes in each bin based on mtDNA from the NADH-1 (ND1) protein-coding gene (969 bp), originally reported in Leaché et al. (2010). Leaché et al. (2010) reported a transition in mtDNA haplotypes (between western 'A1' and eastern 'A2') ca. 0.5 km E of Hetch Hetchy Reservoir (Res.). To ensure that we captured the transition between mtDNA haplotypes, we expanded our mtDNA sampling westward to include sequence data for individuals N of Hetch Hetchy Res. and ca. 12 km SW of the O'Shaughnessy Dam (the western boundary of the Hetch Hetchy Res.). We recalculated one-dimensional distances between elevation bins for the expanded sampling scheme (see above) and scaled them so that the distance still increased from 0 to 21 km along the gradient and decreased from 0 to -12 km west of the gradient. We assigned mtDNA haplotypes based on the haplotype

network reported by Leaché et al. (2010). We calculated the haplotype frequencies within each elevation bin.

Morphological clines. We fit clines to morphological traits originally measured by Leaché et al. (2010), including snout-vent-length (SVL) in mm and proportion of ventral pigmentation at 100 ppi (See Leaché et al. [2010] for methods). We were interested in relative body size variation along the gradient, so we drew clines based on the proportion of maximum SVL. To calculate proportions of maximum SVL, we divided each individual's SVL by the maximum SVL observed along the elevation gradient (MVZ 245786 ♂; 86.70 mm). We calculated the maximum of the standardized SVL within each elevation bin. Leaché et al. (2010) calculated proportions of ventral coloration by dividing areas of blue, dark blue, and black pigmentation by the total area. We fit clines to the proportion of coloration on (1) the throat, (2) the abdomen, and (3) the total ventral surface (throat + abdomen), averaged across individuals within each elevation bin.

Demographic model selection

We used a model selection approach based on the site frequency spectrum (SFS) to determine the demographic history of populations along the elevation gradient. The specific aspects of demographic history that we sought were magnitude and direction of gene flow, timing of divergence, and effective population size. We excluded 15 individuals from two localities at mid-elevations (1670–1870 m) to infer long-term trends in gene flow between populations at the extremes of the elevation gradient (Schield et al., 2017). We generated the folded 2D SFS for the reduced dataset, which included 28 individuals from low elevation and 35 individuals from the high elevation. We evaluated 20 competing models, including: divergence with continuous symmetric migration; divergence with continuous asymmetric migration;

divergence in isolation with symmetric secondary contact; and divergence in isolation with asymmetric secondary contact (First 20 models; http://github.com/dportik/dadi_pipeline/Two_Population_Pipeline/Models_2D.pdf).

We performed a thorough parameter search over two iterations of the demographic modeling optimization routine developed by Portik et al. (2017; https://github.com/dportik/dadi_pipeline). The goal of the optimization routine was to conduct multiple replicate parameter searches within a 'round' of analysis and seed consecutive rounds with the best (maximum log likelihood) set of parameters from the previous round. Over multiple rounds of analysis models converged on a consistent set of parameters. Using the *moments* translation of the optimization routine (Jouganous et al., 2017; Leaché et al., in prep), we executed three primary runs, each from an independent and random set of starting parameter values. The three independent runs each contained four rounds of optimization per model with 20, 40, 60, and 80 replicates per round, respectively (600 total replicates per model across independent runs). We increased the stringency of the optimization algorithm (*maxiters* = 10, 15, 20, 30) and decreased the starting parameter perturbation factor (*folds* = 3, 2, 2, 1) for each consecutive round. We combined replicates across the three independent runs and identified sets of parameters that maximized log likelihood for each model. We executed a secondary run of the optimization routine and seeded the first round of analysis with the optimized parameter values for each model. The secondary run contained four rounds of optimization for each model with 10, 20, 30, 40 replicates (100 total replicates per model), respectively. The *maxiters* and *folds* specifications for the model search remained constant.

Genome-environmental correlation

Gene-environment association studies (GEAS) are aimed at investigating potential signatures of local adaptation by identifying loci that correlate with environmental variables (Coop et al., 2010; Frichot et al., 2013). These loci may underlie traits that increase fitness and provide a starting point for functional genomics studies. Latent factor mixed models (LFMM) are used in GEAS to control for false discoveries and variation due to isolation-by-distance by correcting for unobserved confounders by treating them as fixed effects (Frichot et al., 2013). LFMM's include an explanatory variable (e.g., environmental condition) and a response variable (e.g., genotype, methylation level, gene expression).

We used the R package LFMM (Frichot et al., 2013) to test for correlations between SNPs (response variable) and elevation (explanatory variable). Increasing elevation correlates with decreasing temperature and increasing solar radiation, which are both environmental conditions that are potentially relevant to fitness in lizards (Moreno Azócar et al., 2016). We incorporated neutral genetic structure along the gradient by assigning the number of latent factors equal to the number of genetic clusters (*K*) selected by ADMIXTURE (Rellstab et al., 2015). To maximize our chances of identifying correlated SNPs, we included all of the SNPs from the dataset, rather than one per locus (N = 761). We fit the LFMM using regularized least squares (ridge regression with *K* latent factors), which enabled fitting a linear model to multicolinear data while factoring out genetic variation due to isolation-by-distance. We selected the exact ("analytical") algorithm for smaller datasets and set the regularization parameter to 10^{-5}. We calibrated significance values for the association between predictor and response variables using the Genomic Control statistical method (Devlin & Roeder, 1999).

We explored the potential function of loci containing SNPs significantly correlated with elevation by mapping loci to the annotated reference genome of *Sceloporus undulatus* (Schwartz et al., in prep). We obtained full-length FASTA alignments of SNP loci from STACKS and cleaved the additional bp returned by Illumina to render sequences 39 bp in length. We used BOWTIE 2 version 2.3.5.1 (Langmead & Salzberg, 2012) to map FASTA alignments for each locus. We ran BOWTIE 2 in the default "end-to-end" mode, which required alignment scores to be calculated using all characters in the sequence. We initiated searches with a 22 bp 'seed', and allowed 0 mismatches in the seed alignment. We allowed 15 consecutive seed extension attempts and 2 re-seeding attempts before moving on to the next sequence in the alignment. We used SAMTOOLS version 1.9 (Li et al., 2009) to summarize and sort matching genome coordinates. We visualized the relative positions of gene annotations from the *S. undulatus* genome and mapped loci in the Integrative Genomics Viewer (IGV) version 2.5.2 (Robinson et al., 2011). We reported the match coordinates of the locus in the genome and the annotated gene or, if the locus did not overlap with an annotated gene, we reported the distance to the nearest annotated gene. The genome is composed of long genetic sequences containing assembled contigs from sequencing, or scaffolds.

Results

Bioinformatics

We retained 78 individuals in the final dataset, which required that (1) loci had non-missing data for a minimum of 73 individuals (90% of total); and (2) individuals had no more than 50% missing data across all loci. The prefiltered ddRADseq dataset contained 2,040 loci, of which 1,214 were invariant, 105 had more than 2 haplotypes per individual, and 0 were non-

biallelic. The filtered dataset contained 721 unlinked and biallelic SNPs with an average of 4.5% missing data per individual. Additional characteristics of the ddRADseq data are provided in Table S2.

Population structure

Genetic variation along the elevation gradient was best explained by grouping individuals into two populations. Cross-validation error from ADMIXTURE was minimized when $K = 2$. (Fig. 2a). Populations were separated between low and high elevation ends of the gradient, and admixed individuals occurred at intermediate localities. Population membership proportions transitioned from the low elevation population to the high elevation population between 1545–1865 m elevation (Fig. 2b).

Cline analysis

We fit ML clines to characterize clinal variation in multiple traits and to estimate the strength of selection along the elevation gradient. For each trait (SNPs, mtDNA, SVL, pigmentation), we used AICc to compare 4 different cline models and a null model.

SNP clines. We used two approaches to fit clines to SNP data: a summary approach in which we used average admixture proportions (Q) and a single-SNP approach in which we used average allele frequencies in each elevation bin. We identified 430 "cline-like" SNPs and excluded 291 SNPs from downstream cline analyses. AICc scores supported the null model (no cline) for 49 SNPs. We visualized clines for the remaining 381 SNPs in a "DensiCline" plot (similar to DensiTree; Bouckaert, 2010) at 60% transparency to identify a consensus in cline shape and position (Fig. 3a). We estimated the Gaussian kernel density of cline centers with a

bandwidth of 1.23 and identified the highest density of clines centered at 16.46 km (Fig. 3b). We selected one representative SNP centered at 16.46 km for comparisons with other trait clines. AICc scores support Model 1 (trait interval between 0 and 1 with no exponential tails) for the *Q* cline and Model 2 (observed trait interval with no exponential tails) for the single SNP cline (Table 1). Centers of the *Q* and representative SNP clines are offset by approximately 2.23 km, with the SNP cline center (16.46 km; 2 log-likelihood unit support limits, 2LL = 14.75–18.50 km; Fig. 4; Table 1) located east of the *Q* cline center (14.23 km; 2LL = 13.10–15.28 km). The point estimate for the width of the SNP cline (0.082 km; 2LL = $1.9e^{-4}$–7.19 km) is smaller than the point estimate for the *Q* cline (7.43 km; 2LL = 5.59–9.97 km) (Fig. 4).

mtDNA cline. Statistical parsimony was able to connect all mtDNA haplotypes at the 95% significance level. We recovered a haplotype network composed of two major clusters separated by 11 mutational steps, which corresponded to individuals west and east of the eastern edge of Hetch Hetchy Reservoir. The center of the mtDNA cline (-2.04 km; 2LL = -5.63–0.39 km; Table 1) is located west of the beginning of the elevation gradient (Fig. 4). Leaché et al. (2010) found that haplotypes sharply transitioned from the western 'A1' to the eastern 'A2' at the eastern edge of Hetch Hetchy Res., meaning that all individuals along the elevation gradient beginning 0.16 km E of Hetch Hetchy share the same mtDNA haplotype. AICc scores support Model 1 (trait interval between 0 and 1 with no exponential tails) for the mtDNA haplotype cline (Table 1).

Morphological clines. Leaché et al. (2010) found strong evidence for differences in body size (SVL) and coloration between low and high elevation lizards from the GCT. AICc scores supported Model 2 (observed trait interval with no exponential tails) for both the SVL and the total ventral coloration clines (Table 1). AICc scores supported the null model (no cline) for

throat and abdomen coloration. Clines for SVL and total ventral coloration have similar cline center positions (SVL: 12.87 km; 2LL = 6.26–20.19 km; coloration: 14.93 km; 2LL = 8.13–20.64 km) and equivalent cline widths (SVL: 20.99 km; 2LL = 4.45–21.00 km; coloration: 20.96 km; 2LL = 4.55–21.00 km) (Table 1).

Strength of selection. We used equation (3) (above) to calculate the strength of selection (s) needed to maintain a trait cline (Slatkin, 1973). In our calculations, cline width (w) was the ML point estimate and average dispersal distance (l) was either 50 or 500 m. Generally, selection was greater for narrower clines (SNP, mtDNA) and lesser for broader clines (Q, SVL, coloration) (Table 1). Increasing average dispersal distance by an order of magnitude (50 m to 500 m) increased selection by two orders of magnitude (Table 1). A possible explanation for the exceedingly large s estimates for narrow clines is the relationship between the sizes of w and l. For example, the SNP and mtDNA cline widths (0.08 km [80 m] and 0.23 km [230 m], respectively) are both smaller than a dispersal distance of 500 m. If dispersal distance is greater than cline width, the strength of selection must be nonsensically large to maintain a cline. In reality, establishment of a cline requires average dispersal distance to be less than the cline width, so unreasonable estimates of s are not surprising, and suggest that the average dispersal distance of lizards along the gradient is less than 500 m.

Demographic model selection

We used AIC and Akaike weights to select the best demographic model from a panel of 20 candidate models. Models with higher Akaike weights (wAIC) carry a higher probability of being the correct model considering the relative log likelihoods and ΔAIC of other models (Wagenmakers & Farrell, 2004). The best model supports secondary contact with asymmetric

migration and change in effective population size (wAIC = 1.00) (Table 2). The first four trailing models had negligible wAIC's (<< 0.001), meaning that there is no support for alternate demographic scenarios (Table 2). Immediately after initial divergence, the ratio of high elevation population size to low elevation population size was 0.015 (i.e., high elevation was 1.5% the size of low elevation). Currently, the effective size of high elevation is 69.13% that of low elevation. Low and high elevation populations remained in isolation for 15.99 coalescent time units prior to secondary contact 0.13 coalescent time units ago (Table 2). Migration is asymmetric with 4.55 times as many migrants entering high elevation from low elevation than the converse.

Genome-environment correlation

Out of 761 total SNPs, three were highly correlated with elevation at a significance level of $p < 0.05$. All three correlated SNPs mapped to the annotated *S. undulatus* genome, but none of the SNPs overlapped with an annotated gene. Loci were named according to the catalog locus number assigned by STACKS. Locus 1743 and locus 10406 mapped to different positions on Scaffold 8, while locus 9900 mapped to Scaffold 11 (Table 3). Locus 1743 aligned as a complement sequence, with the 3' (left) end 17,312 bp upstream of the 5' end of the mRNA FUN_012199. The hypothetical product of FUN_012199 is a protein. Locus 1743 contained a fixed transversion from T to A at position Scaffold 8: 19,638,091. The 5' (left) end of locus 9900 was 399 bp downstream of the 5' end of the mRNA FUN_006540. The hypothetical product of FUN_006540 is a protein. Locus 9900 contained a SNP transition from G to A at position Scaffold 11: 6,435,599. Locus 10406 aligned as a complement sequence, with the 3' (left) end 23,595 bp downstream of the 5' end of the mRNA FUN_011703. The hypothetical product of

FUN_011703 is a protein. Locus 10406 contained a SNP transition from G to A at position Scaffold 8: 17,886,056.

Discussion

We investigate local adaptation by quantifying migration and selection along a sharp elevation gradient. While *S. occidentalis* exhibits clinal variation in traits along the gradient, explicit tests–using common garden or reciprocal transplant experiments–are still necessary to demonstrate whether native genotypes have a fitness advantage in native environments (Kawecki & Ebert, 2004). We found evidence for genetic divergence between low and high elevation populations and for asymmetric gene flow between populations (Fig. 2; Table 2). Selection was stronger to maintain narrow clines and weaker to maintain broad clines (Table 1). Our hypothesis proposed that clinal variation likely indicates local adaptation if genotypes are divergent and gene flow is limited along the gradient. Our hypothesis was partially supported in that genotypes were divergent, but the presence of strong asymmetric gene flow suggests that additional evidence is needed before concluding whether clinal variation is a product of local adaptation. Explicit tests–using common garden or reciprocal transplant experiments–are still necessary to demonstrate whether native genotypes have a fitness advantage in native environments (Kawecki & Ebert, 2004).

Genetic divergence between low and high elevation has occurred rapidly along the gradient. Leaché et al. (2010) found evidence for divergence in mtDNA along the Tuolumne River drainage, where an ‘A1’ clade occupies the drainage west of Hetch Hetchy Res. and an ‘A2’ clade occupies the GCT. In this study, we sampled SNPs only for members of the ‘A2’ clade in the GCT from Leaché et al. (2010). We found evidence for an additional divergence within the ‘A2’ clade between individuals at low and high elevations (Fig. 1). Despite sharing

mtDNA haplotypes, individuals in the GCT have diverged genetically and morphologically (Fig. 4). This is interesting considering that high elevation was inaccessible until 10,000 ybp and presumably the timeline for divergence has also been limited (Davis, 1988).

Net gene flow along the gradient is 'uphill,' with proportionally more low elevation migrants entering high elevation than the converse (Table 2). Contemporary asymmetric gene flow may be explained by either habitat quality or species interactions. With increasing elevation, suitable habitat for *S. occidentalis*–open, south-facing rocky slopes–becomes patchier as it is interspersed with dense forest (Leaché et al., 2010). Microclimates determine the range of body temperatures ectotherms experience, and thus performance; if on average the thermal quality of high elevation habitats is lower than low elevation habitats one would expect lower population densities at high elevation (Díaz, 1997; Huey, 1991). However, at least one study has found higher densities of lizards in low thermal quality, montane habitats (we also observed higher densities of *S. occidentalis* at high elevation in the GCT), which suggests that temperature is not the only factor relevant to fitness (Díaz, 1997). Other factors relevant to fitness, like food availability and predation intensity, may be better indicators of habitat quality. Western carpenter ants (*Camponotus modoc*) are a locally abundant food source for vertebrates at high elevations (black bears, Graber & White, 1983; western fence lizards, field observations) and predation intensity on lizards is higher at low elevations (Angilletta et al., 2004).

Species interactions are an alternative explanation for asymmetric gene flow. Individuals might have colonized newly available high elevation habitats after the last glacial maximum through passive diffusion from high to low population densities (Hastings, 1982; Travis et al., 1999). We found evidence for a very small effective population size at high elevation immediately following divergence from low elevation, potentially indicating a founder effect

(Table 2). While it remains smaller than low elevation, the contemporary effective population size of high elevation has increased almost 50-fold. As the size of high elevation approaches that of low elevation, if population density increases we expect gene flow to eventually slow and reach equilibrium because darker, high elevation males exhibit more aggression than lighter, low elevation males and juvenile dispersal is male-biased (Massot et al., 2003; Seddon & Hews, 2017).

What additional evidence is needed to evaluate if, and how, high elevation lizards are locally adapted? We identified genomic regions that were highly correlated with elevation, and that might be linked to increasing fitness in native environments (Table 3). These genomic regions are promising starting points for targeted sequencing and gene ontology studies to explore the potential biological functions of genes linked to elevation. Ideally, captive quantitative trait locus (QTL) crosses of phenotypically divergent low and high elevation lizards and linkage mapping of SNPs would reveal alleles underlying differences in traits (Mackay, 2001; Slate, 2004). While strong asymmetric gene flow might indicate that trait variation is produced by adaptive phenotypic plasticity, which is expected to lower the costs of colonizing a new or temporally variable environments, local adaptation is still possible under gene flow (Ghalambor et al., 2007; Gonzalo-Turpin & Hazard, 2009; Keller et al., 2013; Lenormand, 2002; Yeaman & Whitlock, 2011). Recombination and selection facilitate local adaptation under gene flow by creating tightly linked clusters of alleles of large effect that underlie locally adapted traits (Yeaman & Whitlock, 2011). The true test of whether trait clines in the GCT are produced by local adaptation will be a common garden or reciprocal transplant experiment. Rearing both low and high elevation hatchlings together under natural conditions in a common garden, or under a limited number of conditions that impact fitness (i.e., temperature, activity duration,

ppO_2, UV radiation) in a lab reciprocal transplant experiment will enable explicit comparisons of fitness in native and foreign environments (Kawecki & Ebert, 2004). Such studies are currently underway (Chapter 3).

Acknowledgments

We thank the National Park Service for permission to collect specimens from Yosemite National Park. We thank the Museum of Vertebrate Zoology, and especially Carol Spencer and David Wake, for access to tissues collected during the 2003–2006 Grinnell Resurvey Project in Yosemite. We thank Manuel Massot for providing access to hatchling dispersal data. We thank Tonia Schwartz for providing access to the annotated *Sceloporus undulatus* genome and Earl Middlebrook for a genomics tutorial. We thank Ray Huey, Joe Felsenstein, and Josh Schraiber for helpful discussions and suggestions that improved the manuscript. This project was supported by a Society for the Study of Evolution Rosemary Grant Award to N.M.B.

References

Adolph, S. C. (1990). Influence of behavioral thermoregulation on microhabitat use by two *Sceloporus* lizards. Ecology, 71, 315–327.

Adolph, S. C., & Porter, W. P. (1993). Temperature, activity, and lizard life histories. The American Naturalist, 142, 273–295.

Aitken, S. N., & Whitlock, M. C. (2013). Assisted gene flow to facilitate local adaptation to climate change. Annual Review of Ecology, Evolution, and Systematics, 44, 367–388.

Alexander, D. H., Novembre, J., & Lange, K. (2009). Fast model-based estimation of ancestry in unrelated individuals. Genome Research, 19, 1655–1664.

Andrews, R. M. (1998). Geographic variation in field body temperature of *Sceloporus* lizards. Journal of Thermal Biology, 23, 329–334.

Angilletta, Jr, M. J., Niewiarowski, P. H., Dunham, A. E., Leaché, A. D., & Porter, W. P. (2004). Bergmann's clines in ectotherms: illustrating a life-history perspective with sceloporine lizards. The American Naturalist, 164, E168–E183.

Babraham Bioinformatics. (2011). FastQC: a quality control tool for high throughput sequence data. Babraham Institute, Cambridge, United Kingdom.

Barton, N. H. (1979). Gene flow past a cline. Heredity, 43, 333–339.

Bogert, C. M. 1949. Thermoregulation and eccritic body temperatures in Mexican lizards of the genus *Sceloporus*. Sobreiro de los Anales del Instituto de Biologia Mexico, 20, 415–426.

Bouckaert, R. R. (2010). DensiTree: making sense of sets of phylogenetic trees. Bioinformatics, 26, 1372–1373.

Bromwich, C. R., & Schall, J. J. (1986). Infection dynamics of *Plasmodium mexicanum*, a malarial parasite of lizards. Ecology, 67, 1227–1235.

Brown, J. S., & Pavlovic, N. B. (1992). Evolution in heterogeneous environments: effects of migration on habitat specialization. Evolutionary Ecology, 6, 360–382.

Buckley, L. B. (2010). The range implications of lizard traits in changing environments. Global Ecology and Biogeography, 19, 452–464.

Camp, C. L. (1916). The subspecies of *Sceloporus occidentalis* with description of a new form from the Sierra Nevada, and systematic notes on other California lizards. University of California Publications in Zoology, 17, 63–74.

Catchen, J., Hohenlohe, P. A., Bassham, S., Amores, A., & Cresko, W. A. (2013). Stacks: an analysis tool set for population genomics. Molecular Ecology, 22, 3124–3140.

Chhatre, V. E., & Emerson, K. J. (2017). StrAuto: Automation and Parallelization of STRUCTURE Analysis. BMC Bioinformatics, 18:192

Chifman, J., & Kubatko, L. (2014). Quartet inference from SNP data under the coalescent model. Bioinformatics, 30, 3317–3324.

Clement, M., Posada, D. C. K. A., & Crandall, K. A. (2000). TCS: a computer program to estimate gene genealogies. Molecular Ecology, 9, 1657–1659.

Clusella-Trullas, S., Terblanche, J. S., Blackburn, T. M., & Chown, S. L. (2008). Testing the thermal melanism hypothesis: a macrophysiological approach. Functional Ecology, 22, 232–238.

Clusella-Trullas, S., van Wyk, J. H., & Spotila, J. R. (2007). Thermal melanism in ectotherms. Journal of Thermal Biology, 32, 235–245.

Coop, G., Witonsky, D., Di Rienzo, A., & Pritchard, J. K. (2010). Using environmental correlations to identify loci underlying local adaptation. Genetics, 185, 1411–1423.

Cope, R. B., Fabacher, D. L., Lieske, C., & Miller, C. A. (2001). Resistance of a Lizard (the Green Anole, *Anolis carolinensis*; Polychridae) to Ultraviolet Radiation–induced Immunosuppression¶. Photochemistry and Photobiology, 74, 46–54.
Crispo, E. (2008). Modifying effects of phenotypic plasticity on interactions among natural selection, adaptation and gene flow. Journal of Evolutionary Biology, 21, 1460–1469.
Davis, P. T. (1988). Holocene glacier fluctuations in the American Cordillera. Quaternary Science Reviews, 7, 129–157.
Davis, J., & Ford, R. G. (1983). Home range in the western fence lizard (*Sceloporus occidentalis occidentalis*). Copeia, 4, 933-940.
Derryberry, E. P., Derryberry, G. E., Maley, J. M., & Brumfield, R. T. (2014). HZAR: hybrid zone analysis using an R software package. Molecular Ecology Resources, 14, 652–663.
Devlin, B., & Roeder, K. (1999). Genomic control for association studies. Biometrics, 55, 997–1004.
Diaz, J. A. (1997). Ecological correlates of the thermal quality of an ectotherm's habitat: a comparison between two temperate lizard populations. Functional Ecology, 11, 79–89.
Du, W., Ji, X., & Shine, R. (2005). Does body-volume constrain reproductive output in lizards?. Biology Letters, 1, 98–100.
Endler, J. A. (1977). Geographic variation, speciation, and clines (No. 10). Princeton University Press.
Falush, D., Stephens, M., & Pritchard, J. K. (2003). Inference of population structure using multilocus genotype data: linked loci and correlated allele frequencies. Genetics, 164, 1567–1587.
Frichot, E., Schoville, S. D., Bouchard, G., & François, O. (2013). Testing for associations between loci and environmental gradients using latent factor mixed models. Molecular Biology and Evolution, 30, 1687–1699.
Ghalambor, C. K., McKay, J. K., Carroll, S. P., & Reznick, D. N. (2007). Adaptive versus non-adaptive phenotypic plasticity and the potential for contemporary adaptation in new environments. Functional Ecology, 21, 394–407.
Gonzalo-Turpin, H., & Hazard, L. (2009). Local adaptation occurs along altitudinal gradient despite the existence of gene flow in the alpine plant species *Festuca eskia*. Journal of Ecology, 97, 742–751.
Gordon, A. & Hannon, G. (2012). Fastx-toolkit. Available at http://hannonlab.cshl.edu/fastx_toolkit.
Graber, D. M., & White, M. (1983). Black bear food habits in Yosemite National Park. Bears: Their Biology and Management, 5, 1–10.
Grinnell, J., & Storer, T. I. (1924). Animal life in the Yosemite: an account of the mammals, birds, reptiles, and amphibians in a cross-section of the Sierra Nevada. University of California Press, Berkeley, CA.
Gutenkunst, R. N., Hernandez, R. D., Williamson, S. H., & Bustamante, C. D. (2009). Inferring the joint demographic history of multiple populations from multidimensional SNP frequency data. PLoS Genetics, 5, e1000695.
Hastings, A. (1982). Dynamics of a single species in a spatially varying environment: the stabilizing role of high dispersal rates. Journal of Mathematical Biology, 16, 49–55.
Hendry, A. P. (2015). Key questions on the role of phenotypic plasticity in eco-evolutionary dynamics. Journal of Heredity, 107, 25–41.

Hereford, J. (2009). A quantitative survey of local adaptation and fitness trade-offs. The American Naturalist, 173, 579–588.
Hoffmann, A. A., & Sgro, C. M. (2011). Climate change and evolutionary adaptation. Nature, 470, 479–485.
Huber, N. K. (1990). The late Cenozoic evolution of the Tuolumne River, central Sierra Nevada, California. Geological Society of America Bulletin, 102, 102–115.
Huey, R. B. (1991). Physiological consequences of habitat selection. The American Naturalist, 137, S91–S115.
Huey, R. B., Gilchrist, G. W., Carlson, M. L., Berrigan, D., & Serra, L. (2000). Rapid evolution of a geographic cline in size in an introduced fly. Science, 287, 308–309.
Jameson Jr, E. W., & Allison, A. (1976). Fat and breeding cycles in two montane populations of *Sceloporus occidentalis* (Reptilia, Lacertilia, Iguanidae). Journal of Herpetology, 10, 211–220.
Jouganous, J., Long, W., Ragsdale, A. P., & Gravel, S. (2017). Inferring the joint demographic history of multiple populations: beyond the diffusion approximation. Genetics, 206 1549–1567.
Kawecki, T. J., & Ebert, D. (2004). Conceptual issues in local adaptation. Ecology Letters, 7, 1225–1241.
Keller, I., Alexander, J. M., Holderegger, R., & Edwards, P. J. (2013). Widespread phenotypic and genetic divergence along altitudinal gradients in animals. Journal of Evolutionary Biology, 26, 2527–2543.
Langmead, B., & Salzberg, S. L. (2012). Fast gapped-read alignment with Bowtie 2. Nature Methods, 9, 357–359.
Leaché, A. D., Helmer, D. S., & Moritz, C. (2010). Phenotypic evolution in high-elevation populations of western fence lizards (*Sceloporus occidentalis*) in the Sierra Nevada Mountains. Biological Journal of the Linnean Society, 100, 630–641.
Lenormand, T. (2002). Gene flow and the limits to natural selection. Trends in Ecology & Evolution, 17, 183–189.
Levins, R., (1968). Evolution in a Changing Environment. Princeton University Press, Princeton, New Jersey.
Levy, O., Buckley, L. B., Keitt, T. H., & Angilletta Jr, M. J. (2016). Ontogeny constrains phenology: opportunities for activity and reproduction interact to dictate potential phenologies in a changing climate. Ecology Letters, 19, 620–628.
Li, H., Handsaker, B., Wysoker, A., Fennell, T., Ruan, J., Homer, N., Marth, G., Abecasis, G., & Durbin, R. (2009). The sequence alignment/map format and SAMtools. Bioinformatics, 25, 2078–2079.
Mackay, T. F. (2001). Quantitative trait loci in *Drosophila*. Nature Reviews Genetics, 2, 11–20.
MacManes, M. MacManes salt extraction protocol, 2013 Figshare. Available from: https://doi.org/10.6084/m9.figshare.658946
Massot, M., Huey, R. B., Tsuji, J., & van Berkum, F. H. (2003). Genetic, prenatal, and postnatal correlates of dispersal in hatchling fence lizards (*Sceloporus occidentalis*). Behavioral Ecology, 14, 650–655.
McKenna, T. M., & Packard, G. C. (1975). Rates of heat exchange in the lizards *Cnemidophorus sexlineatus* and *Sceloporus undulatus*. Copeia, 1, 162–169.

Moreno Azócar, D. L., Bonino, M. F., Perotti, M. G., Schulte, J. A., Abdala, C. S., & Cruz, F. B. (2016). Effect of body mass and melanism on heat balance in *Liolaemus* lizards of the goetschi clade. Journal of Experimental Biology, 219, 1162–1171.

Moritz, C., Patton, J. L., Conroy, C. J., Parra, J. L., White, G. C., & Beissinger, S. R. (2008). Impact of a century of climate change on small-mammal communities in Yosemite National Park, USA. Science, 322, 261–264.

Peterson, B. K., Weber, J. N., Kay, E. H., Fisher, H. S., & Hoekstra, H. E. (2012). Double digest RADseq: an inexpensive method for de novo SNP discovery and genotyping in model and non-model species. PloS One, 7, e37135.

Petkova, D., Novembre, J., & Stephens, M. (2016). Visualizing spatial population structure with estimated effective migration surfaces. Nature Genetics, 48, 94–100.

Portik, D. M., Leaché, A. D., Rivera, D., Barej, M. F., Burger, M., Hirschfeld, M., Rödel, M., Blackburn, D. C., & Fujita, M. K. (2017). Evaluating mechanisms of diversification in a Guineo-Congolian tropical forest frog using demographic model selection. Molecular Ecology, 26, 5245–5263.

Pritchard, J. K., Stephens, M., & Donnelly, P. (2000). Inference of population structure using multilocus genotype data. Genetics, 155, 945–959.

Purcell, S., Neale, B., Todd-Brown, K., Thomas, L., Ferreira, M. A., Bender, D., Maller, J., Sklar, P., de Bakker, P. I. W., Daly, M. J. & Sham, P. C. (2007). PLINK: a tool set for whole-genome association and population-based linkage analyses. The American journal of human genetics, 81, 559–575.

R Core Team. (2017). R: A language and environment for statistical computing. R Foundation for Statistical Computing, Vienna, Austria. https://www.R-project.org/.

Reguera, S., Zamora-Camacho, F. J., & Moreno-Rueda, G. (2014). The lizard *Psammodromus algirus* (Squamata: Lacertidae) is darker at high altitudes. Biological Journal of the Linnean Society, 112, 132–141.

Rellstab, C., Gugerli, F., Eckert, A. J., Hancock, A. M., & Holderegger, R. (2015). A practical guide to environmental association analysis in landscape genomics. Molecular Ecology, 24, 4348–4370.

Robinson, J. T., Thorvaldsdóttir, H., Winckler, W., Guttman, M., Lander, E. S., Getz, G., & Mesirov, J. P. (2011). Integrative genomics viewer. Nature Biotechnology, 29, 24–26.

Ruth, S. B. 1977. A comparison of the demography and female reproduction in sympatric western fence lizards (*Sceloporus occidentalis*) and sagebrush lizards (*Sceloporus graciosus*) on Mounta Diablo, California. Dissertation. University of California, Berkeley, California, USA.

Schield, D. R., Adams, R. H., Card, D. C., Perry, B. W., Pasquesi, G. M., Jezkova, T., Portik, D. M., Andrew, A. L., Spencer, C. L., Sanchez, E. E., Fujita, M. K., Mackessy, S. P. & Castoe, T. A. (2017). Insight into the roles of selection in speciation from genomic patterns of divergence and introgression in secondary contact in venomous rattlesnakes. Ecology and Evolution, 7, 3951–3966.

Sears, M. W., & Angilletta Jr, M. J. (2004). Body size clines in *Sceloporus* lizards: proximate mechanisms and demographic constraints. Integrative and Comparative Biology, 44, 433–442.

Seddon, R. J., & Hews, D. K. (2017). Correlates of melanization in multiple high-and low-elevation populations of the lizard, *Sceloporus occidentalis*: Behavior, hormones, and

parasites. Journal of Experimental Zoology Part A: Ecological and Integrative Physiology, 327, 481–492.
Sheldahl, L. A., & Martins, E. P. (2000). The territorial behavior of the western fence lizard, *Sceloporus occidentalis*. Herpetologica, 56, 469–479.
Sinervo, B. (1990). The evolution of maternal investment in lizards: an experimental and comparative analysis of egg size and its effects on offspring performance. Evolution, 44, 279–294.
Sinervo, B. (1990). Evolution of thermal physiology and growth rate between populations of the western fence lizard (*Sceloporus occidentalis*). Oecologia, 83, 228–237.
Sinervo, B., & Adolph, S. C. (1994). Growth plasticity and thermal opportunity in Sceloporus lizards. Ecology, 75, 776–790.
Sinervo, B., Mendez-De-La-Cruz, F., Miles, D. B., Heulin, B., Bastiaans, E., Villagrán-Santa Cruz, M., Lara-Resendiz, R., Martínez-Méndez, N., Calderón-Espinosa, M. L., Meza-Lázaro, R. N., Gadsden, H., Avila, L. J., Morando, M., De la Riva, I. J., Sepulveda, P. V., Duarte Rocha, C. F., Ibargüengoytía, N., Puntriano, C. A., Massot, M., Lepetz, V., Oksanen, T. A., Chapple, D. G., Bauer, A. M., Branch, W. R., Clobert, J., Sites, J. W. (2010). Erosion of lizard diversity by climate change and altered thermal niches. Science, 328, 894–899.
Slate, J. (2005). INVITED REVIEW: Quantitative trait locus mapping in natural populations: progress, caveats and future directions. Molecular Ecology, 14, 363–379.
Slatkin, M. (1973). Gene flow and selection in a cline. Genetics, 75, 733–756.
Slatkin, M. (2008). Linkage disequilibrium—understanding the evolutionary past and mapping the medical future. Nature Reviews Genetics, 9, 477–485.
Travis, J. M., Murrell, D. J., & Dytham, C. (1999). The evolution of density–dependent dispersal. Proceedings of the Royal Society of London. Series B: Biological Sciences, 266, 1837–1842.
Wagenmakers, E. J., & Farrell, S. (2004). AIC model selection using Akaike weights. Psychonomic Bulletin & Review, 11, 192–196.
Wakabayashi, J., & Sawyer, T. L. (2001). Stream incision, tectonics, uplift, and evolution of topography of the Sierra Nevada, California. The Journal of Geology, 109, 539–562.
Yeaman, S., & Whitlock, M. C. (2011). The genetic architecture of adaptation under migration–selection balance. Evolution: International Journal of Organic Evolution, 65, 1897–1911.

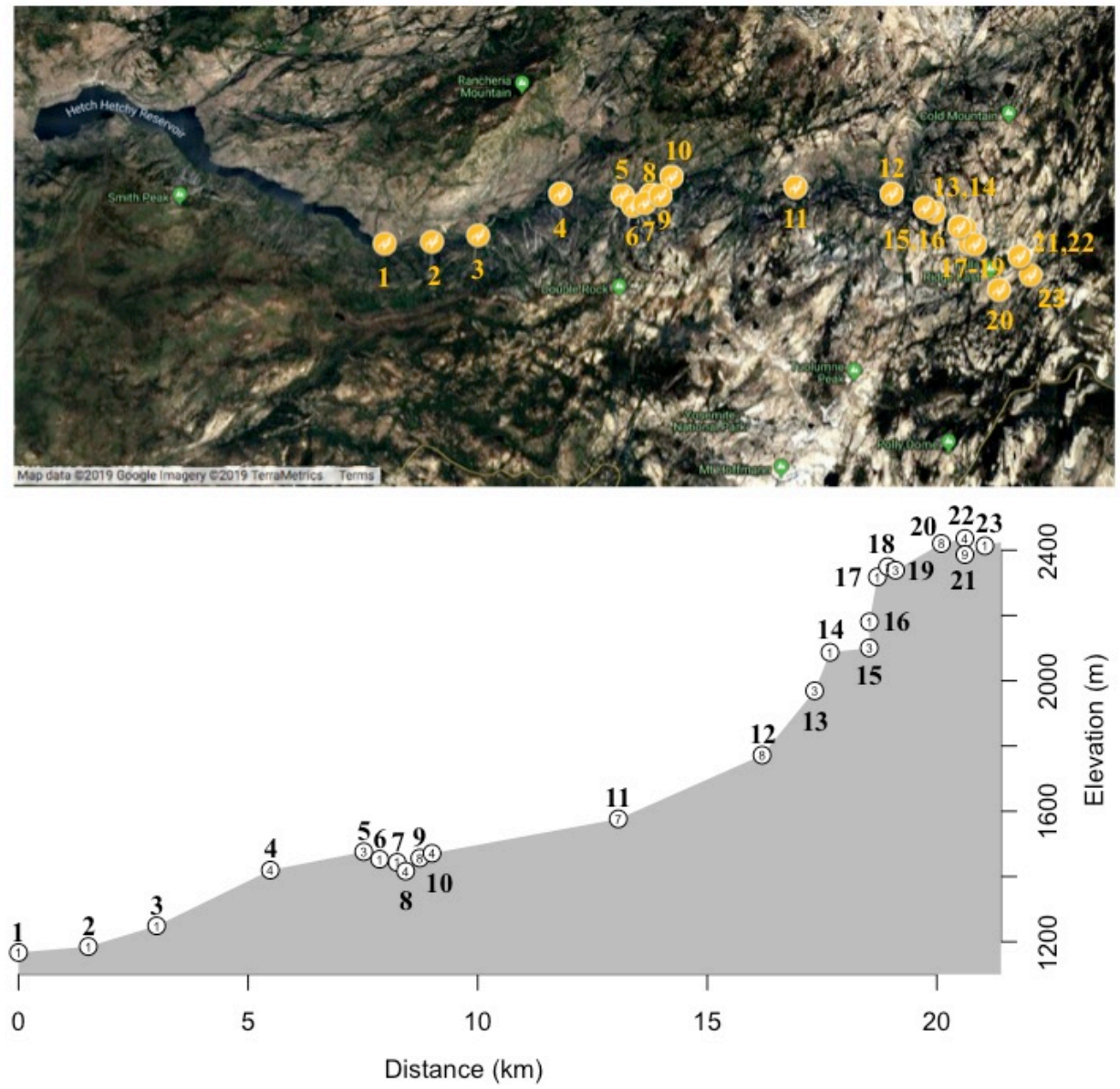

Figure 1. Sampling of the elevation gradient from E Hetch Hetchy Reservoir (low elevation) to E Glen Aulin/Falls Ridge East (high elevation). (bottom) Elevation profile, smoothed by a simple moving average of 2 localities; numbers within points are the sample sizes for each locality.

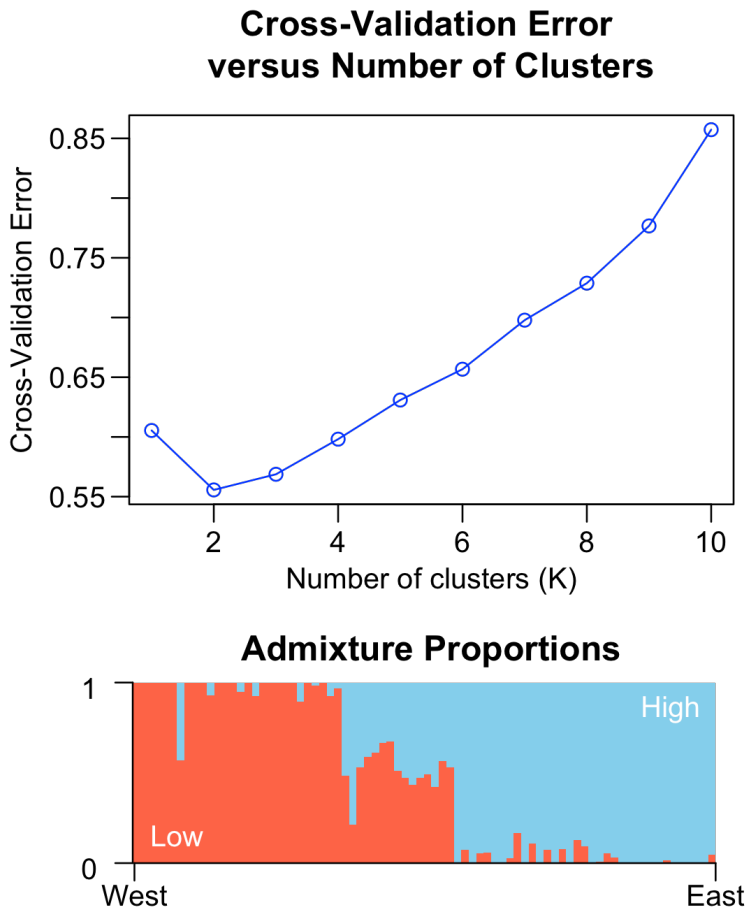

Figure 2. Population structure results for the GCT gradient. (top) Analyses supported 2 populations. (bottom) Proportion of admixture among individuals (vertical bars), ordered from west to east. Individuals with > 50% admixture (center bars) occurred between 1545–1865 m elev.

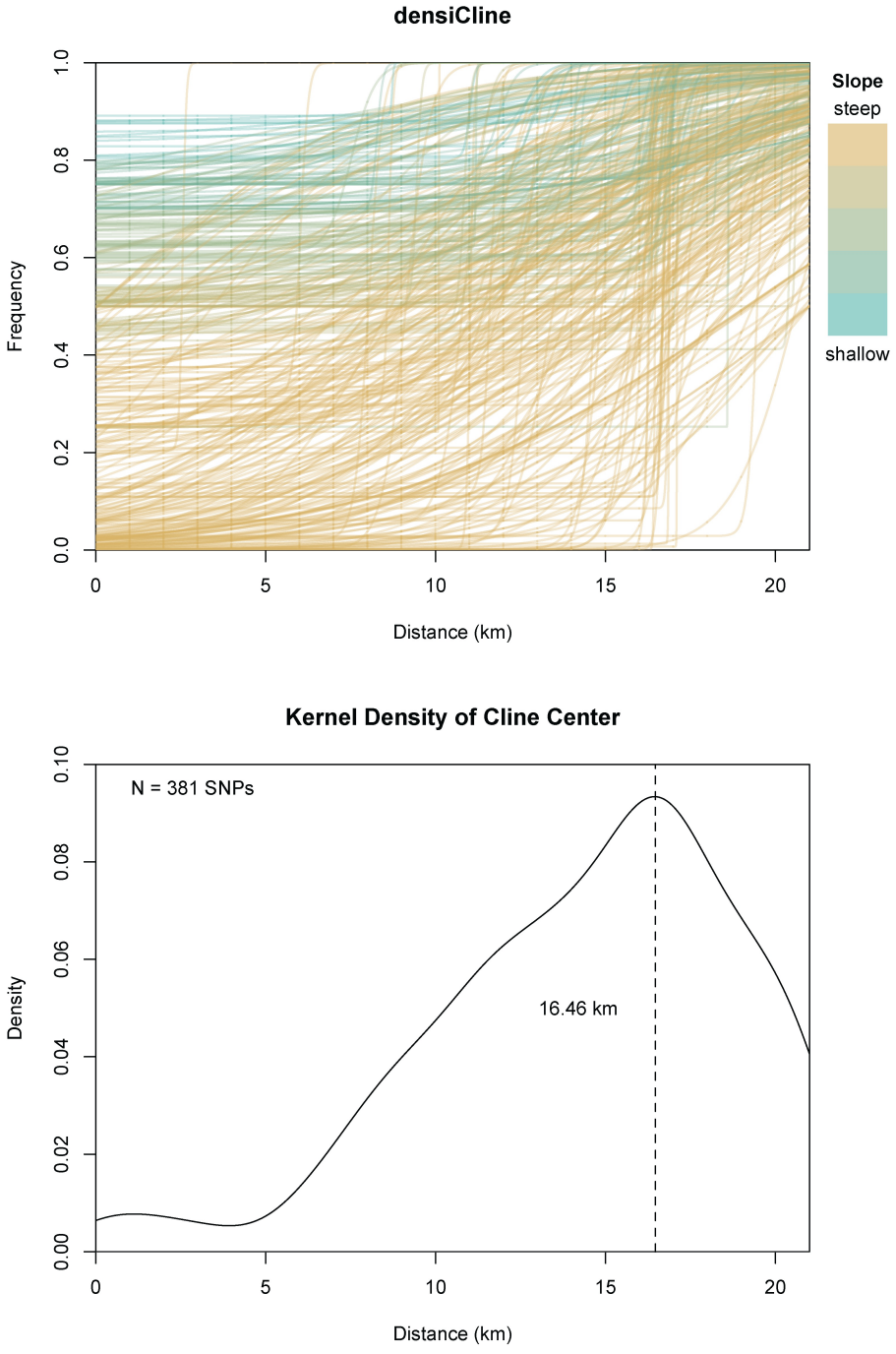

Figure 3. Single SNP DensiCline plot. (top) Each line represents a cline fit to allele frequencies of one SNP. Clines are colored according to slope at cline center. (bottom) Kernel density of cline centers shows a consensus at 16.46 km.

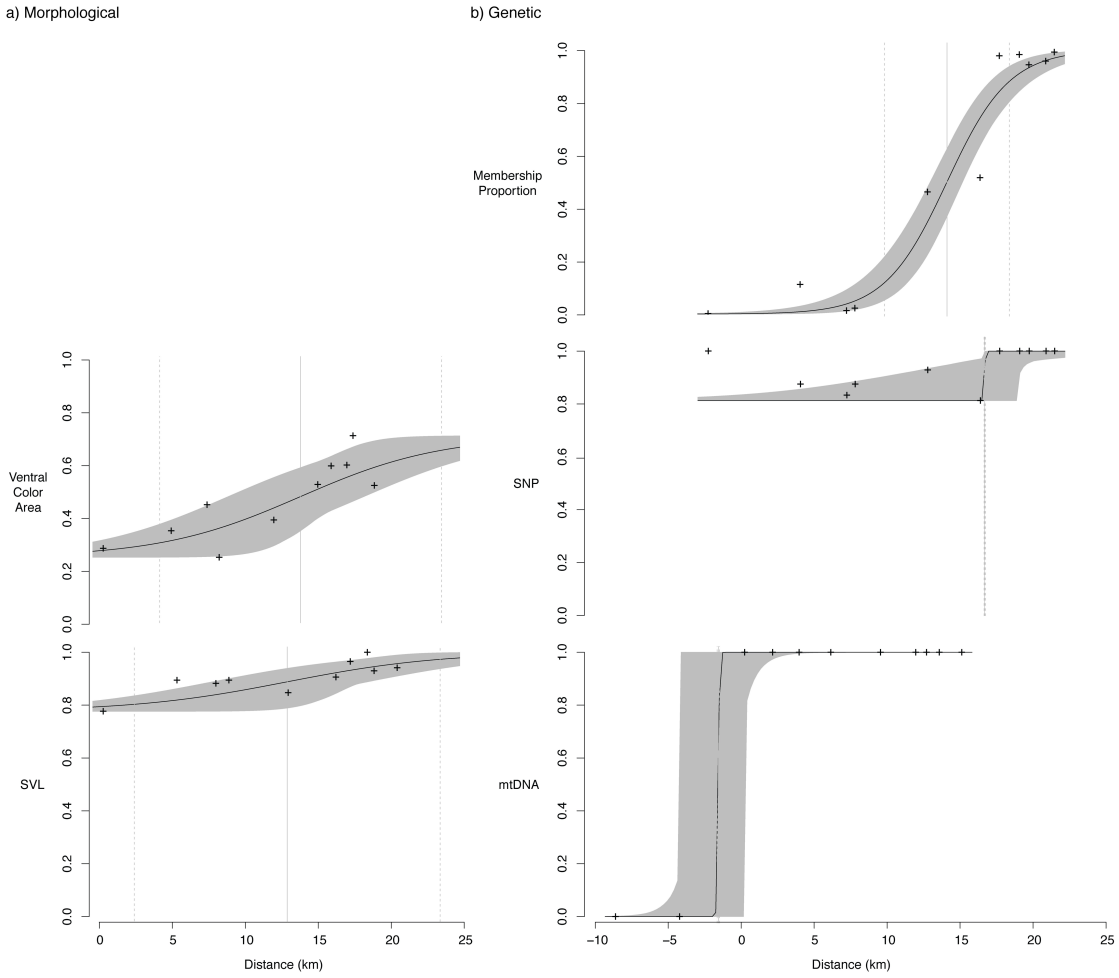

Figure 4. Trait cline comparisons, (a) morphological, (b) genetic, along the GCT elevation gradient. ML cline is in black, confidence intervals are shaded, cline center is the solid vertical line, cline width is denoted by dotted vertical lines, and observed trait frequencies are indicated by '+' symbols.

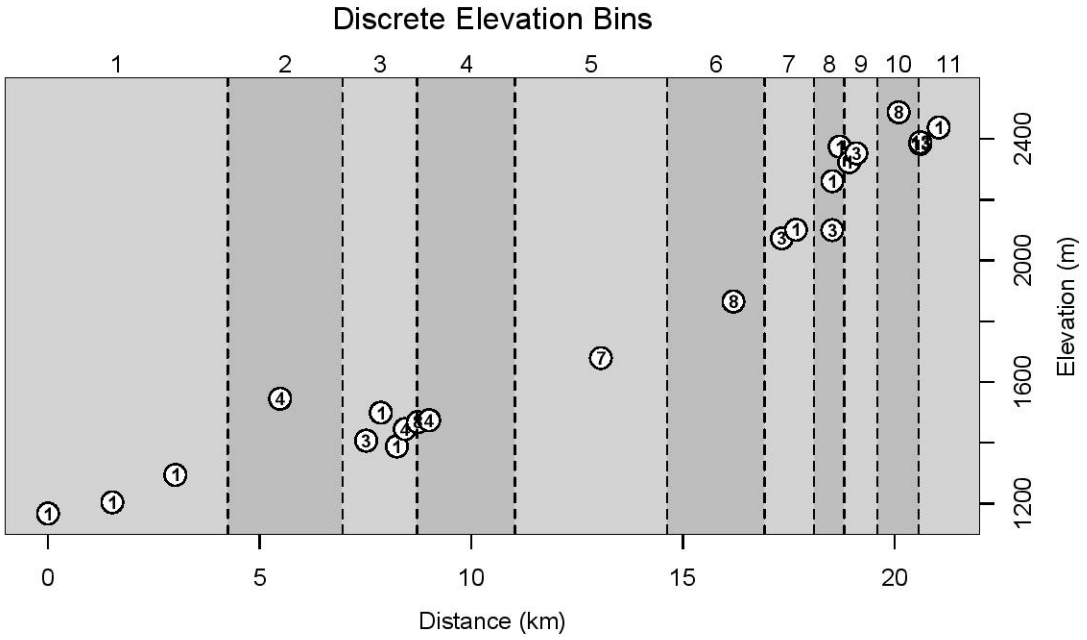

Figure S1. Binning scheme for calculating trait averages along the elevation gradient.

Table 1. Comparison of cline characteristics for each trait. Log likelihoods (LL) are reported for the best model, selected using AICc. Units for maximum likelihood (ML) and 2 log-likelihood support limits for cline centers and widths are in km. Strength of selection (s) when dispersal distance is 50 m and 500 m.

Trait	**Model**	**LL**	**Center**		**Width**		***s***	
			ML Estimate	**2LL**	**ML Estimate**	**2LL**	**50 m**	**500 m**
Admixture Proportion (*Q*)	Model 1	-5.70	14.23	13.10–15.28	7.43	5.59–9.97	4.53E-05	4.53E-03
SNP	Model 2	-2.50	16.46	14.75–18.50	0.08	1.85E-04–7.19	0.37	37.18
mtDNA	Model 1	0.00	-2.04	-5.63–0.39	0.23	1.12E-04–7.50	0.047	4.73
SVL	Model 2	-0.99	12.87	6.26–20.19	20.99	4.45–21.00	5.67E-06	5.67E-04
Coloration	Model 2	-0.78	14.93	8.13–20.64	20.96	4.55–21.00	5.69E-06	5.69E-04

Table 2. Results of demographic model selection using AIC. Akaike weights (wAIC) calculated using log-likelihood (LL) and change in AIC (ΔAIC). Optimized parameters are: low elevation population size (nu1a, nu2a); high elevation population size (nu1b, nu2b); migration into low from high (m12); migration into high from low (m21); coalescent time interval prior to secondary contact or size change (T1); coalescent time interval following secondary contact or size change.

Model	**LL**	**ΔAIC**	**wAIC**	**Optimized Parameters**							
				nu1a	**nu1b**	**nu2a**	**nu2b**	**m12**	**m21**	**T1**	**T2**
Secondary contact, asymmetric migration with size change	-892.4	0	1.00	24.72	0.37	0.16	0.11	4.24	19.29	15.99	0.13
Symmetric migration with size change	-906.8	26.7	0	2.35	7.07	0.053	0.056	23.19	-	4.34	0.063
Secondary contact, asymmetric migration	-908.8	28.7	0	0.17	-	0.058	-	5.04	30.00	24.93	0.19
Secondary contact, symmetric migration with size change	-909.9	32.9	0	2.97	3.26	0.086	0.083	16.66	-	2.92	0.084
Asymmetric migration with size change	-918.0	51.2	0	27.56	2.79	0.29	0.12	1.05	14.62	27.22	0.23

Table 3. Elevation-correlated loci, mapped to the *S. undulatus* genome. Scaffold and coordinates denote the match position. We report the distance to the nearest annotated gene in base pairs (bp) and whether the locus is upstream or downstream of the annotated gene.

Locus	Scaffold	Coordinates	Nearest Gene	Upstream (U) or Downstream (D)	Distance (bp)
1743	8	19,638,055–19,638,093	FUN_012199	U	17,312
9900	11	6,435,583–6,435,621	FUN_006540	D	399
10406	8	17,886,051–17,886,089	FUN_011703	D	23,595

Table S1. Individuals used in this study. Distance refers to the scaled one-dimensional distance along the gradient. Bin refers to scheme used to group individuals into discrete bins. Additional data can be accessed through the Arctos museum database.

Catalog Number	Specific Locality	Latitude	Longitude	Elevation (m)	Distance	Bin
MVZ 245735	0.16 km E Hetch Hetchy Reservoir, Yosemite National Park	37.91682	-119.65948	1167	0.00	1
MVZ 245778	1.0 mi E of Hetch Hetchy Reservoir on N side of Tuolumne River, Yosemite National Park	37.91747	-119.64195	1204	1.52	1
MVZ 245792	2.0 mi E of Hetch Hetchy Reservoir on S side of Tuolumne River, Yosemite National Park	37.91930	-119.62457	1294	3.01	1
MVZ 245779	near footbridges, Pate Valley, Yosemite National Park	37.93151	-119.59417	1545	5.48	2
MVZ 245780	near footbridges, Pate Valley, Yosemite National Park	37.93151	-119.59417	1545	5.48	2
MVZ 245782	near footbridges, Pate Valley, Yosemite National Park	37.93151	-119.59417	1545	5.48	2
MVZ 245783	near footbridges, Pate Valley, Yosemite National Park	37.93151	-119.59417	1545	5.48	2
MVZ 245740	1.3 mi E of footbridges, Pate Valley, Yosemite National Park	37.93101	-119.57091	1407	7.52	3
MVZ 245741	1.3 mi E of footbridges, Pate Valley, Yosemite National Park	37.93101	-119.57091	1407	7.52	3
MVZ 245742	1.3 mi E of footbridges, Pate Valley, Yosemite National Park	37.93101	-119.57091	1407	7.52	3
MVZ 245743	1.5 mi E of footbridges, Pate Valley, Yosemite National Park	37.92791	-119.56746	1499	7.86	3
MVZ 245768	2.75 km E Footbridge, Pate Valley, Yosemite National Park	37.92863	-119.56297	1388	8.24	3
MVZ 245748	1.8 mi E of footbridges, Pate Valley, Yosemite National Park	37.93109	-119.56042	1445	8.43	3

Catalog Number	Specific Locality	Latitude	Longitude	Elevation (m)	Distance	Bin
MVZ 245749	1.8 mi E of footbridges, Pate Valley, Yosemite National Park	37.93109	-119.56042	1445	8.43	3
MVZ 245750	1.8 mi E of footbridges, Pate Valley, Yosemite National Park	37.93109	-119.56042	1445	8.43	3
MVZ 245751	1.8 mi E of footbridges, Pate Valley, Yosemite National Park	37.93109	-119.56042	1445	8.43	3
MVZ 245752	2.0 mi E of footbridges, Pate Valley, Yosemite National Park	37.93106	-119.55691	1468	8.74	4
MVZ 245753	2.0 mi E of footbridges, Pate Valley, Yosemite National Park	37.93106	-119.55691	1468	8.74	4
MVZ 245754	2.0 mi E of footbridges, Pate Valley, Yosemite National Park	37.93106	-119.55691	1468	8.74	4
MVZ 245755	2.0 mi E of footbridges, Pate Valley, Yosemite National Park	37.93106	-119.55691	1468	8.74	4
MVZ 245757	2.0 mi E of footbridges, Pate Valley, Yosemite National Park	37.93106	-119.55691	1468	8.74	4
MVZ 245759	2.0 mi E of footbridges, Pate Valley, Yosemite National Park	37.93106	-119.55691	1468	8.74	4
MVZ 245769	3.27 km E Footbridge, Pate Valley, Yosemite National Park	37.93106	-119.55691	1468	8.74	4
MVZ 245772	3.27 km E Footbridge, Pate Valley, Yosemite National Park	37.93106	-119.55691	1468	8.74	4
MVZ 245763	2.3 mi E of footbridges, Pate Valley, Yosemite National Park	37.93647	-119.55295	1474	9.01	4
MVZ 245764	2.3 mi E of footbridges, Pate Valley, Yosemite National Park	37.93647	-119.55295	1474	9.01	4
MVZ 245765	2.3 mi E of footbridges, Pate Valley, Yosemite National Park	37.93647	-119.55295	1474	9.01	4
MVZ 245766	2.3 mi E of footbridges, Pate Valley, Yosemite National Park	37.93647	-119.55295	1474	9.01	4

Catalog Number	Specific Locality	Latitude	Longitude	Elevation (m)	Distance	Bin
MVZ 241032	ca. 7.5 mi W of Glen Aulin along Trail, N of Tuolumne River, Yosemite National Park	37.93339	-119.50691	1679	13.06	5
MVZ 241035	ca. 7.5 mi W of Glen Aulin along Trail, N of Tuolumne River, Yosemite National Park	37.93339	-119.50691	1679	13.06	5
MVZ 241037	ca. 7.5 mi W of Glen Aulin along Trail, N of Tuolumne River, Yosemite National Park	37.93339	-119.50691	1679	13.06	5
MVZ 241038	ca. 7.5 mi W of Glen Aulin along Trail, N of Tuolumne River, Yosemite National Park	37.93339	-119.50691	1679	13.06	5
MVZ 241040	ca. 7.5 mi W of Glen Aulin along Trail, N of Tuolumne River, Yosemite National Park	37.93339	-119.50691	1679	13.06	5
MVZ 241041	ca. 7.5 mi W of Glen Aulin along Trail, N of Tuolumne River, Yosemite National Park	37.93339	-119.50691	1679	13.06	5
MVZ 241042	ca. 7.5 mi W of Glen Aulin along Trail, N of Tuolumne River, Yosemite National Park	37.93339	-119.50691	1679	13.06	5
MVZ 241022	ca. 500 m W of Return Creek, ca. 5 mi W of Glen Aulin along Trail, N of Tuolumne River, Yosemite National Park	37.93150	-119.47130	1865	16.19	6
MVZ 241024	ca. 500 m W of Return Creek, ca. 5 mi W of Glen Aulin along Trail, N of Tuolumne River, Yosemite National Park	37.93150	-119.47130	1865	16.19	6

Catalog Number	Specific Locality	Latitude	Longitude	Elevation (m)	Distance	Bin
MVZ 241025	ca. 500 m W of Return Creek, ca. 5 mi W of Glen Aulin along Trail, N of Tuolumne River, Yosemite National Park	37.93150	-119.47130	1865	16.19	6
MVZ 241026	ca. 500 m W of Return Creek, ca. 5 mi W of Glen Aulin along Trail, N of Tuolumne River, Yosemite National Park	37.93150	-119.47130	1865	16.19	6
MVZ 241027	ca. 500 m W of Return Creek, ca. 5 mi W of Glen Aulin along Trail, N of Tuolumne River, Yosemite National Park	37.93150	-119.47130	1865	16.19	6
MVZ 241028	ca. 500 m W of Return Creek, ca. 5 mi W of Glen Aulin along Trail, N of Tuolumne River, Yosemite National Park	37.93150	-119.47130	1865	16.19	6
MVZ 241029	ca. 500 m W of Return Creek, ca. 5 mi W of Glen Aulin along Trail, N of Tuolumne River, Yosemite National Park	37.93150	-119.47130	1865	16.19	6
MVZ 241031	ca. 500 m W of Return Creek, ca. 5 mi W of Glen Aulin along Trail, N of Tuolumne River, Yosemite National Park	37.93150	-119.47130	1865	16.19	6
MVZ 241019	ca. 4 km W of Glen Aulin along trail, N side of Tuolumne River, Waterwheel Falls, Yosemite National Park	37.92746	-119.45884	2073	17.34	7

Catalog Number	Specific Locality	Latitude	Longitude	Elevation (m)	Distance	Bin
MVZ 241020	ca. 4 km W of Glen Aulin along trail, N side of Tuolumne River, Waterwheel Falls, Yosemite National Park	37.92746	-119.45884	2073	17.34	7
MVZ 241021	ca. 4 km W of Glen Aulin along trail, N side of Tuolumne River, Waterwheel Falls, Yosemite National Park	37.92746	-119.45884	2073	17.34	7
MVZ 241010	ca. 3.5 km W of Glen Aulin along trail, N side of Tuolumne River, between LeConte and Waterwheel Falls, Yosemite National Park	37.92617	-119.45523	2101	17.67	7
MVZ 241016	ca. 3 km W of Glen Aulin along trail, N side of Tuolumne River, between LeConte and Waterwheel Falls, Yosemite National Park	37.92164	-119.44615	2100	18.53	8
MVZ 241017	ca. 3 km W of Glen Aulin along trail, N side of Tuolumne River, between LeConte and Waterwheel Falls, Yosemite National Park	37.92164	-119.44615	2100	18.53	8
MVZ 241018	ca. 3 km W of Glen Aulin along trail, N side of Tuolumne River, between LeConte and Waterwheel Falls, Yosemite National Park	37.92164	-119.44615	2100	18.53	8
MVZ 241013	ca. 3 km W of Glen Aulin along trail, N side of Tuolumne River, between LeConte and Waterwheel Falls, Yosemite National Park	37.92189	-119.44608	2261	18.53	8

Catalog Number	Specific Locality	Latitude	Longitude	Elevation (m)	Distance	Bin
MVZ 241005	ca. 2.5 km W of Glen Aulin along trail, N side of Tuolumne River, between LeConte and Waterwheel Falls, Yosemite National Park	37.92148	-119.44415	2375	18.71	9
MVZ 241006	ca. 2 km W of Glen Aulin along trail, California Falls, Tuolumne River, Yosemite National Park	37.91681	-119.44236	2324	18.93	9
MVZ 241007	ca. 2 km W of Glen Aulin along trail, California Falls, Tuolumne River, Yosemite National Park	37.91665	-119.44044	2353	19.10	9
MVZ 241008	ca. 2 km W of Glen Aulin along trail, California Falls, Tuolumne River, Yosemite National Park	37.91665	-119.44044	2353	19.10	9
MVZ 241009	ca. 2 km W of Glen Aulin along trail, California Falls, Tuolumne River, Yosemite National Park	37.91665	-119.44044	2353	19.10	9
MVZ 241067	SW corner of McGee Lake on rocky hillside, ca. 1 km SW of Glen Aulin, Yosemite National Park	37.90319	-119.43123	2488	20.10	10
MVZ 241069	SW corner of McGee Lake on rocky hillside, ca. 1 km SW of Glen Aulin, Yosemite National Park	37.90319	-119.43123	2488	20.10	10
MVZ 241070	SW corner of McGee Lake on rocky hillside, ca. 1 km SW of Glen Aulin, Yosemite National Park	37.90319	-119.43123	2488	20.10	10

Catalog Number	Specific Locality	Latitude	Longitude	Elevation (m)	Distance	Bin
MVZ 241071	SW corner of McGee Lake on rocky hillside, ca. 1 km SW of Glen Aulin, Yosemite National Park	37.90319	-119.43123	2488	20.10	10
MVZ 241072	SW corner of McGee Lake on rocky hillside, ca. 1 km SW of Glen Aulin, Yosemite National Park	37.90319	-119.43123	2488	20.10	10
MVZ 241073	SW corner of McGee Lake on rocky hillside, ca. 1 km SW of Glen Aulin, Yosemite National Park	37.90319	-119.43123	2488	20.10	10
MVZ 241074	SW corner of McGee Lake on rocky hillside, ca. 1 km SW of Glen Aulin, Yosemite National Park	37.90319	-119.43123	2488	20.10	10
MVZ 241076	SW corner of McGee Lake on rocky hillside, ca. 1 km SW of Glen Aulin, Yosemite National Park	37.90319	-119.43123	2488	20.10	10
MVZ 240990	ca. 0.5 mi E of Glen Aulin along trail, Yosemite National Park	37.91295	-119.42372	2384	20.61	11
MVZ 240991	ca. 0.5 mi E of Glen Aulin along trail, Yosemite National Park	37.91295	-119.42372	2384	20.61	11
MVZ 240992	ca. 0.5 mi E of Glen Aulin along trail, Yosemite National Park	37.91295	-119.42372	2384	20.61	11
MVZ 240994	ca. 0.5 mi E of Glen Aulin along trail, Yosemite National Park	37.91295	-119.42372	2384	20.61	11
MVZ 240995	ca. 0.5 km W of Glen Aulin, N side of Tuolumne River, Yosemite National Park	37.91295	-119.42372	2389	20.61	11

Catalog Number	Specific Locality	Latitude	Longitude	Elevation (m)	Distance	Bin
MVZ 240997	ca. 0.5 km W of Glen Aulin, N side of Tuolumne River, Yosemite National Park	37.91295	-119.42372	2389	20.61	11
MVZ 240998	ca. 0.5 km W of Glen Aulin, N side of Tuolumne River, Yosemite National Park	37.91295	-119.42372	2389	20.61	11
MVZ 240999	ca. 0.5 km W of Glen Aulin, N side of Tuolumne River, Yosemite National Park	37.91295	-119.42372	2389	20.61	11
MVZ 241000	ca. 0.5 km W of Glen Aulin, N side of Tuolumne River, Yosemite National Park	37.91295	-119.42372	2389	20.61	11
MVZ 241001	ca. 0.5 km W of Glen Aulin, N side of Tuolumne River, Yosemite National Park	37.91295	-119.42372	2389	20.61	11
MVZ 241002	ca. 0.5 km W of Glen Aulin, N side of Tuolumne River, Yosemite National Park	37.91295	-119.42372	2389	20.61	11
MVZ 241003	ca. 0.5 km W of Glen Aulin, N side of Tuolumne River, Yosemite National Park	37.91295	-119.42372	2389	20.61	11
MVZ 241004	ca. 0.5 km W of Glen Aulin, N side of Tuolumne River, Yosemite National Park	37.91295	-119.42372	2389	20.61	11
MVZ 240989	ca. 0.5 mi E of Glen Aulin along trail, Yosemite National Park	37.90764	-119.41962	2438	21.05	11

Chapter 3: Genetic divergence and phenotypic plasticity underlie trait differentiation in Western Fence Lizards (*Sceloporus occidentalis*)

NASSIMA M. BOUZID[1,2,*], LAUREN B. BUCKLEY[1], REGINA R. SPRANGER[3], BARRY SINERVO[3], & ADAM D. LEACHÉ[1,2]

[1]*Department of Biology, University of Washington, Box 351800, Seattle WA 98195–1800, USA*

[2]*Burke Museum of Natural History and Culture, University of Washington, Seattle, WA 98195, USA*

[3]*Department of Ecology and Evolutionary Biology, University of California, Santa Cruz, CA, 95064, USA*

**E-mail: bouzidnm@uw.edu*

Introduction

Species often exhibit variation in traits along environmental gradients. Trait variation may reflect adaptation to local environments along gradients, but explicit tests are needed to identify sources of trait variation (Kawecki & Ebert, 2004; Moran et al., 2016). Different sources of trait variation–including genetic adaptation, phenotypic plasticity, and drift–have different potential outcomes for future responses to climate change (Crispo, 2008; Moran et al., 2016). Trait variation produced by heritable differences between individuals is capable of evolving by natural selection, and therefore more likely to respond to new selective regimes produced by climate change (Hoffman & Sgrò, 2011). Trait variation produced by phenotypic plasticity enables maintenance of high fitness across spatially or temporally variable environments but may buffer organisms from selection and hinder future adaptation (Buckley & Huey, 2016; Chevin et al, 2010; Ghalambor et al., 2007; Huey et al., 2012). Genetic drift, which is most relevant for isolated or small populations subject to demographic stochasticity, can produce random trait variation with respect to environment (Bolnick et al., 2011).

Sceloporus lizards in the *undulatus* group (Leaché, 2010) exhibit variation in life history and phenotypic traits along environmental gradients. Variation in body size and growth rates of *S. graciosus* have been shown to vary with potential activity time, meaning that individuals in environments that provide more opportunities for foraging and growth generally grow faster and achieve larger adult body sizes (Adolph & Porter, 1993; Tinkle et al., 1993). Relationships between phenotypically variable populations and species have been explored with genetic data, enabling identification of genotypes that might be locally adapted (Chapter 1; Chapter 2; Leaché & Reeder, 2002; Leaché et al.,

2010). Foundational links between environmental conditions and variation in life-history and behavior have elucidated traits that are relevant to fitness in different environments (Jameson & Allison, 1976; Sears & Angilletta, 2004). Multiple lab rearing experiments have identified potential for phenotypic plasticity (acclimation) among populations and within clutches (Buckley et al., 2009; Sinervo & Adolph, 1989; Sinervo & Adolph, 1994; Tsuji, 1988). While temperature certainly factors into biological processes relevant to fitness, like growth and energy assimilation, in *Sceloporus* careful behavioral thermoregulation dampens its effects (Adolph & Porter, 1993; Huey et al., 2003; Sears & Angilletta, 2004; but see Grant, 1990).

Duration of activity impacts fitness of behavioral thermoregulators in contrasting thermal environments more directly than temperature (Sears & Angilletta, 2004; Sinervo et al., 2010). Preferred body temperatures of *Sceloporus* species are narrow–constrained by phylogeny and local environmental temperatures–and maintained via behavioral plasticity (Andrews, 1998; Bogert, 1949; McGinnis, 1970). As a result, lizards in high quality thermal environments (i.e., environments that support activity at preferred body temperatures) have prolonged activity periods, while lizards in low quality thermal environments have limited activity periods (Adolph & Porter, 1993; Huey, 1991; Sinervo & Adolph, 1994). The fitness implications of limited activity periods–and therefore limited opportunities for feeding, growth, and reproduction–can be dire; activity periods shortened by warming midday temperatures are expected to cause widespread declines in *Sceloporus* (Sinervo et al., 2010; but see Kearney, 2013). Warming is expected to lengthen activity periods in cold environments at high latitudes and elevations, but may

result in phenological shifts that increase juvenile mortality (e.g. exposure to freezing temperatures during incubation, starvation due to late emergence) (Levy et al., 2016).

Rapid local adaptation, resulting from genetic divergence, or phenotypic plasticity may facilitate colonization of new environments by enabling species to maintain high fitness across environmental gradients (Ghalambor et al., 2007; Kawecki & Ebert, 2004). Along elevation gradients, populations living in cold high elevation environments may suffer fitness consequences due to reduced daily and seasonal activity periods (Adolph & Porter, 1993; Sinervo & Adolph, 1994). In *Sceloporus* lizards, larger body sizes and darker coloration might ameliorate fitness consequences of life in cold, high elevation environments. For example, *S. undulatus* exhibit larger body sizes with increasing elevation and latitude, which are linked to a combination of genetically-based variation in growth rates, delayed maturation, and lower mortality rates (Blackburn et al., 1999; Sears & Angilletta, 2004). In contrast, cold environment *S. graciosus* achieve smaller body sizes; mortality rates are higher and growth rates are environmentally plastic, not genetically-based, potentially because of gene flow along elevation gradients (Sears & Angilletta, 2003; Tinkle et al., 1993). Lizards in cold environments may also increase heating rates by darkening skin color according to the thermal melanism hypothesis (Clusella-Trullas et al., 2007). Darker skin colors reflect less and absorb more radiant heat, enabling ectotherms to lengthen activity periods in cold environments (Gibson & Falls, 1979; Sherbrooke et al., 1994). While ample evidence supports the incidence of darker ectotherms in cold environments, the relative contributions of genetics and plasticity to fitness await further study (Clusella-Trullas et al., 2007; Moreno Azócar et al., 2015; Stevenson, 1985).

Western Fence Lizards (*Sceloporus occidentalis*) along elevation gradients in Yosemite National Park, California exhibit larger body sizes and darker, more melanistic coloration at high elevation (Leaché et al., 2010). The case study of *S. occidentalis* along the Grand Canyon of the Tuolumne River (GCT) is particularly well suited to testing whether trait clines have resulted from local adaptation or adaptive plasticity. Due to recent glaciation of high elevations in the Sierra Nevada, suitable habitat for *S. occidentalis* at high elevations has only become available within the last 10,000 years, meaning that trait differentiation has occurred recently (Chapter 1; Chapter 2). Phenotypically divergent populations at low and high elevations are also genetically divergent, which is a requirement for local adaptation (Chapter 2; Kawecki & Ebert, 2004). High elevation populations experience restricted daily and seasonal activity periods that put growth rates at a premium, especially for hatchling lizards that may have as little as 20 days between hatching and the first snowfall (Bouzid, field observations; Jameson & Allison, 1976; Sears & Angilletta, 2004). The short activity period at high elevation constrains both survival and energetics, and is therefore likely the primary selective pressure impacting *S. occidentalis* hatchlings (Jameson & Allison, 1976). A study comparing overwintering energetics and life histories of low (1500 m) and high (2200 m) elevation *S. occidentalis* from the central Sierra Nevada revealed that larger individuals amass larger energy reserves (fat bodies) and rely on these reserves for overwintering survival and spring reproduction (Jameson & Allison, 1976). Because energy acquisition and storage is paramount to overwintering survival of hatchlings, we expect adaptive traits to facilitate longer activity in short activity periods (e.g., traits that increase heating rates and heat retention or behaviors that maximize available time).

We determined whether trait clines along the GCT were produced by genetic divergence or phenotypic plasticity by rearing 36 low elevation (5 families) and 52 high elevation (8 families) hatchling lizards in a lab reciprocal transplant experiment. Building on knowledge that for thermoregulating ectotherms durations of activity periods are more relevant to fitness than thermal environment, we modified activity periods directly in two treatments and equally distributed low and high elevation hatchings among treatments in a factorial design. We quantified variation among and between populations and treatments in life history traits (clutch size, clutch mass, egg mass, incubation period, body size), growth rates, color, thermal preference, and activity. We evaluated three hypotheses to determine the underlying mechanism of trait divergence among low and high elevation hatchlings:

H_0: Neither population nor treatment affects trait variation, suggesting that neither local adaptation nor adaptive plasticity is the underlying mechanism.

H_1: Population and treatment affect trait variation, suggesting that local adaptation is the underlying mechanism.

H_2: Treatment, but not population, affects trait variation, suggesting that adaptive plasticity is the underlying mechanism.

Materials and methods

Ethical note

We collected wild lizards with permission from the National Park Service (Permit# YOSE-2018-SCI-0008) and California Department of Fish and Wildlife (SCP-13699). Lab husbandry and experiments were approved by Institutional Animal Care and

Use Committee (IACUC) protocol Sineb1802 (UC Santa Cruz). Field collection, euthanasia, and specimen preparation methods were approved by IACUC protocol 4209–01: Burke Collections (University of Washington).

Animal handling and care

Field collection. We conducted collection trips in Yosemite National Park, CA from May 20–24; May 28–Jun 1; Jun 11–14; Jun 20–24; and Jun 27–29, for a total of 22 days, all in 2018. We focused our efforts at one low elevation site and two high elevation sites. The low elevation site was located immediately east of the O'Shaugnessy Dam, along the Hetch Hetchy-Rancheria Falls trail north of Hetch Hetchy Reservoir (37.96°N, -119.78°W). We began lizard surveys each day at approximately 0600 hours (hrs), walking at a slow pace along the trail to Wapama Falls (4 km) and back, ending our survey between 1700–1900 hrs. Each day, we saw between 20 and 30 lizards, of which 1–2 were gravid females.

The high elevation sites were located just north of Tenaya Lake on the north side of Highway 120 (37.83°N, -119.46°W) and in the vicinity of Glen Aulin, ca. 6 miles (by foot) northwest of Tuolumne Meadows (37.91°N, -119.43°W). We began lizard surveys at approximately 0700 hrs, walking at a slow pace between the Glen Aulin High Sierra Camp and Waterwheel Falls along the Grand Canyon of the Tuolumne trail, ending our survey between 1600–1800 hrs. Each day, we saw between 30 and 50 lizards, of which 1–3 were gravid females. At all sites we caught lizards using a small loop of braided nylon thread attached to an expandable fishing pole. We noted that lizards at high elevation would allow us to approach to a closer distance than did those at low elevation.

We collected 13 *S. occidentalis*, all gravid (pregnant) females, between May 29 and June 24, 2018 (Table S1). Of these, 5 females were collected from low elevation (Hetch Hetchy [1200 m]) and 8 females were collected from high elevation (Tenaya Lake [2474 m] and Glen Aulin [2400 m]). In 2017, we were only able to sample one female from high elevation due to the high snowpack and delayed opening of Hwy 120 (on June 28, 2017). In 2018, Tioga Pass and Hwy 120 opened on May 21, enabling us to access high elevation sites and sample gravid females from high elevation. We report that in 2018 the narrow window of reproduction in which high elevation females carry fertilized eggs occurred between the second and fourth weeks of June.

Adult care. We transported gravid female lizards from Yosemite National Park to the UC Santa Cruz Coastal Science Campus within 3 days of collection. We housed lizards individually in 6 qt. (13 5/8" L x 8 1/4" W x 4 7/8" H) plastic containers with wire lids with 3" of 50:50 ground sphagnum moss:sand (moistened just until clumping) substrate to encourage egg laying (Appendix A). We kept enclosures in a climate-controlled greenhouse (21–25°C) with a natural photoperiod (ca. 14 hr day:10 hr night). We supplied females with 40 W incandescent bulbs (on for 9 hrs/day), rocks for basking, and hides opposite the heat lamp. We provided females with *Acheta domestica* crickets dusted with Reptivite calcium and mineral supplement (Zoo Med Laboratories, Inc., San Luis Obispo, CA) *ad libitum* and provided water by spraying sides of enclosures with water daily. We checked enclosures for the presence of eggs twice daily (mornings and evenings). At least 1 week after egg laying, we euthanized and prepared females as museum specimens, and collected liver tissue in RNAlater.

Egg care. Upon discovery during twice-daily checks, we excavated and weighed eggs to the nearest 0.00 g, and placed them individually in 2 oz deli cups filled with a 1:12 mixture of water and vermiculite. We recorded the combined weight of cup (minus lid), vermiculite, and egg as a target weight for replenishing water each week. We incubated eggs in a Percival environmental chamber (Percival Scientific, Inc., Perry, Iowa) at constant temperature (28°C). We kept egg-cups for each clutch in plastic containers, covered loosely with a plastic bag to prevent moisture loss. We rotated egg-cups within containers and containers throughout the chamber each week to ensure that all eggs experienced uniform conditions during incubation. From incubation days 1–29, we examined eggs and replenished the weight of evaporated water in the water:vermiculite mixture weekly. Following incubation day 29, we checked eggs daily for signs of hatching: small droplets of liquid on the egg surface, dimpling, or rupture.

Hatchling care. Following discovery of hatchling lizards, we measured mean thermal preference, snout-vent length (SVL), mass, and assigned unique toe-clip identifiers for each individual. We randomly assigned members of each clutch to either "long day" or "short day" treatments, which differed in the amounts of time hatchlings could access a thermal gradient produced by a radiant heat source (based on Sinervo & Adolph, 1989). During the "long day" treatment hatchlings could access the gradient for 12 hrs (0700–1900 hrs), while during the "short day" treatment hatchlings could access the gradient for 6 hrs (0800–1400 hrs). Low and high elevation hatchlings were raised in both treatments. We kept "long day" and "short day" enclosures on wire shelving racks, separated by 3 ft. Apart from the duration of thermal gradient access, all other rearing conditions (e.g., enclosure set-up, food, water) were identical among individuals.

We individually housed hatchlings in medium-sized plastic “Kritter Keeper” enclosures (11.9” L x 7.8” W x 8.1” H), filled with 0.5” of washed play sand. We provided hatchlings with two basking substrates in the enclosure corner closest to the heat source, a small rock and a nugget of pine bark. We arranged enclosures in groups of four, such that each group shared one radiant heat source (Appendix A). We used a 50 W UVB/UVA halogen bulb to provide both radiant heat and UVB radiation necessary for normal growth and development (Pough, 1991; but see Gehrmann et al., 1991). We fed each lizard 6 approximately equal-sized *Acheta domestica* crickets dusted with Rep-Cal Herptivite Multivitamin and Rep-Cal Calcium with Vitamin D3 (Rep-Cal Research Labs, Los Gatos, CA) and provided water by spraying sides of enclosures with water daily. To ensure that all hatchlings experienced uniform conditions within treatments, we randomly redistributed enclosures on shelves weekly. We reared hatchlings to 6-weeks of age.

We measured ambient air temperature and relative humidity in the greenhouse with a HOBO U23 Pro v2 Temperature/Relative Humidity Data Logger (U23-001). We set up two “dummy” enclosures for each treatment (4 enclosures total) on either end of the wire shelving rack to measure operative temperature differences between basking (rock) and hiding (under sand, opposite heat source). We used a HOBO 2x External Temperature Data Logger (U23-003) with two metal probes to measure substrate temperatures; we attached one probe to the basking rock (directly under the heat source) and the other probe to the bottom of the enclosure (under 0.5” sand, opposite the heat source) (Fig. S1; Appendix A).

Life-history variation

Clutch size and egg mass. Variation in *Sceloporus* body size has been explained by trade-offs between clutch size, egg mass, and time to reach maturity (Sears & Angilletta, 2004). Larger body sizes of hatchlings might increase fitness by supporting larger energy stores and increasing heat retention, which would facilitate greater overwintering success and longer activity, respectively (Jameson & Allison, 1976; Moreno Azócar et al., 2015). We investigated inter-population variation in clutch size and egg mass to determine whether life-history trade-offs explain variation in hatchling body size. Specifically, we compared hatchling and egg mass to determine if differences in maternal investment impact hatchling size and performance (Sinervo, 1990; Sinervo et al., 1991; Van Berkum et al., 1989). We also compared clutch sizes and egg mass of low and high elevation dams and tested for correlations between dam mass and clutch size and dam mass and egg mass.

Morphology and growth rate

Mass and SVL. Adult *S. occidentalis* achieve larger maximum body sizes at high elevation than at low elevation, but the mechanism is unclear (Jameson & Allison, 1976; Leaché et al., 2010). Unlike high latitude and high elevation *S. undulatus*, high elevation *S. occidentalis* do not delay maturation and instead mature at the same age as their low elevation counterparts (ca. 20 months; Jameson & Allison, 1976). The extremely short window for growth after hatching (< 50 days) and obligate hibernation period (6–9 months) suggests that to achieve larger body sizes in less time high elevation lizards must

have accelerated growth rates. We tested this hypothesis by calculating instantaneous growth rates (IGR) for mass and length between time intervals *i* and *i*-1:

$$IGR = ln(mass_i/mass_{i-1})/(time_i - time_{i-1})$$

Within 12 hrs of hatching, we weighed hatchlings to the nearest 0.00 g, measured snout-vent length (SVL) to the nearest mm, and assigned a unique identifier by clipping the end of one digit per hand/foot immediately below the nail. Each week thereafter, we re-weighed hatchlings to the nearest 0.000 g and measured SVL to the nearest mm; in total we collected seven weight and length measurements per individual over the course of the experiment. To ensure that we recorded measurements for the correct individual, we matched toe-clip and hatchling identifiers prior to each measurement. We evaluated whether hatchlings exhibited differences in SVL immediately after hatching, and whether interactions of population and treatment produced different SVL by the end of the experiment.

Body shape. To quantify changes in overall body shape, we calculated body condition index (BCI) with the following equation:

$$BCI = \sqrt[3]{mass}/SVL$$..

Body condition is a measurement that incorporates both mass and SVL and has been shown to be repeatable over short time periods in *S. occidentalis* hatchlings (Van Berkum et al., 1989). In other words, body shape at hatching is an accurate predictor of body shape and performance (e.g. sprint speed, Sinervo et al., 1991) later in development. We evaluated whether hatchlings exhibited differences in BCI immediately after hatching, and whether interactions of population and treatment produced different BCI by the end of the experiment.

Color

Illuminance. Properties of reptile skin impact the flux of heat, and can facilitate activity by enabling individuals to reach preferred active body temperatures quicker (Clusella-Trullas et al., 2009; Gibson & Falls, 1979; Sherbrooke et al., 1994). Physiological mechanisms behind lightening and darkening of reptile skin involve changes in the distribution and density of melanin stored in melanophores (Merchant et al., 2018). Changes in color for the purpose of thermoregulation has been well-documented in lizards (Fan et al., 2014; Geen et al., 2014; Langkilde & Boronow, 2012). Plastic color changes in response to developmental and environmental temperatures have been documented in *Sceloporus* and other ectotherms (Davis et al., 2005; Gibson & Falls, 1979; Kingsolver & Buckley, 2018; Langkilde & Boronow, 2012; Michie et al., 2010; Sherbrooke et al., 1994), but not in response to activity period. We evaluated genetic and plastic constituents of hatchling color, by directly modifying activity period. We measured illuminance, the amount of light reflected per image pixel, as an estimate of "darkness" of dorsal coloration (Troscianko & Stevens, 2015). Larger illuminance values correspond to lighter colors with higher reflectances. We photographed the dorsal surface of hatchlings at three time points in development (2-weeks, 4-weeks, and 6-weeks of age) to track ontogenetic shifts in coloration. We took photos in RAW format with a Nikon D3300 DSLR camera and AF-S DX Micro-NIKKOR 40 mm f/2.8G lens. We included a metric ruler and two reflectance standards (40% Gray [60% reflectance] and 80% Gray [20% reflectance]; SpyderCHECKR® 24 color standards) within the same plane as the hatchling in each photo. Including reflectance standards enabled us to correct for differences in illumination between photos (Troscianko & Stevens, 2015). We restrained

and positioned hatchlings on black cardstock with clear athletic tape, and released hatchlings by wetting the athletic tape.

We used ImageJ version 1.51 (Schneider at al., 2012) and the Multispectral Image Calibration and Analysis Toolbox (Troscianko & Stevens, 2015) to process 261 photos for 87 individuals. For each photo, we set a 10 mm scale bar and selected the dorsal surface of the hatchling and the lighter reflectance standard (40% Gray) as a measurement control. To standardize the areas measured across hatchlings, we drew a polygon with vertices at the armpits of the forelimbs and at the inguinal regions anterior to the hind limbs (Fig. S2). We repeated measurements for which the control illuminance fell outside of the interquartile range (outliers). We quantified total illuminance by adding together illuminances detected by the red, green, and blue channels (Corl et al., 2018; Troscianko & Stevens, 2015).

Thermal Preference

Preferred body temperatures of hatchlings and juveniles have received little attention compared to preferred body temperatures of adults (Angilletta et al., 1999). However, habitat selection and foraging behavior are known to vary ontogenetically, which might impact microhabitat availability and thermoregulatory behavior of hatchlings (Congdon et al., 1993; Huey, 1991; Huey & Pianka, 1981; Huey & Slatkin, 1976; Magnuson et al., 1976; Rose, 1976). In the few cases that have been studied, hatchlings prefer higher body temperatures than older juveniles and adults, but the point at which preferred body temperatures lower remains unclear (Lang, 1981; Perez-Quintero, 1994).

Preferred body temperatures of hatchlings vary across environments and might contribute to rapid initial growth after hatching (Sinervo, 1988; Sinervo & Adolph, 1989). In a common garden experiment of *S. occidentalis* hatchlings from Oregon and California, hatchlings experienced rapid growth between 3–7 days of age and hatchlings that selected higher body temperatures had faster growth rates (Sinervo, 1990; Sinervo & Adolph, 1989). Northern *S. occidentalis* hatchlings from Oregon (cold environments) selected lower preferred temperatures than southern hatchlings from California (warm environments) (Sinervo, 1988). In contrast, adult *S. occidentalis* from different habitats do not exhibit differences in field body temperatures or preferred body temperatures; instead, adults modify activity periods by becoming inactive when temperatures are too hot or too cold for effective thermoregulation (McGinnis, 1966; McGinnis, 1970; McMillan, 2010). According to previous studies, high elevation hatchings in Yosemite should select higher body temperatures to optimize growth and increase chances of overwintering survival. We evaluated whether thermal preference of high elevation hatchlings is locally adapted or adaptively plastic by comparing low and high elevation hatchlings reared in short and long activity periods. We also compared thermal preference of low and high elevation post-gravid adult females.

Adults. We measured thermal preference for females during daylight hours (between 1100–1700 hrs) one week after laying eggs to standardize any potential variation related to differences in reproductive state. We acclimated females to 20–22°C for at least 15 minutes before placing them in a thermal gradient (40°C hot end, 20°C cool end). The multi-lane thermal gradient was constructed out of medium density fiberboard and each lane measured 36” L x 8” W x 15” H (Appendix A). We inserted an ultrathin “Type T”

thermocouple probe, blunted by a small amount of epoxy resin, 1 cm into the cloaca and secured it which a piece of clear athletic tape. We acclimated lizards for an additional 15 minutes within the thermal gradient, and then recorded internal body temperature readings every 5 minutes for 2 hrs with an Omega^{TM} 8-channel USB Temperature Data Logger (model TC08). We discarded temperature readings during which the thermocouple broke or was extruded from the lizard. We averaged temperature readings for each individual to calculate a single preferred body temperature.

Hatchlings. We measured thermal preference of hatchlings at three time points: immediately after hatching, at 3-weeks, and at 6-weeks. We measured multiple time points to determine whether hatchlings ontogenetically shift thermal preference according to activity period. We constructed thermal gradients out of plastic, terra cotta colored planter boxes, each with a 100 W incandescent bulb suspended over one end (Appendix A). The thermal gradient varied from 20°C on the cool end to 55°C on the hot end. We acclimated hatchlings for 10 minutes within the thermal gradient, and then measured body temperatures every 5 minutes for 1 hour. We used an Amprobe (IR-750) infrared temperature gun to record temperatures of the dorsal midbody. We took care to avoid disturbing hatchlings during thermal preference trials, but if one was disturbed we waited an additional five minutes before recording body temperature. We averaged recorded temperatures for each individual to calculate a single preferred body temperature.

Behavior

Proportion of 'active' behaviors. Lizards maintain stable active body temperatures by selecting microhabitats within their environments (e.g., shuttling between sun and shade),

altering their positions relative to the sun, and modifying activity periods (Adolph, 1990; Anderson et al., 1986; Huey & Slatkin, 1976; Sears & Angilletta, 2004). Thus, thermoregulation is an 'active' behavior, meaning that lizards must actively maintain body temperatures suitable for efficient foraging, digestion, and assimilation (Adolph & Porter, 1993). However, thermoregulation may not always be beneficial; costs like exposure to predation, high energy expenditure, or inefficient energy processing might outweigh the benefits of continued thermoregulation (Huey & Slatkin, 1976).

Hatchlings at low and high elevations in Yosemite occupy different environments in terms of predation pressure, temperature, and seasonal activity restrictions. Adult *S. occidentalis* from different habitats cope with different environmental conditions by modifying thermoregulatory behavior (McGinnis, 1970; McMillan, 2010). To determine whether thermoregulatory behavior under activity restrictions is plastic or genetically hardwired, we scored the proportion of time engaged in 'active' behaviors throughout the day. On Sep 22, when hatchlings were between 3–6 weeks of age, we scored behaviors as either active or inactive for each hatchling at 30 min intervals. Hatchlings remained undisturbed in their enclosures and treatments. We began recording 30 minutes before heat/UV lamps turned on (0630 hrs) and ended 30 minutes after lamps turned off (1930 hrs). We categorized basking, moving, and feeding as active behaviors (scored as 1) and hiding under sand or under rock as inactive behaviors (scored as 0). We obtained 25 total observations per individual and did not record behaviors between 1200–1300 hrs while we fed hatchlings. We calculated the proportion of activity by dividing the sum of the scores by the total number of observations.

Analysis

Our primary goals were: (1) to determine whether hatchlings from the same population, but reared in different treatments, exhibited the same (genetics) or different (plasticity) traits; and (2) to determine whether hatchlings from different populations, but reared in the same treatment, exhibited the same (plasticity) or different (genetics) traits. Within populations (i.e., low elevation or high elevation), we interpreted similarities in traits of individuals reared in different treatments as evidence for an underlying genetic basis. We interpreted differences in traits of individuals reared in different treatments as evidence for an underlying plastic response to activity period. We considered traits to be adaptive and increase fitness for high elevation hatchlings if they facilitated extended activity and/or faster growth under restricted activity periods. Low elevation hatchlings may not be under strong selective pressure to maximize activity and growth because daily and seasonal activity periods are longer (Sinervo & Adolph, 1989). Low elevation lizards mature at smaller adult sizes in the same time period as larger high elevation lizards, meaning that growth rates of low elevation lizards are comparatively slower (Jameson & Allison, 1976). Furthermore, predation pressure is higher at low elevation, so increased activity is a cost of thermoregulation (Huey & Slatkin, 1976). Therefore, we considered traits to be adaptive and increase fitness for low elevation hatchlings if they facilitated reduced activity and/or slower growth under restricted activity periods.

Local adaptation in traits should manifest as a gene-environment interaction in which native genotypes have a home-site fitness advantage, therefore locally adapted traits must have a genetic component (Kawecki & Ebert, 2004). Locally adapted traits must also exhibit fitness trade-offs in different environments (e.g., high growth rates in

low elevation environments may not be energetically feasible) (Storm & Angilletta, 2007). Adaptive plasticity should manifest as similar traits in similar environments for different populations (e.g., similar growth rates for both low and high elevation lizards raised in the same environment). In both cases, traits should increase fitness in respective treatments.

We conducted all statistical analyses in R version 3.3.3 (R Core Team, 2017) and we considered p values less than 0.05 to be significant.

Life history variation. We used t-tests to test for differences between low and high elevation populations in the following life history traits: dam mass (after egg laying), egg mass, total clutch mass, clutch size, incubation time, mass at hatching, and SVL at hatching. We identified potential origins of life history variation by testing for correlations between life history traits. We used linear regression to test for associations between the following independent and dependent variables, respectively: dam mass and mean egg mass; dam mass and total clutch mass; dam mass and clutch size; clutch size and mean egg mass; egg mass and hatchling mass; and egg mass and incubation time.

Tests of local adaptation and adaptive plasticity. We used factorial repeated measures analysis of variance (ANOVA, three-way) to test for differences in trait means across time, population, and treatment. We followed significant factor interactions from the ANOVA with post hoc Tukey tests or pairwise t-tests for all 6 possible comparisons of 2 populations (low and high elevation) and 2 treatments (long and short activity period). We used the Bonferroni multiple-comparison correction method to adjust p values of post hoc tests. We evaluated the following traits for local adaptation and adaptive plasticity: mass-specific growth rate, color (illuminance), thermal preference, and activity

proportion. We also tested for correlations between fitness related traits: mass-specific growth rate and color; color and thermal preference; color and activity proportion, and mass-specific growth rate and activity proportion.

Results

Life history variation

High elevation gravid females were significantly heavier and produced more eggs than low elevation females, but population-level differences in total clutch mass and egg mass were not significant (Table 1). Larger egg mass as a proxy for increased maternal investment has been shown to explain larger hatchling size and longer incubation time between populations (Sinervo, 1990). However, despite lacking population-level differences in egg mass, high elevation hatchlings hatched sooner (~ 2 days) and were heavier and longer than low elevation hatchlings (Table 1). This suggests that genetic variation between populations also factors into hatchling traits.

Associations between life history traits are possible explanations for body size variation between low and high elevation hatchlings. Dam mass was not significantly associated with mean egg mass, total clutch mass, or clutch size, which suggests that low and high elevation females do not differ in tradeoffs between maternal provisioning and offspring number (Niewiarowski et al., 2004; Sinervo, 1990; Table 2). Clutch size was not significantly associated with single egg mass, which further supports the lack of a tradeoff between offspring number and maternal provisioning. Egg mass was significantly and positively associated with hatchling mass immediately after hatching. However, variation in egg mass reduced variation in hatchling mass in the linear model by only 28% for the high elevation population, compared with 74% for the low elevation

population (Fig. 1a; Table 2). This suggests that egg mass is a better predictor of hatchling mass at low elevations, but that additional sources of variation, like genetics or content of maternal provisioning, factor into hatchling mass at high elevation (Storm & Angilletta, 2007). Egg mass was significantly and positively associated with incubation time for high elevation hatchlings, which suggests that heavier eggs take longer to incubate and is consistent with previous work (Fig. 1b; Table 2; Sinervo, 1990).

Morphology and growth rates

We compared body conditions of hatchlings to assess the influence of activity period on growth in the first 6 weeks after hatching. Immediately after hatching, mean body condition of low elevation hatchlings (0.033 ± 0.0008) was greater than mean body condition of high elevation hatchlings (0.032 ± 0.0008) ($t(70.52) = -4.72$, $p < 0.001$). At 6 weeks of age, we found no differences in body condition between any pairwise comparison of population and treatment.

Body size differences between low and high elevation hatchlings were apparent at hatching. High elevation hatchlings were significantly heavier and longer than low elevation hatchlings (Fig. 2; Table 3). In another study, hatchlings with larger body sizes had higher mass specific growth rates, which would be beneficial for hatchlings in environments with restricted activity periods (Sinervo & Adolph, 1989). A three-way repeated measures ANOVA yielded a main effect of time point (week) on hatchling mass ($F(1, 84) = 2133.78$, $p < 0.001$), meaning that hatchlings increased in mass from week to week. The interaction effects of time point and population ($F(1, 84) = 30.44$, $p <0.001$) and of time point and treatment ($F(1, 84) = 16.89$, $p <0.001$) both significantly impacted

hatchling mass. The time point-population effect indicates that population impacted change in mass from week to week; the time-point-treatment interaction effect indicates that treatment impacted change in mass from week to week. The interaction effect of time point, population, and treatment was not significant ($F(1, 84) = 0.003$, $p = 0.95$).

After 6 weeks, high elevation hatchlings reared in the same and in different treatments had significantly different mass and SVL (Fig. 2; Table 3). Generally, high elevation hatchlings were larger than low elevation hatchlings when reared in the same treatment, which suggests that genetics underlies differences in body size between populations. High elevation hatchlings from long activity periods were larger than high elevation hatchlings from short activity periods; the difference in size stems from faster mass-specific growth rates of high elevation hatchlings in long activity periods between 1 and 2 weeks of age (Fig. 3). In long activity periods, low elevation hatchlings were smaller than high elevation hatchlings; the difference in size stems from faster growth rates of high elevation hatchlings between 2 and 4 weeks of age. Low elevation hatchlings reared in different treatments did not significantly differ in body size by the end of the experiment, despite faster growth of low elevation hatchlings in long activity periods between 4 and 5 weeks of age (Fig. 3; Table 3). Interestingly, the body sizes of populations reared in 'native' conditions–high elevation in short activity periods and low elevation in long activity periods–did not differ. If our lab-simulated activity restrictions reasonably reflect those in nature, we expect wild hatchlings to be indistinguishable in body size if trait variation is produced exclusively by phenotypic plasticity. Currently, body size clines in *Sceloporus* are explained by differences in time to reach maturity; similarities in growth rates and body sizes of hatchlings reared in 'native' conditions

supports this theory, but a long-term study of Sierra Nevada *S. occidentalis* has confirmed that low and high elevation lizards reach maturity at the same age (Jameson & Allison, 1976; Sears & Angilletta, 2004).

Mass-specific growth rates underwent two phases of rapid growth before beginning to decelerate (Fig. 3). We observed an initial phase of rapid growth between 1 and 2 weeks of age in all population-treatment combinations. High and low elevation hatchlings in long activity periods grew fastest during this phase. We observed a second phase of rapid growth between 3 and 4 weeks of age, during which high elevation hatchlings in both treatments and low elevation hatchlings in long activity periods accelerated growth, but growth rates of low elevation hatchlings in short activity periods began to plateau.

Tests for local adaptation in growth rates were inconclusive. We compared growth rates among and between populations and treatments at time points during which growth rates different significantly (weeks 2, 3, 4, 5; Fig. 3). At 2 weeks of age, growth rates were in the opposite direction of our expectations for local adaptation; low elevation hatchlings grew faster in short activity periods and high elevation hatchlings grew faster in long activity periods (Fig. 1a; Fig. S3). By 5 weeks of age, the pattern had reversed and was consistent with our expectations for local adaptation; high elevation hatchlings grew faster in short activity periods and low elevation hatchlings grew faster in long activity periods. If hatchlings continued growth trajectories apparent at 6 weeks of age, local adaptation of growth rates would be supported.

Color

Hatchlings from both populations are capable of plastically changing color. Illuminance of low elevation hatchlings in long activity periods remained consistently and significantly higher than illuminance of low elevation hatchlings in short activity periods (Fig. 4). High elevation hatchlings in long activity periods trended lighter than high elevation hatchlings in short activity periods until 6 weeks of age, at which point high elevation hatchlings in long activity periods became significantly lighter. Low elevation hatchlings were lighter in long activity periods than high elevation hatchlings in long activity periods, but at 6 weeks of age high elevation hatchlings began to lighten. In all population-treatment combinations, hatchlings became lighter with age. According to the thermal melanism hypothesis, darker coloration (lower reflectance) should facilitate faster heating rates and therefore be adaptive in cold environments (Clusella-Trullas et al., 2007). Under activity period restrictions, faster heating rates would be adaptive if they facilitated extended activity and/or growth. Illuminance was significantly and negatively associated with mass-specific growth rate (Fig. 5). In both low and high elevation populations variation in color explained approximately 25% of variation in mass-specific growth rates. Darker individuals (lower illuminance) grew faster than lighter individuals; significant color differences under native conditions suggest that trait divergence in color is produced by local adaptation. However, the demonstrated ability of high elevation hatchlings to change color in adaptive directions (light in long and dark in short activity periods) indicates that variation in color might be at least partially produced by adaptive plasticity (Fig. 4 Fig. 5).

Thermoregulatory behavior

Preferred body temperatures measured within 12 hrs of hatching indicated that low elevation hatchlings might select higher preferred body temperatures (34.47°C ± 4.19) than high elevation hatchlings (33.57°C ± 3.32) ($t(71.56) = -2.00$, $p = 0.05$) (Fig. S3). Subsequent measurements of thermal preference at 3 weeks and 6 weeks of age did not yield significant differences between any combination of population and treatment, meaning that preferred body temperatures were essentially the same. Adult females measured 1 week after laying eggs did not have significantly different preferred body temperatures (HE: 34.53°C ± 2.79; LE: 35.78°C ± 1.87; $t(11.46) = 1.06$, $p = 0.31$).

Thermoregulatory behavior appears to have a genetic basis and may be suggestive of local adaptation in behavioral strategies. The proportion of active behaviors differed significantly between populations ($F(2, 82) = 15.21$, $p < 0.001$) and between treatments ($F(1, 82) = 17.42$, $p < 0.001$). However, the interaction between population and treatment on proportion of active behaviors was not significant ($F(2, 82) = 2.42$, $p = 0.10$); low elevation hatchlings did not significantly differ between treatments. High elevation hatchlings in long activity periods were active for longer than hatchlings in any other treatment (Tukey HSD, Fig. S4). While the difference in activity time for high elevation hatchlings in short activity periods was not significantly different from that of low elevation hatchlings in short activity periods (Tukey HSD, Fig. S4), it trended towards being longer for high elevation hatchlings (Fig. 4; Fig. S4). Activity time of low elevation hatchlings, regardless of treatment, trended towards being shorter.

Discussion

Variation between low and high elevation *S. occidentalis* populations in the central Sierra Nevada has been investigated in two previous studies (Jameson & Allison, 1976; Leaché et al., 2010). Both studies found evidence for significantly larger body sizes of high elevation *S. occidentalis.* Jameson and Allison (1976) noted a trend in which high elevation lizards had larger clutches and postulated that larger body sizes might accommodate larger fat stores needed for overwintering and reproduction. We built on these foundational studies by investigating life history variation within our sample of gravid females and eggs from Yosemite National Park.

Activity period restrictions are the primary environmental constraints on growth and body size for *Sceloporus* (Levy et al., 2016; Sears & Angilletta, 2003; Sinervo & Adolph, 1994; Sinervo et al., 2010). Recently established high elevation populations of *S. occidentalis* in the Sierra Nevada face extreme activity restrictions (up to 9 months of hibernation), yet they mature in the same amount of time as their low elevation counterparts (Jameson & Allison, 1976). High elevation *S. occidentalis* exhibit trait clines in color and body size along elevation gradients that are consistent with the thermal melanism hypothesis and Bergman's clines, respectively, but links between differences in traits and fitness remain to be investigated (Clusella-Trullas et al., 2007; Leaché et al., 2010; Sears & Angilletta, 2004). Recent studies of correlations between hormone levels, behavior, and color in low and high elevation *S. occidentalis* have been unable to identify the underlying mechanisms of trait differentiation along elevation gradients in the Sierra Nevada, and urge additional studies aimed at disentangling genetic and plastic constituents of phenotypes (Seddon & Hews, 2017; Seddon & Hews, 2016). We

employed an integrative reciprocal transplant approach to investigating both the underlying mechanisms of trait differentiation and the potential fitness implications of trait variation in restricted activity periods.

High elevation hatchlings are under strong selection within the first 2 months of hatching; hatchlings begin emerging in early July, and continue hatching until the onset of snowfall at high elevation, so hatchlings have a limited window for growth before first overwintering (Jameson & Allison, 1976). High elevation males and females rely on large energy stores for overwintering success and spring reproduction, so faster growth rates and larger body sizes to accommodate energy stores provide a fitness advantage in environments with activity period restrictions (Jameson & Allison, 1976). Low and high elevation dams did not produce clutches of different size or mass, yet high elevation hatchlings were heavier and longer (Fig. 2). Even though high elevation dams did not provide additional maternal provisioning to jump-start growth in the form of larger eggs with larger yolks, hatchlings might be larger because of differences in embryo respiration or yolk assimilation rates (Storm & Angilletta, 2007).

We found evidence for both genetic and plastic constituents of divergent low and high elevation phenotypes. High elevation hatchlings were genetically-hardwired to maximize activity and take advantage of longer activity periods and tended to be larger and darker in coloration (Fig. 2; Fig. 4; Fig. 6). At hatching, high elevation hatchlings appeared 'preset' for short activity periods; darker coloration and larger body size of hatchlings might enable faster heating rates–and longer activity periods–and faster growth rates (Gibson & Falls, 1979; Sinervo & Adolph, 1989). High elevation hatchlings exhibited plasticity in growth rates and in color (Fig. 3; Fig. 4). By 6 weeks of age

'foreign' high elevation hatchlings became significantly lighter than their 'native' counterparts and trended towards becoming lighter than 'native' low elevation hatchlings (Fig. 4). While 'foreign' high elevation hatchlings shifted thermoregulatory behavior and color in a direction that would enable more activity and faster growth in environments with long activity periods, maximizing activity might not be beneficial in all environments (Huey & Slatkin, 1976).

High elevation hatchlings appeared to be genetically hardwired to be more active in all activity periods, but at low elevations where activity periods are longer and predation risk is higher their canalized behavioral strategy would reduce fitness by increasing exposure to predators. High elevation hatchlings appear to be "growth opportunists," meaning that they utilize all available activity time and resources to increase growth. This is an interesting counterexample to Sinervo and Adolph (1994), who found that *S. occidentalis* hatchlings from high latitude, activity restricted populations in Oregon were "short-day specialists" instead of "growth opportunists". Oregon hatchlings had similar behavioral strategies to low elevation Yosemite hatchlings–despite ample thermal opportunity in the lab, hatchlings were inactive for a greater proportion of time, were smaller, and grew more slowly (Sinervo, 1988; Sinervo & Adolph, 1989). At low elevation in Yosemite this strategy is consistent with high predation (Leaché, Bouzid, field observations). At high elevation in Yosemite either predation pressure is lower, or the benefits of prolonged activity for growth outweigh the potential costs. Prolonged activity at high elevation, where thermal opportunity is lower, might be a locally adapted behavioral strategy; the benefits of prolonged activity in foreign, low elevation environments in nature would not outweigh the cost of predation

(Huey & Slatkin, 1976). Similarly, conservative activity at low elevation, where predation pressure is higher, might be indicative of local adaptation; the benefits of conservative activity in foreign, high elevation environments in nature might not outweigh the cost of overwintering without sufficient energy stores. Choosing to be inactive in long activity periods–even in lab conditions where thermal opportunity was high, food was abundant, and the chance of predation was close to zero–may reflect a canalized behavioral strategy to increase chances of survival and avoid predation (Ghalambor et al., 2010). In this case, voluntarily limiting activity periods in low elevation environments with higher predation pressure might be a behavioral adaptation to local selection (Fig. 6). In native environments (long activity period treatment) reduced activity might increase fitness by limiting exposure to predators, but reduced activity in foreign, high elevation environments would decrease fitness by slowing growth and preventing hatchlings from achieving large body sizes (Fig. 6). Field studies of behavioral strategies and growth rates of low and high elevation *S. occidentalis* populations will provide further evidence for evaluating local adaptation.

Rather than being directly under selection, dark color might be an accessory to increasing activity and therefore growth rates at high elevation. Darker coloration to increase heating rates is beneficial in cold environments, but may be maladaptive in warm environments (Clusella-Trullas et al., 2007; Gibson & Falls, 1979). However, even in cold, high elevation environments heat stress is a risk because of the intensity of solar radiation (Stevenson, 1985). Plasticity in color may be a safety measure to prevent overheating; the relative costs and benefits of color vary dramatically under different environmental conditions, so maintaining a constant color is not beneficial (Langkilde &

Boronow, 2012). The short time frame over which hatchlings changed color suggests that plastic changes in color may be more pervasive across ontogeny, and potentially across seasons, than previously thought. Plastic color change to facilitate background matching and thermoregulation in lizards has been documented (Corl et al., 2018; Langkilde & Boronow, 2012; Porter, 1967). However, interactions between seasonal variation in thermoregulatory behavior and variation in color have received relatively little attention. Variation in skin reflectance of *S. occidentalis* in different habitats has been attributed to local adaptation, but might be an accessory to support canalized behavioral strategies (Porter & Norris, 1969). We urge those studying local adaptation of coloration in ectotherms to also consider potential interactions with other fitness-related traits like thermoregulatory behavior and growth rates.

Acknowledgments

We thank the National Park Service and California Department of Fish and Wildlife for allowing us to collect lizards from Yosemite National Park. Thanks to Ammon Corl and Pauline Blaimont for providing animal husbandry and experimental training and troubleshooting. Thanks to Ann Trápaga, Charlotte Jennings, Ellen Murphy, Natasha Stepanova, Dana Lin, Leonard Jones, Rachel Gittelman, Petr Novodvorskiy for providing help in the field. This project was funded by an NSF DDIG (DEB- 1701231) awarded to A.D.L., N.M.B., and L.B.B.

References

Adolph, S. C. (1990). Influence of behavioral thermoregulation on microhabitat use by two *Sceloporus* lizards. Ecology, 71, 315–327.

Adolph, S. C., & Porter, W. P. (1993). Temperature, activity, and lizard life histories. The American Naturalist, 142, 273–295.

Anderson, D. K., Bowker, R. G., Damschroder, S., & Sweet, A. M. (1986). Thermoregulatory behavior of the North American lizards *Cnemidophorus velox* and *Sceloporus undulatus*. Amphibia-Reptilia, 7, 335–346.

Andrews, R. M. (1998). Geographic variation in field body temperature of *Sceloporus* lizards. Journal of Thermal Biology, 23, 329–334.

Angilletta Jr, M. J., Montgomery, L. G., & Werner, Y. L. (1999). Temperature preference in geckos: diel variation in juveniles and adults. Herpetologica, 212–222.

Blackburn, T. M., Gaston, K. J., & Loder, N. (1999). Geographic gradients in body size: a clarification of Bergmann's rule. Diversity and Distributions, 5, 165–174.

Bogert, C. M. 1949. Thermoregulation and eccritic body temperatures in Mexican lizards of the genus *Sceloporus*. Sobreiro de los Anales del Instituto de Biologia Mexico, 20, 415–426.

Bolnick, D. I., Amarasekare, P., Araújo, M. S., Bürger, R., Levine, J. M., Novak, M., Rudolf, V. H. W., Schreiber S. J., Urban, M. C., & Vasseur, D. A. (2011). Why intraspecific trait variation matters in community ecology. Trends in Ecology & Evolution, 26, 183–192.

Buckley, C. R., Irschick, D. J., & Adolph, S. C. (2009). The contributions of evolutionary divergence and phenotypic plasticity to geographic variation in the western fence lizard, *Sceloporus occidentalis*. Biological Journal of the Linnean Society, 99, 84–98.

Buckley, L. B. (2007). Linking traits to energetics and population dynamics to predict lizard ranges in changing environments. The American Naturalist, 171, E1–E19.

Buckley, L. B., & Huey, R. B. (2016). How extreme temperatures impact organisms and the evolution of their thermal tolerance. Integrative and Comparative Biology, 56, 98–109.

Buckley, L. B., Nufio, C. R., & Kingsolver, J. G. (2014). Phenotypic clines, energy balances and ecological responses to climate change. Journal of Animal Ecology, 83, 41–50.

Cabezas-Cartes, F., Boretto, J. M., & Ibargüengoytía, N. R. (2018). Effects of Climate and Latitude on Age at Maturity and Longevity of Lizards Studied by Skeletochronology. Integrative and Comparative Biology, 58, 1086–1097.

Campbell-Staton, S. C., Bare, A., Losos, J. B., Edwards, S. V., & Cheviron, Z. A. (2018). Physiological and regulatory underpinnings of geographic variation in reptilian cold tolerance across a latitudinal cline. Molecular Ecology, 27, 2243–2255.

Castella, B., Golay, J., Monney, J. C., Golay, P., Mebert, K., & Dubey, S. (2013). Melanism, body condition and elevational distribution in the asp viper. Journal of Zoology, 290, 273–280.

Chevin, L. M., Lande, R., & Mace, G. M. (2010). Adaptation, plasticity, and extinction in a changing environment: towards a predictive theory. PLoS Biology, 8, e1000357.

Clusella-Trullas, S., van Wyk, J. H., & Spotila, J. R. (2007). Thermal melanism in ectotherms. Journal of Thermal Biology, 32, 235–245.

Clusella-Trullas, S., van Wyk, J. H., & Spotila, J. R. (2009). Thermal benefits of melanism in cordylid lizards: a theoretical and field test. Ecology, 90, 2297–2312.
Congdon, J. D., Gotte, S. W., & McDiarmid, R. W. (1993). Ontogenetic changes in habitat use by juvenile turtles (*Chelydra serpentina* and *Chrysemys picta*). Canadian Field-Naturalist, 106, 241–248.
Corl, A., Bi, K., Luke, C., Challa, A. S., Stern, A. J., Sinervo, B., & Nielsen, R. (2018). The genetic basis of adaptation following plastic changes in coloration in a novel environment. Current Biology, 28, 2970–2977.
Crispo, E. (2008). Modifying effects of phenotypic plasticity on interactions among natural selection, adaptation and gene flow. Journal of Evolutionary Biology, 21, 1460–1469.
Davis, A. K., Farrey, B. D., & Altizer, S. (2005). Variation in thermally induced melanism in monarch butterflies (Lepidoptera: Nymphalidae) from three North American populations. Journal of Thermal Biology, 30, 410–421.
Fan, M., Stuart-Fox, D., & Cadena, V. (2014). Cyclic colour change in the bearded dragon *Pogona vitticeps* under different photoperiods. PloS one, 9, e111504.
Geen, M. R., & Johnston, G. R. (2014). Coloration affects heating and cooling in three color morphs of the Australian bluetongue lizard, *Tiliqua scincoides*. Journal of Thermal Biology, 43, 54–60.
Ghalambor, C. K., Angeloni, L. M., & Carroll, S. P. (2010). Behavior as phenotypic plasticity. Evolutionary Behavioral Ecology. In: Evolutionary Behavioral Ecology (D.F. Westneat & C.W. Fox, eds), pp. 161–187. Oxford University Press, New York.
Ghalambor, C. K., McKay, J. K., Carroll, S. P., & Reznick, D. N. (2007). Adaptive versus non-adaptive phenotypic plasticity and the potential for contemporary adaptation in new environments. Functional Ecology, 21, 394–407.
Gibson, A. R., & Falls, B. B. (1979). Thermal biology of the common garter snake *Thamnophis sirtalis* (L.). Oecologia, 43, 79–97.
Grant, B. W. (1990). Trade-offs in activity time and physiological performance for thermoregulating desert lizards, *Sceloporus merriami*. Ecology, 71, 2323‑2333.
Hoffmann, A. A., & Sgrò, C. M. (2011). Climate change and evolutionary adaptation. Nature, 470, 479–485.
Huey, R. B. (1991). Physiological consequences of habitat selection. The American Naturalist, 137, S91–S115.
Huey, R. B., & Pianka, E. R. (1981). Ecological consequences of foraging mode. Ecology, 62, 991-999.
Huey, R. B., & Slatkin, M. (1976). Cost and benefits of lizard thermoregulation. The Quarterly Review of Biology, 51, 363-384.
Huey, R. B., Hertz, P. E., & Sinervo, B. (2003). Behavioral drive versus behavioral inertia in evolution: a null model approach. The American Naturalist, 161, 357-366.
Huey, R. B., Kearney, M. R., Krockenberger, A., Holtum, J. A., Jess, M., & Williams, S. E. (2012). Predicting organismal vulnerability to climate warming: roles of behaviour, physiology and adaptation. Philosophical Transactions of the Royal Society B: Biological Sciences, 367, 1665–1679.

Jameson Jr, E. W., & Allison, A. (1976). Fat and breeding cycles in two montane populations of *Sceloporus occidentalis* (Reptilia, Lacertilia, Iguanidae). Journal of Herpetology, 211–220.

Kawecki, T. J., & Ebert, D. (2004). Conceptual issues in local adaptation. Ecology letters, 7, 1225–1241.

Kearney, M. R. (2013). Activity restriction and the mechanistic basis for extinctions under climate warming. Ecology Letters, 16, 1470-1479.

Kingsolver, J. G., & Buckley, L. B. (2018). How do phenology, plasticity, and evolution determine the fitness consequences of climate change for montane butterflies?. Evolutionary Applications, 11, 1231-1244.

Lang, J. W. (1981). Thermal preferences of hatchling New Guinea crocodiles: effects of feeding and ontogeny. Journal of Thermal Biology, 6, 73-78.

Langkilde, T., & Boronow, K. E. (2012). Hot boys are blue: temperature-dependent color change in male eastern fence lizards. Journal of Herpetology, 461-465.

Leaché, A. D. (2010). Species trees for spiny lizards (genus *Sceloporus*): identifying points of concordance and conflict between nuclear and mitochondrial data. Molecular Phylogenetics and Evolution, 54, 162–171.

Leache, A. D., Helmer, D. S., & Moritz, C. (2010). Phenotypic evolution in high-elevation populations of western fence lizards (*Sceloporus occidentalis*) in the Sierra Nevada Mountains. Biological Journal of the Linnean Society, 100, 630–641.

Leaché, A. D., & Reeder, T. W. (2002). Molecular systematics of the eastern fence lizard (*Sceloporus undulatus*): a comparison of parsimony, likelihood, and Bayesian approaches. Systematic Biology, 51, 44–68.

Levy, O., Buckley, L. B., Keitt, T. H., & Angilletta Jr, M. J. (2016). Ontogeny constrains phenology: opportunities for activity and reproduction interact to dictate potential phenologies in a changing climate. Ecology Letters, 19, 620–628.

Mazzotti, F. J., Bohnsack, B., McMahon, M. P., & Wilcox, J. R. (1986). Field and laboratory observations on the effects of high temperature and salinity on hatchling *Crocodylus acutus*. Herpetologica, 42, 191–196.

McGinnis, S. M. (1966). Sceloporus occidentalis: preferred body temperature of the western fence lizard. Science, 152, 1090–1091.

McGinnis, S. M. (1970). Flexibility of thermoregulatory behavior in the western fence lizard *Sceloporus occidentalis*. Herpetologica, 26, 70–76.

McMillan, D. M. (2010). Functional Consequences of Acute Temperature Stress in the Western Fence Lizard, *Sceloporus occidentalis*. Open Access Dissertations, 156.

Merchant, M., Hale, A., Brueggen, J., Harbsmeier, C., & Adams, C. (2018). Crocodiles alter skin color in response to environmental color conditions. Scientific Reports, 8, 6174.

Michie, L. J., Mallard, F., Majerus, M. E. N., & Jiggins, F. M. (2010). Melanic through nature or nurture: genetic polymorphism and phenotypic plasticity in *Harmonia axyridis*. Journal of Evolutionary Biology, 23, 1699-1707.

Moran, E. V., Hartig, F., & Bell, D. M. (2016). Intraspecific trait variation across scales: implications for understanding global change responses. Global Change Biology, 22, 137–150.

Moreno Azócar, D. L., Perotti, M. G., Bonino, M. F., Schulte, J. A., Abdala, C. S., & Cruz, F. B. (2015). Variation in body size and degree of melanism within a lizards clade: is it driven by latitudinal and climatic gradients?. Journal of Zoology, 295, 243–253.

Niewiarowski, P. H., Angilletta Jr, M. J., & Leaché, A. D. (2004). Phylogenetic comparative analysis of life-history variation among populations of the lizard *Sceloporus undulatus*: an example and prognosis. Evolution, 58, 619–633.

Perez-Quintero, J. C. (1994). Thermal ecology in a saltmarsh population of Chalcides chalcides. In Resumenes, Herpetologia, III Congreso Luso-Espanol & VII Congreso Espanol, Badajoz (pp. 19–23).

Porter, W. P. (1967). Solar radiation through the living body walls of vertebrates with emphasis on desert reptiles. Ecological Monographs, 37, 273-296.

Porter, W. P., & Norris, K. S. (1969). Lizard reflectivity change and its effect on light transmission through body wall. Science, 163, 482-484.

Pough, F. H. (1991). Recommendations for the care of amphibians and reptiles in academic institutions. ILAR Journal, 33, S1–S21.

R Core Team (2017). R: A language and environment for statistical computing. R Foundation for Statistical Computing, Vienna, Austria. URL https://www.R-project.org/.

Rose, B. R. (1976). Habitat and prey selection of *Sceloporus occidentalis* and *Sceloporus graciosus*. Ecology, 57, 531–541.

Schneider, C. A., Rasband, W. S., & Eliceiri, K. W. (2012). NIH Image to ImageJ: 25 years of image analysis. Nature Methods, 9, 671.

Sears, M. W., & Angilletta, M. J. (2003). Life-history variation in the sagebrush lizard: phenotypic plasticity or local adaptation?. Ecology, 84, 1624-1634.

Sears, M. W., & Angilletta Jr, M. J. (2004). Body size clines in *Sceloporus* lizards: proximate mechanisms and demographic constraints. Integrative and Comparative Biology, 44, 433-442.

Seddon, R. J., & Hews, D. K. (2016). Phenotypic correlates of melanization in two *Sceloporus occidentalis* (Phrynosomatidae) populations: Behavior, androgens, stress reactivity, and ectoparasites. Physiology & Behavior, 163, 70-80.

Seddon, R. J., & Hews, D. K. (2017). Correlates of melanization in multiple high-and low-elevation populations of the lizard, *Sceloporus occidentalis*: Behavior, hormones, and parasites. Journal of Experimental Zoology Part A: Ecological and Integrative Physiology, 327, 481-492.

Sherbrooke, W. C., de L. Castrucci, A. M., & Hadley, M. E. (1994). Temperature effects on in vitro skin darkening in the mountain spiny lizard, *Sceloporus jarrovi*: a thermoregulatory adaptation?. Physiological Zoology, 67, 659-672.

Sinervo, B. (1988) The evolution of growth rate in *Sceloporus* lizards: environmental, behavioral, maternal, and genetic aspects. Dissertation, University of Washington, Seattle, WA.

Sinervo, B. (1990). Evolution of thermal physiology and growth rate between populations of the western fence lizard (*Sceloporus occidentalis*). Oecologia, 83, 228–237.

Sinervo, B., & Adolph, S. C. (1989). Thermal sensitivity of growth rate in hatchling *Sceloporus* lizards: environmental, behavioral and genetic aspects. Oecologia, 78, 411–419.

Sinervo, B., & Adolph, S. C. (1994). Growth plasticity and thermal opportunity in *Sceloporus* lizards. Ecology, 75, 776–790.

Sinervo, B., Hedges, R., & Adolph, S. C. (1991). Decreased sprint speed as a cost of reproduction in the lizard *Sceloporus occidentalis*: variation among populations. Journal of Experimental Biology, 155, 323–336.

Sinervo, B., Mendez-De-La-Cruz, F., Miles, D. B., Heulin, B., Bastiaans, E., Villagrán-Santa Cruz, M., Lara-Resendiz, R., Martínez-Méndez, N., Calderón-Espinosa, M. L., Meza-Lázaro, R. N., Gadsden, H., Avila, L. J., Morando, M., De la Riva, I. J., Sepulveda, P. V., Duarte Rocha, C. F., Ibargüengoytía, N., Puntriano, C. A., Massot, M., Lepetz, V., Oksanen, T. A., Chapple, D. G., Bauer, A. M., Branch, W. R., Clobert, J., Sites, J. W. (2010). Erosion of lizard diversity by climate change and altered thermal niches. Science, 328, 894–899.

Stevenson, R. D. (1985). The relative importance of behavioral and physiological adjustments controlling body temperature in terrestrial ectotherms. The American Naturalist, 126, 362-386.

Storm, M. A., & Angilletta, M. J. (2007). Rapid assimilation of yolk enhances growth and development of lizard embryos from a cold environment. Journal of Experimental Biology, 210, 3415-3421.

Tinkle, D. W., Dunham, A. E., & Congdon, J. D. (1993). Life-history and demographic variation in the lizard *Sceloporus graciosus*: a long-term study. Ecology, 74, 2413-2429.

Troscianko, J., & Stevens, M. (2015). Image calibration and analysis toolbox–a free software suite for objectively measuring reflectance, colour and pattern. Methods in Ecology and Evolution, 6, 1320-1331.

Tsuji, J. S. (1988). Thermal acclimation of metabolism in *Sceloporus* lizards from different latitudes. Physiological Zoology, 61, 241-253.

Van Berkum, F. H., Huey, R. B., Tsuji, J. S., & Garland, T. (1989). Repeatability of individual differences in locomotor performance and body size during early ontogeny of the lizard *Sceloporus occidentalis* (Baird & Girard). Functional Ecology, 97–105.

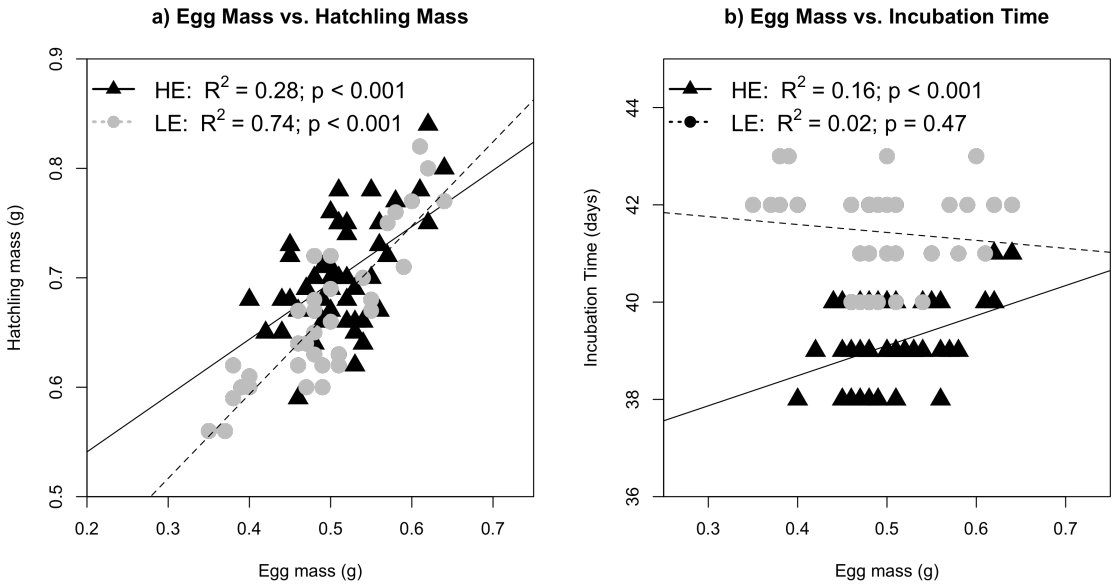

Figure 1. Significant associations between life history traits. (a) Egg mass had more power to predict hatchling mass at low elevation (LE; R^2=0.74) than at high elevation (HE; R^2=0.28). (b) Variation in egg mass explained 16% of variation in incubation time at high elevation.

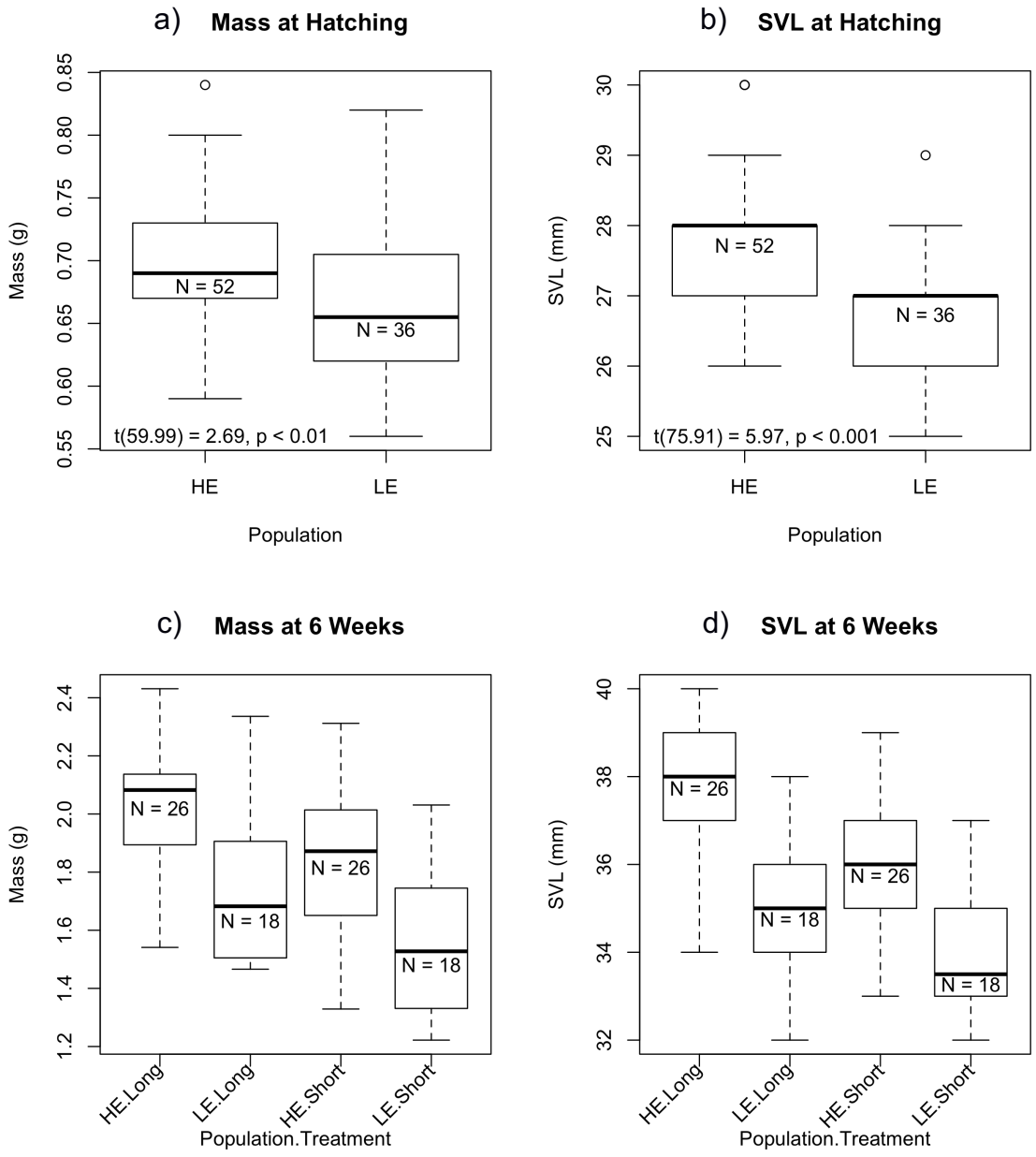

Figure 2. Variation in body size at hatching and at 6 weeks of age. (a) High elevation (HE) hatchlings were heavier than low elevation (LE) hatchlings. (b) HE hatchlings were longer than LE hatchlings. (c) High elevation (HE) hatchlings in long activity periods were heavier than hatchlings in all other population.treatment combinations. (d) High elevation (HE) hatchlings in long activity periods were longer than hatchlings in all other population.treatment combinations.

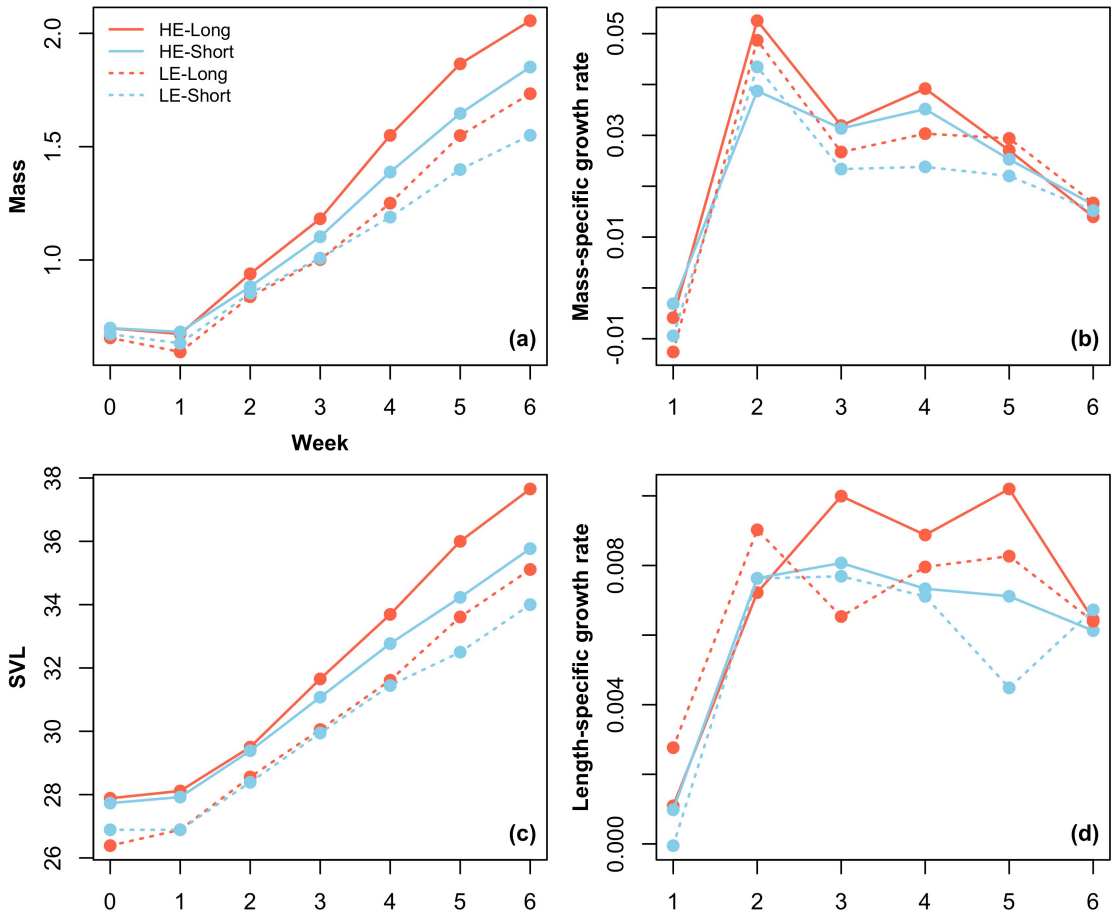

Figure 3. Full factorial comparison of mass and snout-vent length (SVL) trajectories and mass-specific and length-specific growth rates among two populations (high elevation [HE-solid lines]; low elevation [LE-dashed lines]) and two treatments (short-blue lines; long-red lines). (a) Change in mass (g). (b) Change in mass-specific growth rates ($\ln(mass_j\text{-}mass_i)/time_j\text{-}time_i$). (c) Change in SVL (mm). (d) Change in length-specific growth rates ($\ln(SVL_j\text{-}SVL_i)/time_j\text{-}time_i$).

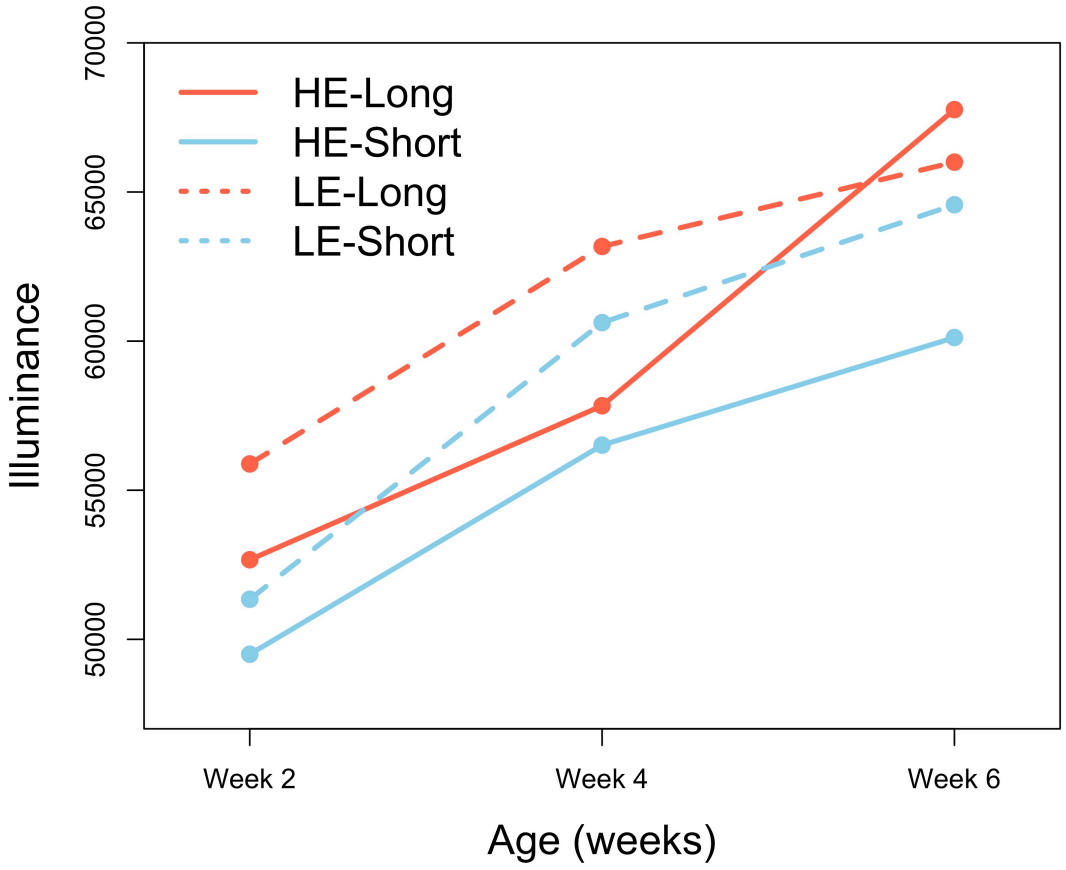

Figure 4. Full factorial comparison of color among two populations (high elevation [HE-solid lines]; low elevation [LE-dashed lines]) and two treatments (short-blue lines, long-red lines). Larger illuminance values represent lighter colors

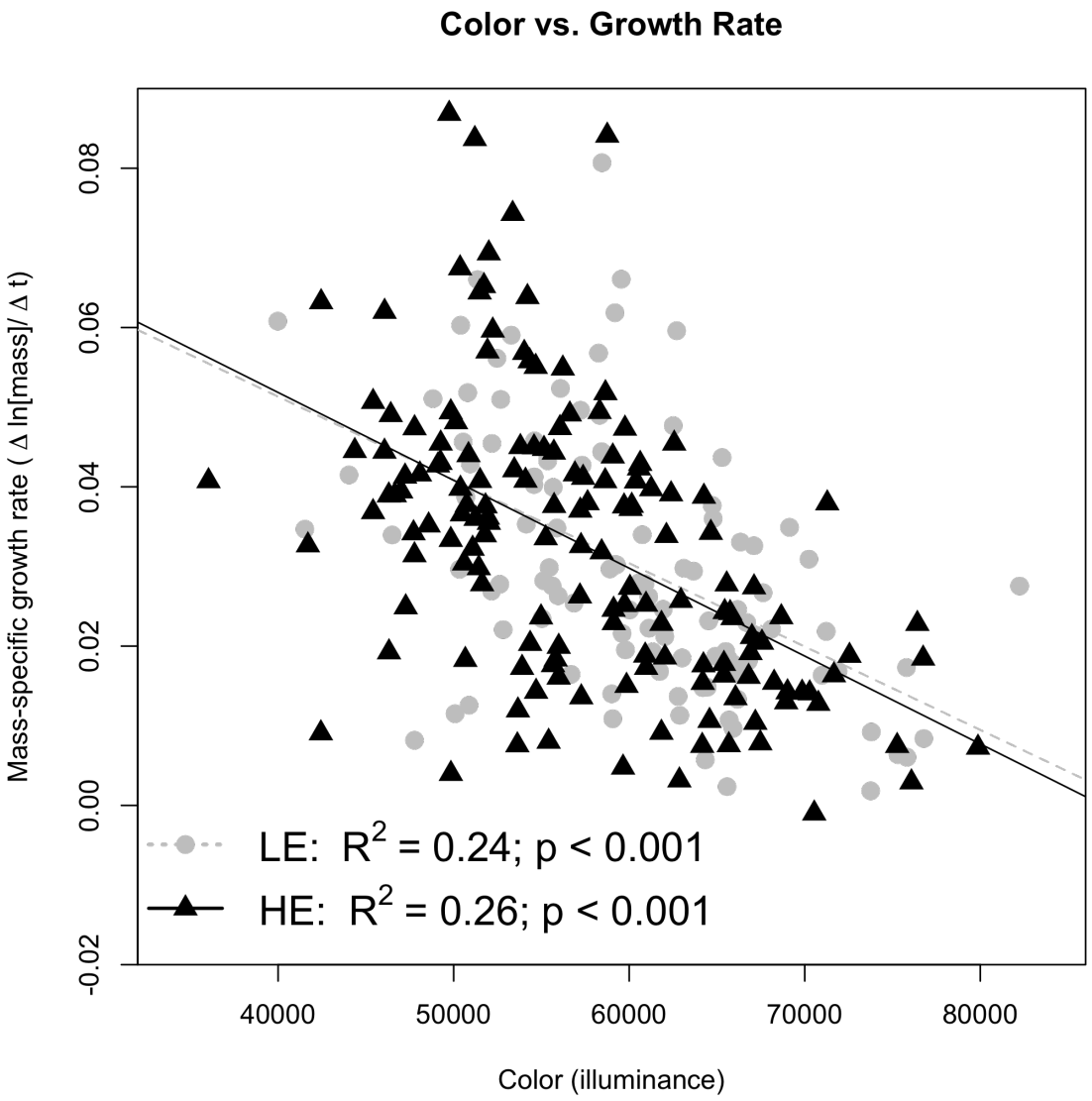

Figure 5. Association between color (illuminance) and mass-specific growth rate. Larger illuminance values represent lighter colors. In both populations variation in color explains ca. 25% of variation in growth rates.

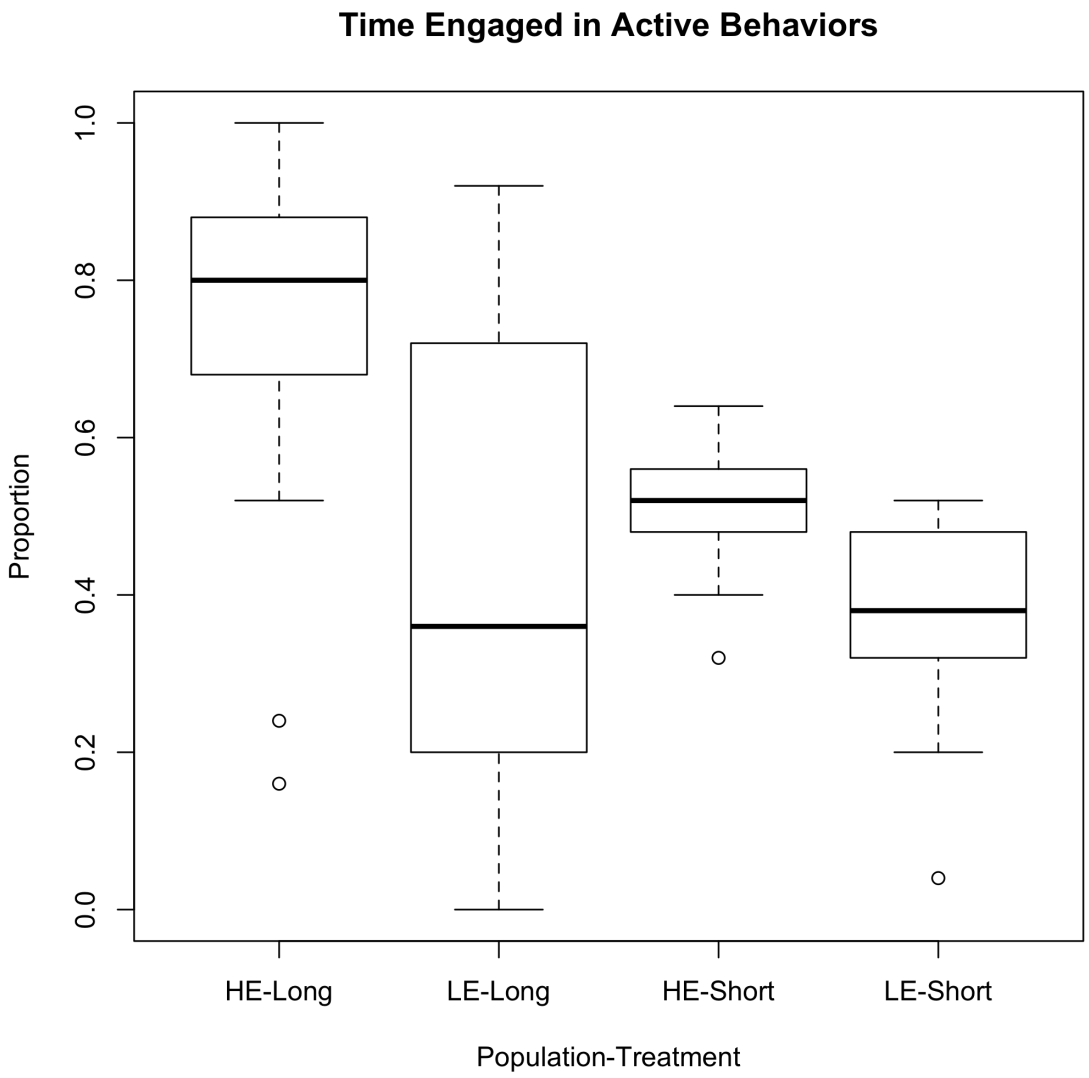

Figure 6. Differences in the proportions of activity among treatments. High elevation (HE) hatchlings in long activity periods were active significantly more often than hatchlings in any other treatment.

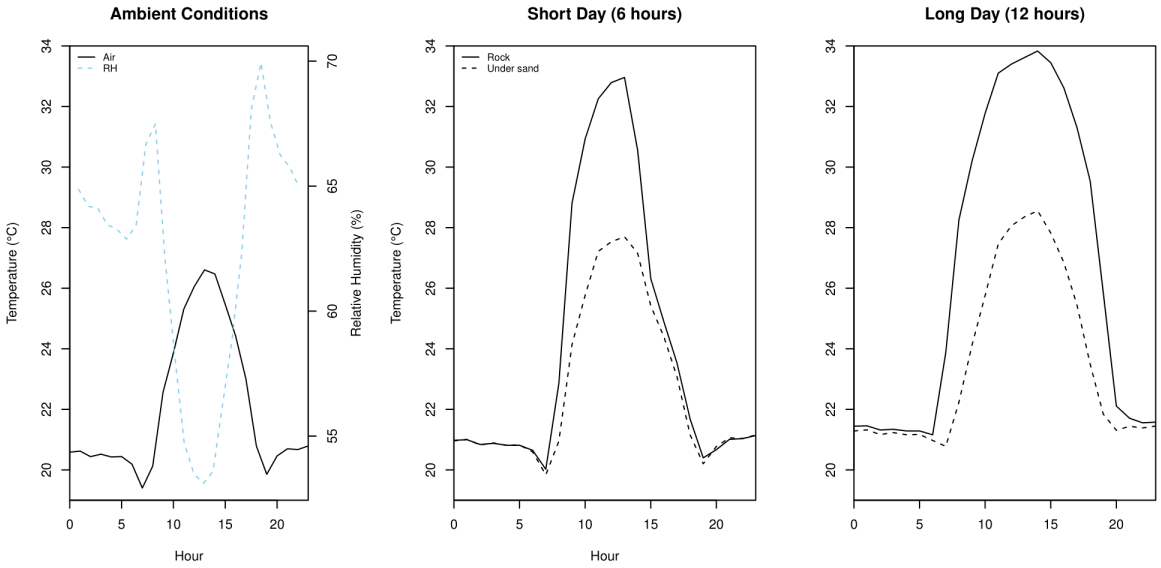

Figure S1. Average air and substrate temperatures within treatments. 'Rock' represents the hot extreme and 'under sand' represents the cold extreme. Ambient conditions were shared between treatments.

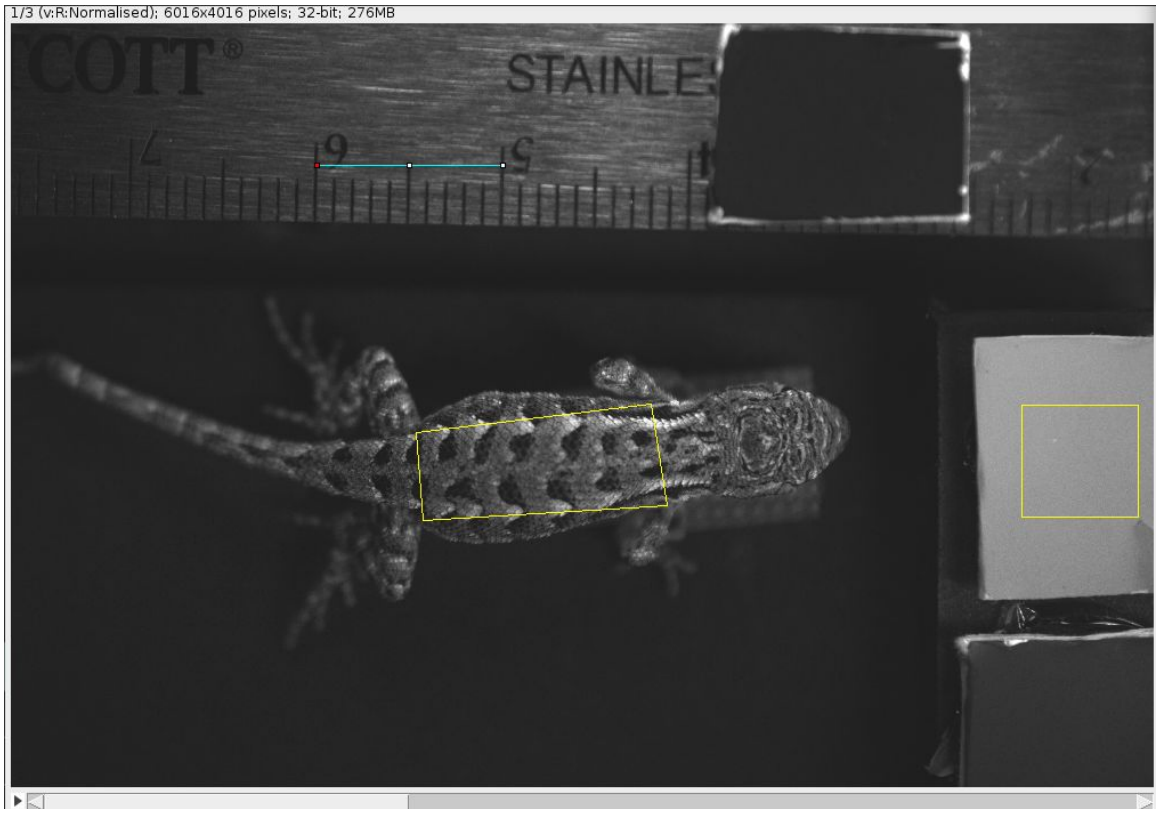

Figure S2. Area selections for measuring illuminance in ImageJ. Gray reflectance standards were used to standardize illuminance among photos. The light gray standard was measured as a control.

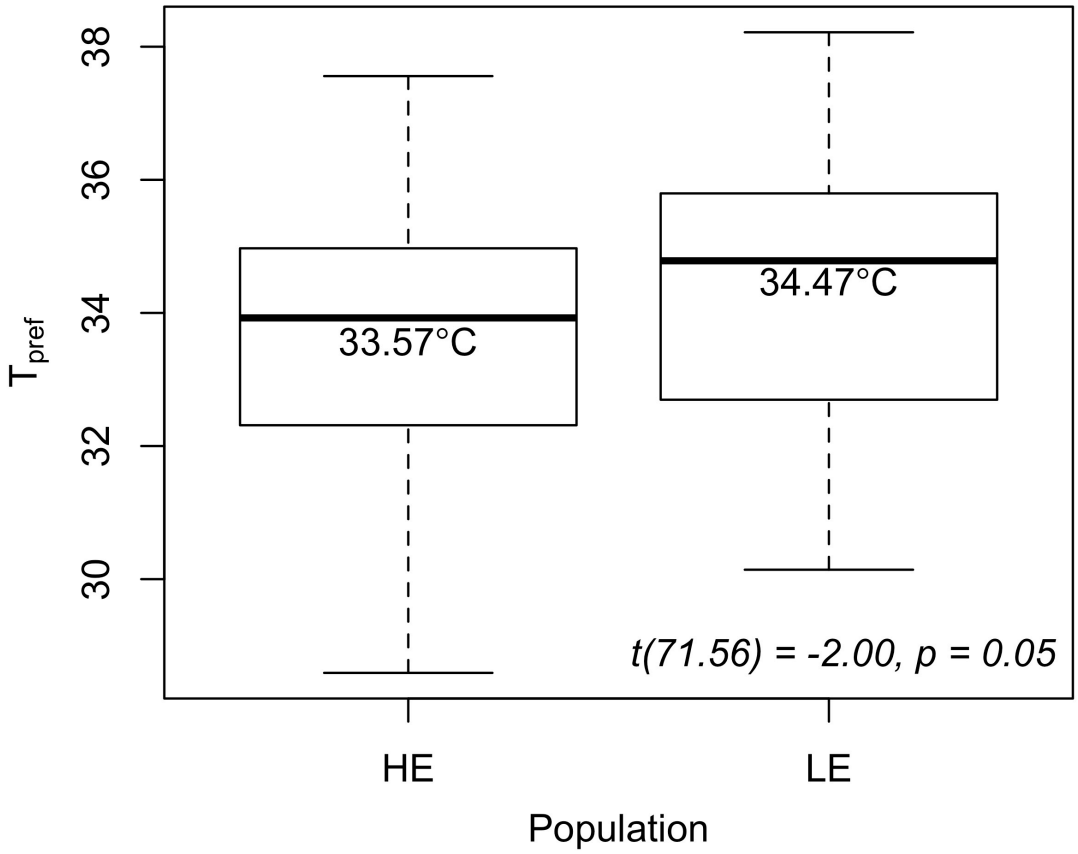

Figure S3. Differences in mean preferred body temperatures (T_{pref}) of hatchlings within 12 hours of hatching. Low elevation (LE) hatchings appear to select higher temperatures than high elevation (HE) hatchlings, but the difference is not significant at the $p < 0.05$ level.

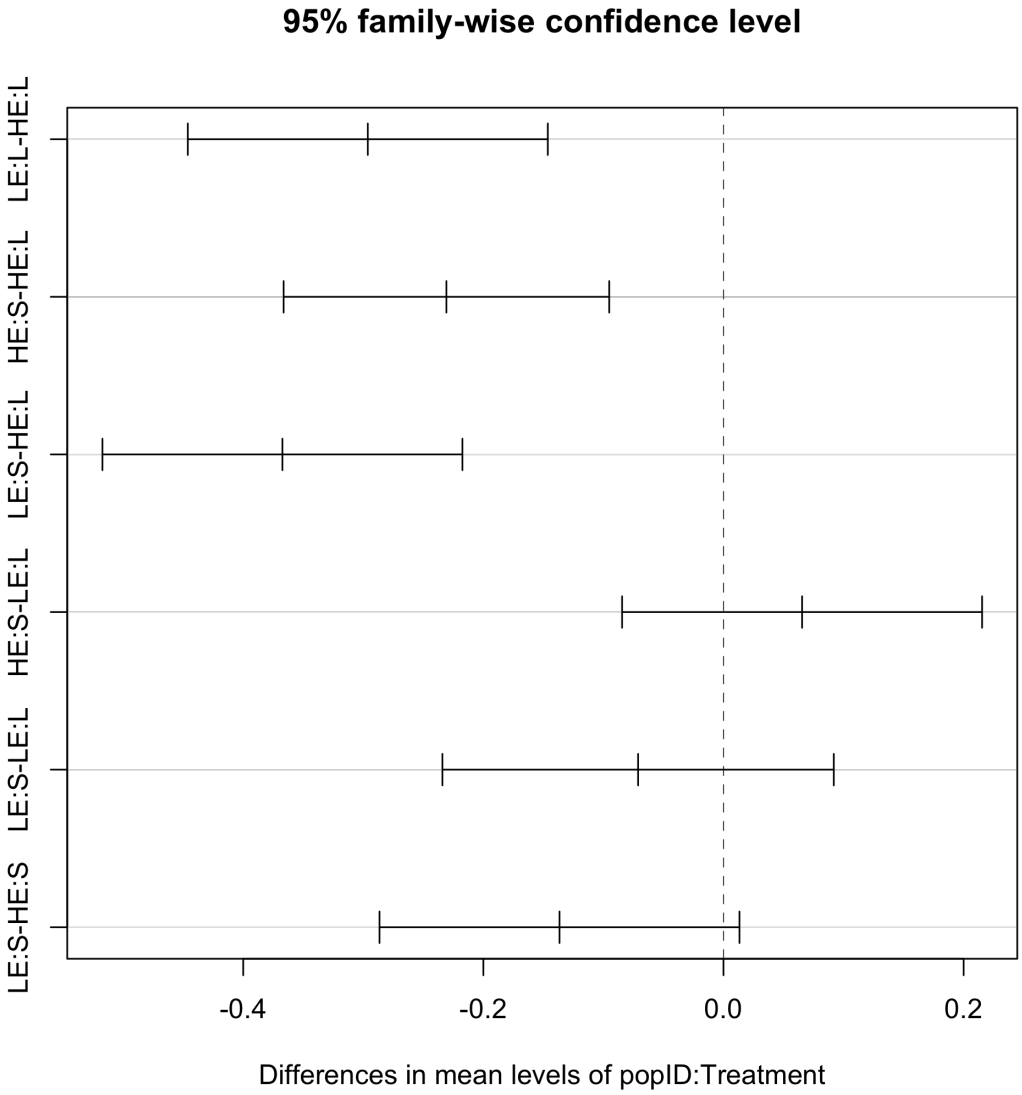

Figure S4. Tukey HSD post hoc test for mean proportion of active behaviors. Full factorial comparison of color among two populations (high elevation [HE]; low elevation [LE]) and two treatments (short [S], long [L]). Significantly different mean comparisons do not cross the dashed line.

Table 4. Summary of differences in life history traits between low elevation (LE) and high elevation (HE) populations. Means are reported with standard deviation in parentheses. Units for mass are grams, units for incubation time are days, and units for snout-vent length (SVL) are millimeters. P values that satisfy $p < 0.05$ are bold.

Trait	LE	HE	*p*
Dam mass	7.26 (±0.90)	9.34 (±0.89)	**< 0.001**
Egg mass	0.50 (±0.07)	0.51 (±0.05)	0.26
Clutch mass	3.55 (±0.52)	4.20 (±0.70)	0.07
Clutch size	7.17 (±0.41)	8.25 (±1.04)	**0.02**
Incubation time	41.44 (±0.97)	39.17 (± 0.78)	**< 0.001**
Hatchling mass	0.67 (±0.07)	0.70 (±0.05)	**< 0.01**
Hatchling SVL	26.60 (±0.90)	27.8 (±0.949)	**< 0.001**

Table 5. Associations between life history traits of low elevation (LE) and high elevation (HE) populations. Slope is the slope of the relationship between traits from linear regression. R^2 is the power of the predictive model, or the amount of variation in the dependent variable that is reduced by variation in the independent variable. P values that satisfy $p < 0.05$ are bold.

Association	Population	slope	R^2	*p*
Dam mass vs. Mean egg mass	HE	0.02	0.12	0.41
	LE	0.04	0.36	0.21
Dam mass vs. Clutch mass	HE	0.30	0.17	0.32
	LE	0.34	0.41	0.17
Dam mass vs. Clutch size	HE	0.31	0.08	0.51
	LE	0.08	0.03	0.73
Clutch size vs. Mean egg mass	HE	0.01	0.02	0.75
	LE	-0.01	4.00E-03	0.90
Egg mass vs. Hatchling mass	HE	0.52	0.28	**< 0.001**
	LE	0.77	0.74	**< 0.001**
Egg mass vs. Incubation days	HE	6.18	0.16	**< 0.001**
	LE	-1.63	0.02	0.47

Table 6. Variation in body sizes among populations after hatching (0 weeks) and at the termination of the experiment (6 weeks). Mean mass (g) and SVL (mm) are reported with the standard deviation in parentheses. * denotes 'native' conditions: high elevation (HE) hatchlings reared in short activity periods and low elevation (LE) hatchlings reared in long activity periods. P values are corrected for multiple comparison, and bold if significant.

0 weeks

	LE	**HE**	***p***
Mass	0.66 (±0.07)	0.70 (±0.05)	< 0.01
SVL	26.64 (±0.91)	27.81 (±0.90)	< 0.001

6 weeks

Mass			
	LE-short	**LE-long***	**HE-short***
LE-long*	p = 0.15	-	-
HE-short*	**p < 0.001**	p = 0.69	-
HE-long	**p < 0.001**	**p < 0.001**	**p = 0.02**
SVL			
	LE-short	LE-long*	HE-short*
LE-long*	p = 0.16	-	-
HE-short*	**p = 0.001**	p = 0.91	-
HE-long	**p < 0.001**	**p < 0.001**	**p < 0.001**

Table S1. Gravid female Sceloporus occidentalis collected for this study. Experiment ID is the identifier used throughout the experiment as the root of hatchling ID. Additional data can be accessed through the Arctos museum database.

Catalog Number	Collector Number	Experiment ID	Locality	Latitude	Longitude	Elevation
UWBM 9723	NMB 141	HH-02	Hetch Hetchy	37.95756	-119.78369	1235 m
UWBM 9724	NMB 142	HH-04	Hetch Hetchy	37.95874	-119.77845	1196 m
UWBM 9725	NMB 143	HH-03	Hetch Hetchy	37.95771	-119.78446	1228 m
UWBM 9726	NMB 144	HH-05	Hetch Hetchy	37.95077	-119.78939	1169 m
UWBM 9727	NMB 145	HH-06	Hetch Hetchy	37.95373	-119.78815	1153 m
UWBM 9728	NMB 146	TL-02	Tenaya Lake	37.83458	-119.46170	2474 m
UWBM 9730	NMB 148	GA-02	Glen Aulin	37.91413	-119.43148	2379 m
UWBM 9731	NMB 149	GA-03	Glen Aulin	37.91404	-119.42954	2414 m
UWBM 9732	NMB 150	GA-04	Glen Aulin	37.91404	-119.42954	2414 m
UWBM 9734	NMB 152	GA-06	Glen Aulin	37.91073	-119.42105	2333 m
UWBM 9736	NMB 154	GA-08	Glen Aulin	37.91716	-119.44254	2333 m
UWBM 9737	NMB 155	GA-09	Glen Aulin	37.91716	-119.44254	2333 m
UWBM 9738	NMB 156	GA-10	Glen Aulin	37.91661	-119.44130	2333 m

Appendix A – Photos of enclosures and experimental set-up

Gravid adult female enclosures

Hatchling enclosures

“Dummy” enclosure for measuring operative temperature range

Adult female thermal preference tracks

Hatchling thermal preference tracks